Fundamental Studies on the Novel Cancer Immunotherapy for Canine Lymphoid Malignancies

（犬のリンパ系腫瘍に対する新規免疫療法の基礎的検討）

The United Graduate School of Veterinary Science
Yamaguchi University

Osamu SAKAI

March 2021

TABLE OF CONTENTS

GENERAL INTRODUCTION

Cancer is one of the main causes of death in older dogs, and canine B cell lymphoma is the most common hematopoietic neoplasms in veterinary medicine (Zandvliet, M., 2016). Most cases show a good response with the standard treatment, generally consists of a multi-drug chemotherapy regimen. However, it is ultimately only a small population which is truly cured, and the treatment is often challenging because many cases develop relapsed or refractory disease. The efficacy of treatment is also limited because of the drug resistance and the limited alternative treatment options (Zandvliet, M. and Teske, E., 2015). Therefore, there is a distinct need for novel therapeutic option.

Canine cancer is not only clinically important, but also attracting attention as an ideal model relevant to human cancer. The relevance between human and canine cancers has reported in many types of cancer, such as osteosarcoma, transitional cell carcinoma, soft tissue sarcoma, and melanoma (Gardner, HL. *et al*., 2016). Canine lymphoma also shares many characteristics with human lymphoma, and canine lymphoma is considered as a comparative model for human non-Hodgkin lymphoma (Hansen, K. and Khanna, C., 2004, Ito, D. *et al*., 2014). The importance of canine

cancer as relevant model for human cancer is emphasized, especially in the field of immunotherapy, because immunocompetent dogs have an immunosuppressive cancer microenvironment that enables evaluation of the interaction between cancer and immune cells. As with human medicine, the novel immunotherapy has been developed in canine medicine.

Analysis of tumor-associated antigens (TAAs) provides fundamental information for cancer immunotherapy. To date, many TAAs, such as NY-ESO-1, MUC1, HER2, CEA, and MART-1, have been identified and molecularly characterized (Tagliamonte, M. *et al*., 2014). Among them, the Wilms' tumor 1 (WT1) protein is one of the most common TAAs. The WT1 gene was first identified as a gene responsible for Wilms' tumor, a common renal cancer in children. Although WT1 gene was categorized at first as a tumor-suppressor gene, now it is considered that the wild-type WT1 plays an oncogenic role in various kinds of human cancers (Yang, L. *et al*., 2007). High expression of WT1 has been detected in hematological malignancies such as acute myeloid leukemia (AML), acute lymphocytic leukemia (ALL), chronic myeloid leukemia (CML), and myelodysplastic syndromes (MDS), and its therapeutic potential

as peptide-based cancer vaccine has been investigated (Rosenfeld, C. *et al*., 2003). In contrast, the information about TAAs, including WT1, is scarce in veterinary medicine. In chapter 1, canine WT1 gene was molecularly cloned and the expression of WT1 protein was investigated by immunohistochemical analysis.

Despite the high expectations predicted from preclinical studies, the clinical efficacy of peptide vaccines was limited. Thus, many researchers next focused on the use of immune adjuvants or cancer-specific neoantigens, and other approaches have also investigated. Recent studies have shown the clinical efficacy of novel cancer immunotherapy such as adoptive cell therapy and monoclonal antibody therapy. Adoptive cell therapy with chimeric antigen receptor (CAR) T cells targeting CD19 has demonstrated a high rate of complete remission in clinical trials for human B cell malignancies including acute lymphoblastic leukemia, chronic lymphocytic leukemia, and non-Hodgkin lymphoma (Geyer, MB. and Brentjens, RJ., 2016). The typical CAR is composed of three domains; the extracellular antigen recognition domain derived from single-chain variable fragment (scFv) of monoclonal antibody, transmembrane domain, and intracellular signaling domain. In the basic process of CAR-T generation,

the patient's T cells are isolated, activated, and transduced to express CARs that recognize specific tumor-associated antigens. CAR-T cell therapy was firstly developed for hematopoietic malignancies, and further investigation is underway to expand the scope of application for solid tumor. Monoclonal antibody therapy is another strategy in which an antibody as therapeutic agent specifically binds to a molecule on the surface of cancer cells. Rituximab, a human-mouse chimeric anti-CD20 monoclonal antibody, is the most successful therapeutic antibody, and has established efficacy and tolerability in patients with B cell malignancies (Salles, G. *et al*., 2017).

As with human medicine, the development of cancer immunotherapy has also reported in veterinary medicine. There are a few reports on canine CAR-T cell therapy, however, *in vivo* antitumor efficacy in patients with spontaneous cancer has still not established (Mata, M. *et al*., 2014, Smith, JB. *et al*., 2015, Mata, M. and Gottschalk, S., 2016, Panjwani, MK. *et al*., 2016, Yin, Y. *et al*., 2018). Manufacturing CAR-T cells is a complex process involving many procedures, and basic information about optimal manufacturing protocol for canine CAR-T cells is lacking. Monoclonal antibody therapy is also developed against canine B cell malignancies, and several therapeutic

monoclonal antibodies targeting canine CD20 have been established and reported (Jain, S. *et al*., 2016, Ito, D. *et al*., 2015). Our laboratory recently developed the novel anti-canine CD20 antibody with high *in vitro* antitumor activity, and clinical trials for canine B cell lymphoma is ongoing in our veterinary teaching hospital. These new approaches are expected to be a promising therapeutic option in veterinary oncology.

The main purpose of the studies from chapters 2 to 5 is to investigate the optimal protocol for canine CAR-T cell manufacturing. The optimization of canine CAR-T cell manufacturing has described in chapter 4 and 5. In chapter 4, canine CAR-T cells were prepared under various conditions, and the effects of culture conditions on CAR-T cells were investigated. *In vitro* and *in vivo* antitumor activities of canine CAR-T cell were also described. In chapter 5, based on the results obtained in chapter 4, further investigation was conducted to determine the optimal condition for generation of potent CAR-T cells. The study also aimed to establish the monoclonal antibody against CAR, because monitoring of infused CAR-T cells is indispensable for estimation of the therapeutic potential of CAR-T cells. The immunization with CAR-expressing cells produced two monoclonal antibodies that recognize scFv of CAR and canine CD8. In

chapter 2, the establishment and characterization of CAR-specific monoclonal antibody have been described. This antibody was also tested the reactivity against therapeutic anti-canine CD20 antibody. Our laboratory recently reported a pilot clinical study of antibody therapy against PD-1 in canine patients with spontaneous cancers (Igase, M. *et al*., 2020). To evaluate the therapeutic response in immune checkpoint blockade therapy, the monitoring of immune cells, such as cytotoxic T lymphocyte, in tumor microenvironment is important. The establishment of anti-canine CD8 antibody has described in chapter 3, and immunohistochemical detection of canine and feline CD8 was attempted using this antibody.

CD20-targeted immunotherapy has potential to be a promising treatment option for canine B cell malignancies. All of my studies provide new insight into the development of canine cancer immunotherapy.

Chapter 1

Molecular cloning of canine Wilms' tumor 1 for immunohistochemical analysis in canine tissues

SUMMARY

Wilms' tumor 1 (WT1) expression has been investigated in various human cancers as a target molecule for cancer immunotherapy. However, few studies have focused on WT1 expression in dogs. Firstly, cDNA of canine WT1 (cWT1) was molecularly cloned from normal canine kidney. The cross-reactivity of the anti-human WT1 monoclonal antibody (6F-H2) with cWT1 was confirmed via Western blotting using cells overexpressing cWT1. Immunohistochemical staining revealed that cWT1 expression was detected in all canine lymphoma tissues and in some normal canine tissues, including the kidney and lymph node. cWT1 is a potential immunotherapy target against canine cancers.

INTRODUCTION

Cancer is the most common cause of death in dogs, and even though a lot of efforts have been put into the discovery of novel canine cancer therapeutics, only a hand full of these treatments are available in actual clinical practice. During last two decades, cancer immunotherapy has been expected to be new kinds of therapy, where various therapeutic approaches utilizing the immune system to fight against cancer have been attempted. Among these approaches, peptide immunotherapy is expected to have the highest potential. Along with the development of peptide immunotherapy, a large number of tumor-associated antigens (TAAs) have been identified in human cancer. The Wilms' tumor 1 (WT1) protein is one of the most common TAAs found in human cancers (Cheever, MA. *et al*., 2009).

The WT1 gene was first identified in 1990, and categorized as a tumor-suppressor gene because WT1 gene deletions and mutations were found in Wilms' tumor, a common renal tumor in children. WT1 plays an important role in normal cellular development, differentiation, and cell survival (Call, KM. *et al*., 1990, Gessler, M. *et al*., 1990, Menke, AL. *et al*., 1998). High levels of wild-type WT1 expression

were detected in various kinds of human cancers including hematopoietic malignancies such as leukemia and myelodysplastic syndromes, and solid cancers such as brain cancer, neuroblastoma, lung cancer, breast cancer, head and neck squamous cell carcinoma, thyroid cancer, esophageal cancer, ovarian carcinoma and renal cell carcinoma (Oka, Y. *et al*., 2000, Yang, L. *et al*., 2007). Several studies have shown that induction of WT1-specific cytotoxic T lymphocytes (CTL) by the WT1 peptide vaccine is clinically effective in the treatment of human cancer. It is reported that WT1 peptide vaccination in combination with imatinib decreased bcr-abl transcript level in chronic myeloid leukemia patient and this combination did not induce serious adverse effects (Narita, M. *et al*., 2010, Oji, Y. *et al*., 2010). Oka *et al.* reported the outcome of a phase I clinical study of WT1 peptide immunotherapy in patients with breast cancer, lung cancer, myelodysplastic syndrome and acute myeloid leukemia (Oka, Y. *et al*., 2004). Clinical responses such as reduction in the number of tumor cells and tumor sizes were achieved in twelve out of twenty patients. The study also confirmed a clear correlation between the increment of WT1-specific CTL and clinical responses.

On the other hand, there have been few reports on the expression of canine

WT1 (cWT1) in dogs (Pearson, GR. *et al*., 1997, Kothapalli, K. *et al*., 2005, Ichimura, R. *et al*., 2010) and none of those reports was related to canine tumors. Therefore, evaluation of cWT1 expression in canine tumors will be helpful in the development of immunotherapy for dogs. In this study, we molecularly cloned the cWT1 gene and examined its cross-reactivity with an anti-human WT1 antibody. cWT1 expression was also assessed in canine lymphoma tissues, as well as in normal canine tissues.

MATERIALS AND METHODS

Molecular cloning of cWT1

One microgram of total RNA isolated from normal canine kidney tissue was treated with Turbo DNA-free (Ambion Life Technologies, Austin, TX, USA), and transcribed into cDNA using Superscript III (Invitrogen Life Technologies, Carlsbad, CA, USA) according to manufacturers' instructions. Oligo dT primers were used to prime the first-strand synthesis for each reaction. Primers for the cDNA amplification of cWT1, YTM567 (5' TCTGCAAGGCCGAAGGAG 3') and YTM580 (5' CGTACAGGCATCTTGTCTCG 3'), were designed based on predicted sequences of cWT1 in the canine genomic database (GenBank Accession No. NW_876266.1). Using this primer pair, the cWT1 gene was amplified from the normal canine kidney cDNA using KOD plus kit (Toyobo, Osaka, Japan) according to manufacturer's instructions. Predenaturation at 94 ºC for 2 min was followed by 35 cycles of PCR amplification, which consists of denaturation at 98 ºC for 10 sec, annealing at 56 ºC for 30 sec, extension at 68 ºC for 2 min, and a final extension at 68 ºC for 10 min. The gel-purified PCR product was inserted into SmaI restriction sites of pBluescript SK (-) vector (pBS-

cWT1). The constructed vector was sequenced using BigDyeTerminator v3.1 Cycle Sequencing Kit (Perkin-Elmer, Foster City, CA, USA) and analyzed using ABI377 automated DNA sequencer at Yamaguchi University Center for Gene Research.

Cell cultures

Human embryonic kidney cell line, HEK293T, was maintained in D10 complete medium (DMEM supplemented with 10% fetal bovine serum (FBS), 100 units/ml penicillin and 100 μg/ml streptomycin, and 55 μM 2-mercaptoethanol). These cell lines were cultured in a humidified incubator at 37 ºC and 5% CO2.

Vector construction and transfection

In order to evaluate the cross-reactivity of anti-human WT1 monoclonal antibody (6F-H2) with cWT1, cWT1 was transiently overexpressed in HEK293T cells. The expression vector was constructed by inserting BamHI and EcoRV-digested segments of the pBS-cWT1 into a mammalian expression vector pcDNA3.1(+) (pcDNA3.1(+)-cWT1). Empty vector and pcDNA3.1(+)-cWT1 were transfected into

HEK293T cells using Trans-it LTI (TAKARA BIO INC., Shiga, Japan) according to manufacturer's instructions. The cells were collected 48 hr after transfection, and used in following experiments.

Western blotting

Cells were lysed in lysis buffer [10mM Tris (pH 7.5), 150 mM NaCl, 1 mM EDTA, 1% NP40, protease inhibitor (Complete, Mini, EDTA-free: Roche Diagnostics K.K., Tokyo, Japan)] at 4 ºC for 15 min, centrifuged at 20,000 g at 4 ºC for 15 min before supernatant (cell lysate) was collected. Protein concentration was measured using Micro BCA™ Protein Assay Reagent Kit (Thermo Fisher Scientific, Tokyo, Japan) according to the manufacturer's instructions. Samples of equal concentration were subjected to SDS-PAGE (9% acrylamide gel) and subsequent membrane blotting (Hybond™ ECL membrane, GE Healthcare Japan, Tokyo, Japan). Membrane were blocked with blocking buffer [Tris-buffered saline with 0.05% Tween 20 (TBS-T) and 5% skimmed milk] at RT for 1 hr before incubation with a primary antibody; mouse monoclonal anti-human WT1 antibody (6F-H2, Dako, Glostrup, Denmark, 1:500

dilution in 0.5% skimmed milk/ TBS-T) at 4 ºC overnight or goat anti-actin antibody (Santa Cruz Biotechnology, Inc., Dallas, TX, USA, 1:2000 dilution in 0.5% skimmed milk/ TBS-T) at RT for 2 hr. Washing with TBS-T was carried out for 10 min three times before incubation with horseradish peroxidase-conjugated secondary antibodies; goat anti-mouse IgG antibody (Zymed Laboratories Inc., South San Francisco, CA, USA, 1:4000 dilution in 0.5% skimmed milk/ TBS-T) or rabbit anti-goat IgG antibody (Bethyl Laboratories Inc., Montgomery, TX, USA, 1:4000 dilution in 0.5% skimmed milk/ TBS-T) at RT for 1 hr. Washing with TBS-T was repeated again for three times, and membranes were immersed in Western Lightning Chemiluminescence reagent Plus (Perkin-Elmer) for band visualization.

Immunohistochemical staining of cWT1

cWT1 expression was evaluated using 26 normal tissue specimens of various organs from 15 healthy dogs and 22 tumor specimens from 22 dogs diagnosed with lymphoma. The specimens, which were obtained from the laboratories of veterinary pathology of Yamaguchi University and Gifu University, were fixed in formalin and

embedded in paraffin before immunohistochemical staining (IHC) was performed. IHC was carried out following the method described in previous report (Okawa, T. *et al*., 2012). Anti-WT1 antibody (6F-H2) or normal mouse IgG1 (Santa Cruz Biotechnology, Inc., Dallas, TX, USA) was used as the primary antibody, followed by treatment with horseradish peroxidase (HRP)-conjugated secondary antibody, goat anti-mouse IgG antibody (Histofine Simple Stain MAX PO: Nichirei Corporation, Tokyo, Japan). Finally, color was developed using freshly prepared 3,3-diaminobenzidine tetrachloride (Roche Diagnostics K.K., Tokyo, Japan). The slides were counterstained for 1 min with Carazzi's hematoxylin, washed in distilled water, dehydrated in graded baths of ethanol, cleared in xylene, and mounted with xylene-based mounting solution (Matsunami, Osaka, Japan).

RESULTS

Molecular cloning and sequence analysis of cWT1

Firstly, the cDNA of cWT1 was molecularly cloned for sequence analysis and protein overexpression. PCR amplification of the cWT1 cDNA using the primers YTM567 and YTM580 generated a single DNA fragment with an expected size of approximately 1500 bp.

Nucleotide sequence analysis of the full-length cWT1 revealed a cDNA clone of 1559 bp that has an open reading frame of 1356 bp, encoding 451 amino acids (Fig. I-1). The nucleotide sequence of cWT1 was 94% and 91% identical to the human and mouse WT1. When compared with the predicted partial nucleotide sequence of cWT1 (GenBank Accession No. NW_876266.1), 11 mismatched nucleotides were found in the nucleotide sequence of the coding region of cWT1. The alignment of the predicted amino acid sequence of the cWT1 cDNA, the human WT1 cDNA and the mouse WT1 cDNA are shown in Fig. II-2. The deduced amino acid sequence of the cWT1 cDNA was highly homologous (99% and 97%) with that of the human and mouse WT1 polypeptides.

Crossreactivity of anti-human WT1 antibody to cWT1

The cWT1 was transiently expressed in HEK293T cells to evaluate the crossreactivity of anti-human WT1 antibody (6F-H2) to cWT1. In western blotting analysis, the anti-human WT1 antibody, 6F-H2, recognized a band of the expected molecular weight at 50-55 kDa in the HEK293T cells transfected with pcDNA3.1(+)-cWT1, but not in the control using pcDNA3.1(+) (Fig. I-3). This result strongly indicated that 6F-H2 cross-reacted with cWT1.

Immunohistochemical staining of cWT1 in canine tissues

To evaluate the expression of cWT1 protein, normal and lymphoma tissues were stained immunohistochemically with monoclonal antibody (6F-H2). IHC results of the normal tissue specimens are summarized in Table I-1. cWT1 was clearly detected in the glomerular cells, especially in the outer zone, of the kidney (Fig. I-4A). According to the localization site, WT1-positive cells are considered to be podocytes, as reported (Wagner, N. *et al*., 2004). Furthermore, WT1-positive signals were weakly detected in

renal tubules, as observed in normal rat kidneys (Huang, B. *et al*., 2012). In addition, testis and lymph node (Table I-1) were stained positively for cWT1. On the other hand, cWT1 expression was not detected in the heart, spleen, prostate, skeletal muscle and skin. All of the 22 canine lymphoma tissue specimens, irrespective of the immunophenotypes, anatomic sites and historical grade, were positively stained for cWT1 (Fig. I-4C, 4D and Table I-2). Lymphocytes in all the tumor specimens, as well as the normal control lymph nodes of healthy dogs were stained in a similar pattern (Fig. I-4B).

DISCUSSION

In this study, we showed that the mouse anti-human WT1 monoclonal antibody (6F-H2) cross-reacted with cWT1. This was consistent with the description in the product specification, where the antigen binding site of 6F-H2 is located at the N-terminal amino acids 1-181 of the human WT1, and is expected to bind to cWT1. Previous report has used a polyclonal antibody against human WT1 for IHC in canine tissue specimens, but the specificity of the antibody to cWT1 was never shown (Ichimura, R. *et al*., 2010). Western blotting of canine cell lines carried out in our lab using an anti-human WT1 polyclonal antibody (C-19) has revealed multiple non-specific bands (data not shown). The specificity of the 6F-H2 antibody to cWT1 that was shown in this study will become useful information in future investigations of the cWT1 expression pattern in canine tumors.

The main objective of this study was to investigate the relevance of cWT1 as a tumor associated antigen (TAA) in canine malignancies and its applicability as one of the immunotherapeutic options in the near future. Many TAAs have been identified in various human malignancies, and among them, WT1 was found to be commonly

expressed (Cheever, MA. *et al*., 2009). Drakos *et al.* evaluated the expression of WT1 in 167 non-Hodgkin's lymphoma (NHL) samples using IHC, and found that 80% of Burkitt lymphomas, 75% of ALK-positive ALCLs, 50% of lymphoblastic lymphomas, 45% of ALK-negative ALCLs, 33% of DLBCLs and 17% of cutaneous ALCLs were positive for WT1 expression (Drakos, E. *et al*., 2005). Since lymphoma is the most common hematopoietic malignancy in dogs, we focused on the expression of cWT1 in canine lymphoma. In this study, we revealed that cWT1 expression was detected in all of the canine lymphoma tissue specimens, including low and high grade, as well as both T and B cell lymphoma.

The IHC results have shown that cWT1 expression was detected not only in the lymphoma tissue specimens, but also in some normal tissue specimens. This raises concerns, if cWT1 is used as a TAA for immunotherapy, the possibilities of tolerance to treatment. The expression of WT1 protein in normal tissues is not an exclusive phenomenon in dogs, and has also been reported in various human adult tissues, including tissues of the urogenital system, central nervous system and hematopoietic system such as bone marrow and lymph nodes (Menke, AL. *et al*., 1998). Nonetheless,

the results of several clinical trials have shown that WT1 peptide vaccines in cancer patients are capable of eliciting immune responses with minimal adverse events (Brayer, J. *et al*., 2015, Krug, LM. *et al*., 2010). This suggests that even though WT1 is expressed in normal tissues, treatment tolerance will not be induced. In this study, expression of cWT1 was detected in a wide range of normal tissues as compared to that in human. This indicates that more prudent evaluations will be required in order to predict the autoaggression of the immune response against cWT1 in dogs.

Identification of TAAs for use in cancer immunotherapy for canine lymphoma is of increasing importance. Latest therapeutic advancements in veterinary oncology include cancer vaccines, where treatment efficacy of human tyrosinase was evaluated in advanced canine melanoma, and telomerase in B cell canine lymphoma (Liao, JC. *et al*., 2006, Peruzzi, D. *et al*., 2010). These studies indicate that cancer immunotherapy designed based on appropriate TAAs will exert clinical effectiveness. Therefore, we hope that more studies can be conducted to elucidate the therapeutic potential of cWT1 in canine lymphoma, and to reveal cWT1 expression in other canine malignancies.

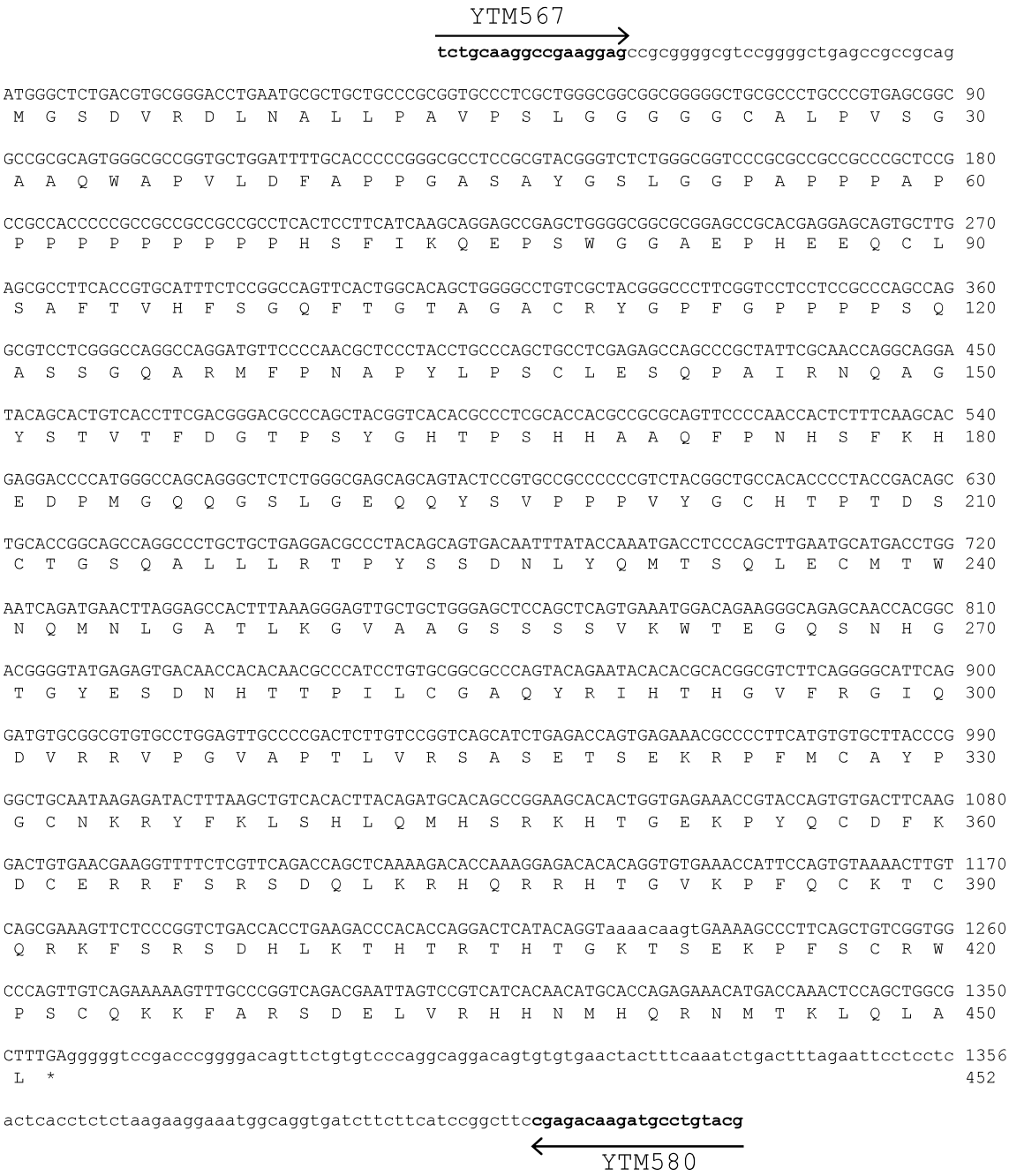

Fig. I-1. Nucleotide sequence (top line) and the predicted amino acid sequence (bottom line) of cWT1.

Letters in upper case represent the coding region of cWT1, and letters in lower case

represent the non-coding region. Asterisk represents the stop codon. Numbers on the right refer to the nucleotide position of the cDNA of cWT1 (top line) and the amino acid sequence position (bottom line). Arrows indicate the primers involved.

```
 Dog   MGSDVRDLNALLPAVPSLGGGGG-CALPVSGAAQWAPVLDFAPPGASAYGSLGGPAPPPA 59
Human  MGSDVRDLNALLPAVPSLGGGGG-CALPVSGAAQWAPVLDFAPPGASAYGSLGGPAPPPA 59
Mouse  MGSDVRDLNALLPAVSSLGGGGGGCGLPVSGARQWAPVLDFAPPGASAYGSLGGPAPPPA 60
       ***************.******* *.****** **************************

Dog    PPPPPPPPPPHSFIKQEPSWGGAEPHEEQCLSAFTVHFSGQFTGTAGACRYGPFGPPPPS 119
Human  PPPPPPPPP-HSFIKQEPSWGGAEPHEEQCLSAFTVHFSGQFTGTAGACRYGPFGPPPPS 118
Mouse  PPPPP--PPPHSFIKQEPSWGGAEPHEEQCLSAFTLHFSGQFTGTAGACRYGPFGPPPPS 118
       *****  ** ************************:************************

Dog    QASSGQARMFPNAPYLPSCLESQPAIRNQAGYSTVTFDGTPSYGHTPSHHAAQFPNHSFK 179
Human  QASSGQARMFPNAPYLPSCLESQPAIRNQG-YSTVTFDGTPSYGHTPSHHAAQFPNHSFK 177
Mouse  QASSGQARMFPNAPYLPSCLESQPTIRNQG-YSTVTFDGAPSYGHTPSHHAAQFPNHSFK 177
       ************************:****. ********:********************

Dog    HEDPMGQQGSLGEQQYSVPPPVYGCHTPTDSCTGSQALLLRTPYSSDNLYQMTSQLECMT 239
Human  HEDPMGQQGSLGEQQYSVPPPVYGCHTPTDSCTGSQALLLRTPYSSDNLYQMTSQLECMT 237
Mouse  HEDPMGQQGSLGEQQYSVPPPVYGCHTPTDSCTGSQALLLRTPYSSDNLYQMTSQLECMT 237
       ************************************************************

Dog    WNQMNLGATLKGVAAGSSSSVKWTEGQSNHGTGYESDNHTTPILCGAQYRIHTHGVFRGI 299
Human  WNQMNLGATLKGVAAGSSSSVKWTEGQSNHSTGYESDNHTTPILCGAQYRIHTHGVFRGI 297
Mouse  WNQMNLGATLKGMAAGSSSSVKWTEGQSNHGIGYESENHTAPILCGAQYRIHTHGVFRGI 297
       ************:*****************. ****:***:********************

Dog    QDVRRVPGVAPTLVRSASETSEKRPFMCAYPGCNKRYFKLSHLQMHSRKHTGEKPYQCDF 359
Human  QDVRRVPGVAPTLVRSASETSEKRPFMCAYPGCNKRYFKLSHLQMHSRKHTGEKPYQCDF 357
Mouse  QDVRRVSGVAPTLVRSASETSEKRPFMCAYPGCNKRYFKLSHLQMHSRKHTGEKPYQCDF 357
       ******.*****************************************************

Dog    KDCERRFSRSDQLKRHQRRHTGVKPFQCKTCQRKFSRSDHLKTHTRTHTGKTSEKPFSCR 419
Human  KDCERRFSRSDQLKRHQRRHTGVKPFQCKTCQRKFSRSDHLKTHTRTHTGKTSEKPFSCR 417
Mouse  KDCERRFSRSDQLKRHQRRHTGVKPFQCKTCQRKFSRSDHLKTHTRTHTGKTSEKPFSCR 417
       ************************************************************

Dog    WPSCQKKFARSDELVRHHNMHQRNMTKLQLAL 451
Human  WPSCQKKFARSDELVRHHNMHQRNMTKLQLAL 449
Mouse  WHSCQKKFARSDELVRHHNMHQRNMTKLHVAL 449
       * *************************::**
```

Fig. I-2. Comparison of the predicted WT1 amino acid sequences among different species.

The amino acid sequence of cWT1 was aligned with its human and mouse counterpart using the “Clustal W” software. “*” indicates that the residue was identical, whereas “:”

and “.” indicate that very similar and similar residues in the alignment were observed. The amino acid sequences of human and mouse WT1 were obtained from the NCBI database (X51630.1 for human and M55512.1 for mouse).

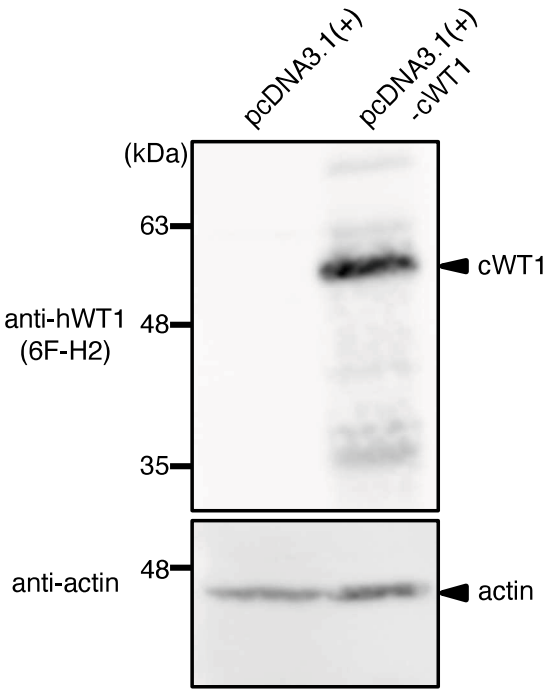

Fig. I-3. Cross-reactivity of the anti-human WT1 antibody with cWT1 overexpressed in HEK293T cells.

HEK293T cells were transiently transfected with pcDNA3.1(+)-cWT1 or pcDNA3.1(+). Forty-eight hours after transfection, whole cell lysates were extracted, and Western blotting using anti-human WT1 antibody (6F-H2) was performed. Arrow indicates a band with the expected molecular weight of cWT1.

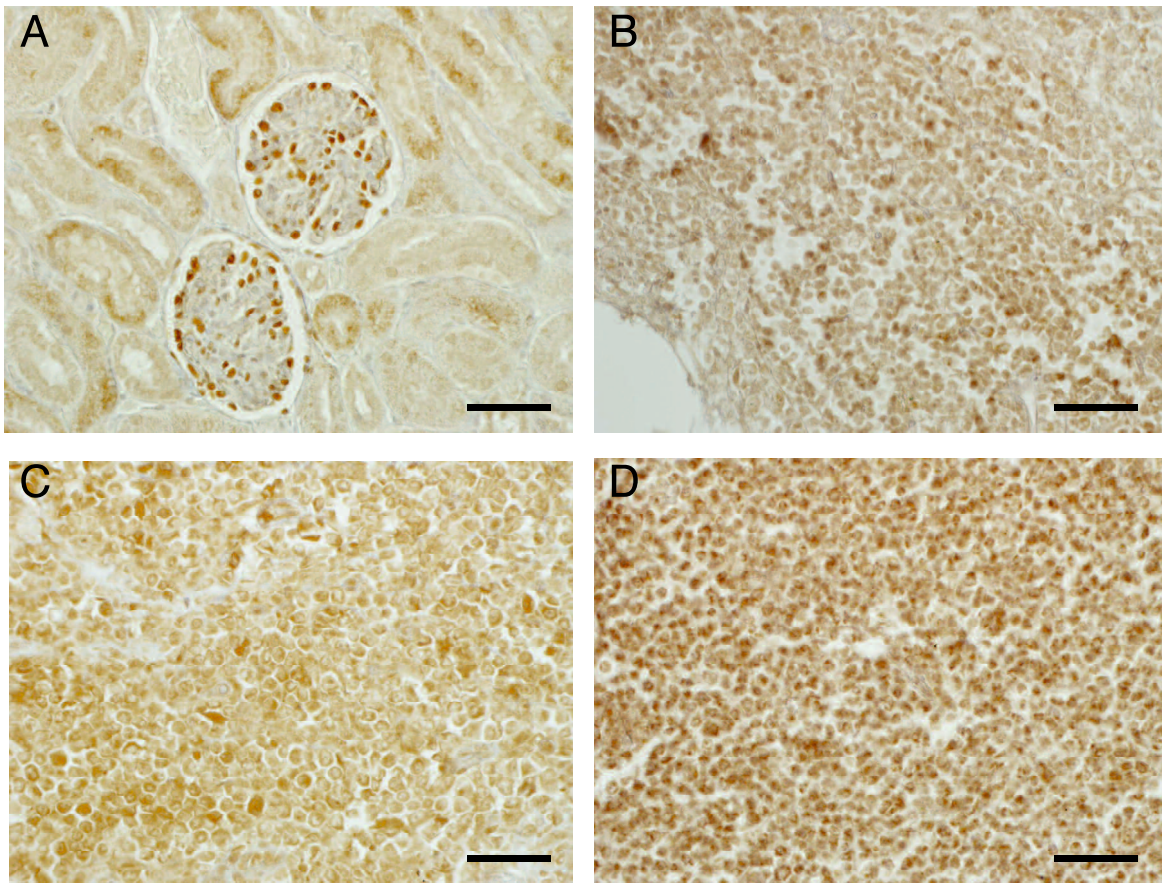

Fig. I-4. Representative results of cWT1 immunohistochemical staining and counterstaining with hematoxylin in normal canine tissue specimens and lymphoma tissue specimens.

(A) Normal kidney, (B) normal lymph node, (C) high grade T cell lymphoma from the intraperitoneal lymph node and (D) high grade B cell lymphoma from the spleen were stained with 6F-H2. Scale bar indicates 50 μm.

Table I-1. Results of the immunohistochemical staining of normal canine tissues

Tissue	n	WT1 expression	Stained cells
Heart	2	−	
Spleen	2	−	
Kidney	3	+	Podocytes
Testis	2	+	Seminiferous tubules epithelium
Prostate gland	2	−	
Skeletal muscle	2	−	
Skin	1	−	
Lymph node	12	+	Lymphocytes

n, number of samples; +, positive staining; −, negative staining

Table II-2. Results of the immunohistochemical staining of lymphoma tissues

Immunophenotype	Grade	Anatomic site			
		Multicentric	Alimentary	Mediastrial	Extranodular
B cell	High	1	4	1	0
	Low	1	1	0	2
T cell	High	3	3	0	0
	Low	5	1	0	0

Chapter 2

Establishment of chimeric antigen receptor (CAR)-specific monoclonal antibody to detect canine CD20-CAR-T cells

SUMMARY

Adoptive cell therapy with chimeric antigen receptor (CAR) T cells is an effective novel treatment for hematopoietic malignancies. CAR-T cell therapy targeting CD20, the target of B cell malignancy, can be a novel adoptive cell therapy for canine patients with B cell malignancy. During the CAR-T therapy, monitoring of circulating CAR-T cells is crucial, because *in vivo* persistence of CAR-T cells correlates with clinical efficacy. This study establishes and evaluates a novel monoclonal antibody against canine CD20-CAR. The antibody was produced by immunization of mice with canine CD20-CAR-expressing cells. Hybridoma cells producing antibody against single-chain variable fragment (scFv) of canine CD20-CAR fragment were selected, and the clone 1F6-11D-1F was established. FACS analysis confirmed that 1F6-11D-1F reacts with canine CD20-CAR-expressing cells. Furthermore, 1F6-11D-1F also detected its reactivity against therapeutic anti-canine CD20 antibody. 1F6-11D-1F is a potential new antibody which provides good tool in both canine CD20-CAR-T cell therapy and anti-canine CD20 antibody therapy for canine lymphoma.

INTRODUCTION

Canine B cell lymphoma is the most common hematopoietic neoplasms in veterinary medicine, and considered as a relevant model for human non-Hodgkin lymphoma (Zandvliet, M., 2016, Ito, D. *et al*., 2014). Many cases show a good response to standard multi-drug chemotherapy, however, the onset of relapsed or refractory disease impedes the long-term control of the disease. Drug resistance is also very common, and makes treatment even more difficult. Therefore, further development of treatment options is needed.

The novel cancer immunotherapy targeting CD19 and CD20, including chimeric antigen receptor (CAR) T cell therapy and monoclonal antibody therapy, has been developed, and proved to be effective for human B cell hematologic malignancies (Chavez, JC. and Locke, FL., 2018, Salles, G. *et al*., 2017). As with human medicine, these novel immunotherapies have been developed in veterinary medicine. There are a few studies on canine CAR-T cell therapy (Mata, M. *et al*., 2014, Smith, JB. *et al*., 2015, Mata, M. and Gottschalk, S., 2016, Panjwani, MK. *et al*., 2016, Yin, Y. *et al*., 2018). For establishing the CAR-T therapy for canine lymphoma, we developed the

strategy preparing canine CD20-CAR-T cells in chapter 4 and 5. It has been suggested that there were many factors influencing the clinical efficacy in CAR-T cell therapy. They were not fully elucidated, however, *in vivo* expansion and persistence of CAR-T cells are considered critical predictive factors of clinical responses (Guedan, S. *et al*., 2018, Rafiq, S. *et al*., 2020). Thus, investigators measure the persistence of adoptively infused T cells to assess the therapeutic potential of CAR-T cells. The main objective of this study is to establish the monoclonal antibody which can detect cell surface expression of CAR.

On the other hands, human studies have shown the effectiveness of anti-CD20 monoclonal antibody therapy against B cell malignancies (Salles, G. *et al*., 2017). Antibody therapy targeting canine CD20 have also been developed and reported. These studies have established the novel anti-canine CD20 monoclonal antibodies, and shown antitumor efficacy *in vitro* (Ito, D. *et al*., 2015, Jain, S. *et al*., 2016). However, the clinical efficacy of these antibodies in patient dogs remain unknown. Our laboratory recently developed the novel anti-canine CD20 antibody showing high *in vitro* antitumor activity, and clinical trials for dogs with B cell lymphoma are under

preparation. In this therapy, pharmacokinetic studies are considered to be essential to determine individual variability and for understanding of relationships between antibody concentration and clinical efficacy.

This study established the new antibody which can detect scFv region of CD20-CAR fragment. We demonstrated that this antibody can be used for detection for CD20-CAR-expressing cells. Moreover, the ELISA assay using established antibody for detection therapeutic anti-canine CD20 antibody was developed.

MATERIALS AND METHODS

Cells

Canine T cell lymphoma cell line, CLC, and murine myeloma cell line, P3U1, were cultured in R10 complete medium (RPMI1640 supplemented with 10% FBS, 100 units/ml penicillin, 100 μg/ml streptomycin, and 55 μM 2-mercaptoethanol). Retroviral packaging cell lines, PG-13 and Plat-E, and murine fibroblast cell line, NIH-3T3, were cultured in D10 complete medium (Dulbecco's modified Eagle's medium supplemented with high glucose, 10% fetal bovine serum (FBS), 100 units/ml penicillin, 100 μg/ml streptomycin, and 55 μM 2-mercaptoethanol). Peripheral blood mononuclear cells (PBMCs) were isolated from a healthy dog and maintained in R10 complete medium. All cells were cultured in a humidified incubator at 37 °C and 5% CO_2.

Cells expressing CD20-CAR

Cell lines stably expressing chimeric antigen receptor (CAR) were established via retrovirus transduction, as described in chapter 4. A third-generation CAR construct was designed and used in this study (Fig. II-1A). The CAR construct was comprised of

the scFv of anti-CD20 antibody, 4E1-7 (Mizuno, T. *et al*., 2020) linked to the canine CD8α hinge and transmembrane domain, followed by the canine CD28 and 4-1BB co-stimulatory domain, and human CD3ζ signaling domain. For the co-expression of CARs together with fluorescent protein, the CAR construct was followed by a P2A peptide fused to Venus fragments. This CAR-P2A-Venus construct was ligated into the MSGV Hu Acceptor PGK-NGFR (Addgene Cambridge, Massachusetts). Retrovirus particles were collected from PG-13 producer cell line, and used to transduce the CLC cells (CLC/CAR). After viral transduction, CD20-CAR-expressing cells were sorted by Venus expression.

To obtain the NIH-3T3 cells expressing CD20-CAR used for immunization, the CAR-P2A-Venus construct was ligated into pMx-IP retroviral vector. Retrovirus particles were generated by transient transfection of Plat-E cells with the CD20-CAR-encoding retrovirus vector. Supernatants containing the retrovirus were collected after 48 hours, and used to transduce the NIH-3T3 cells (NIH-3T3/CAR). The cells were cultured in the presence of puromycin (1 μg/ml) to select the stably transduced cells.

Canine CD20-CAR-T cells were obtained as follows. PBMCs were isolated

using Lymphoprep (Axis-Shield, Oslo, Norway) gradient centrifugation and then stimulated in the presence of 200 U/ml of recombinant human IL-2 (Proleukin; Novartis, Basel, Switzerland) and 5 μg/ml of phytohemagglutinin (PHA) for 72 hours. Retroviral transduction was performed after initial stimulation using recombinant human fibronectin fragment (RetroNectin; TaKaRa Bio, Shiga, Japan). Non-treated 24-well culture plates were coated with 0.5 ml of RetroNectin solution (10 μg/ml) diluted with phosphate-buffered saline (PBS) for 2 hours at room temperature in accordance with the manufacturer's instructions. After removal of the RetroNectin solution, plates were washed with PBS. Then, 0.5 ml of retrovirus-containing supernatants, collected from PG-13 packaging cells, were added to the RetroNectin-coated plate, and preparation of a virus-bound plate was performed using centrifugation methods (2000 × g for 2 hours at 4 °C). A total of 2.5×10^5 stimulated T cells was added to the virus-bound plates and incubated in a 37 °C, 5% CO_2 incubator for 24 hours, followed by the second virus infection in the same manner. To promote contact between T cells and viral particles, plates were centrifuged at 500 × g for 1 min after second infection. After retroviral transduction, CD20-CAR-T cells were subsequently expanded with 200 U/ml

IL-2, and used following experiments.

Production of a mouse monoclonal antibody

All animal studies were carried out in accordance with the Yamaguchi University Animal Care and Use Committee Regulations. A panel of antibodies against CD20-CAR was obtained by immunization with NIH-3T3/CAR cells, as previously described (Umeki, S. *et al*., 2011). In brief, 1×10^7 NIH-3T3/CAR cells in 500 μl of PBS were emulsified with an equal amount of Titer Max Gold (CytRx, California, US), and 50 μl of emulsified products were injected intracutaneously into the hind footpads of 6-week-old BALB/cCrSlc mice (SLC Japan, Shizuoka, Japan). Second immunization was performed without adjuvant ten days after first immunization. Two days after second injection, cells were collected from popliteal lymph nodes and fused with P3U1 myeloma cells. Hybridoma cells that produced antibodies positive for CD20-CAR and anti-canine CD20 antibody, 4E1-7, were identified by cell enzyme-linked immunosorbent assay and flow cytometry, and the resulting hybridoma cells were cloned by limiting dilution. After replacement of the culture media by serum-free

media, the monoclonal antibody was purified using Protein G Sepharose 4 Fast Flow (GE Healthcare Japan, Tokyo, Japan). Immunoglobulin isotyping of purified antibody was conducted using Mouse Immunoglobulin Isotyping kit (Antagen Biosciences, Inc., MA, USA), according to manufacturer's instructions.

Flow cytometry

Cells were collected and washed with PBS, followed by incubation with Fixable Viability Dye eFluor 780 (eBioscience, Inc. Vienna, Austria) for 30 min on ice. Then, cells were resuspended in FACS buffer (PBS containing 2% FBS and 0.1% NaN_3). A total of 2×10^5 cells was stained with each antibody for 30 min on ice. After incubation, cells were washed and fixed in 1% paraformaldehyde and stored until analysis.

Cell surface expression of CD20-CAR was stained with commercially available anti-rat IgG secondary antibodies; goat anti-rat IgG-PE (sc-3740; dilution 1:100; Santa Cruz Biotechnology, Inc., TX, USA), rabbit F(ab')2 anti-rat IgG-RPE (STAR20A; dilution 1:10; Serotec, Oxford, UK), goat anti-rat IgG(H+L)-PE (3050;

dilution 1:250; Southern Biotech, AL, USA), goat anti-rat IgG-Biotin (sc-2041; dilution 1:1000; Santa Cruz Biotechnology, Inc), or DyLight 649 goat anti-rat IgG (405411; dilution 1:500; BioLegend, CA, USA). Incubation with biotin-conjugated antibody was followed by incubation with streptavidin-PE (dilution 1:1000, eBioscience, Inc., Vienna, Austria), or the developed antibody in this study, followed by incubation with DyLight 649-labeled anti-mouse IgG antibody (dilution 1:200, BioLegend, CA, USA).

Samples were analyzed using an Accuri C6 (BD Biosciences, CA, USA), and results were analyzed using FlowJo software (BD Biosciences).

ELISA

Ninety-six-well plates (Maxisorp; Nunc, Roskilde, Denmark) were coated with anti-CD20 antibody (4E1-7-B) for screening or the developed antibody for ELISA confirmation diluted in immobilization buffer (100 μl/well, 0.05 M sodium carbonate solution, pH 9.6) and incubated for 15-18 hours at 4 °C. After incubation, the wells were washed three times with washing buffer (0.05% Tween 20 in PBS), and the nonspecific binding in the wells were blocked with blocking buffer (200 μl/well, 3%

BSA in PBS) for 1 h at 37 °C. After additional washing step, 100 µl of hybridoma supernatant for screening or 4E1-7-B antibody solution for ELISA confirmation, diluted in 1% BSA in PBS, was added to each well, and the plates were incubated for 1 h at 37 °C. After the plates were washed five times, 100 µl of detection antibody solution was added to each well, and then the plates were incubated for 1 h at 37 °C. Either of detection antibody was used; goat anti-mouse IgG (H/L) (Bio-Rad Laboratories, Inc. Hercules, CA, USA) for screening or mouse anti-canine Ig mix secondary antibody (Thermo Fisher Scientific, Tokyo, Japan), labeled with HRP using Peroxidase Labeling Kit-NH_2 (Dojindo, Kumamoto, Japan) for ELISA confirmation. After another washing step, 100 µl of KPL ABTS Peroxidase Substrate Solution (SeraCare, MA, USA) was added to each well, and plates were incubated to react for 10 min at 37 °C in the dark. The absorbance was measured at 405 nm with a microplate reader. All measurements were performed in triplicate.

RESULTS AND DISCUSSION

The main purpose of this study is to establish a method for detection of surface expression of CD20-CAR. First of all, we examined if the commercially available anti-rat IgG secondary antibody could detect CD20-CAR, using CAR-expressing cell line, CLC/CD20-CAR (Fig. II-1B). Since scFv region of CD20-CAR construct derived from rat monoclonal antibody, five kinds of anti-rat IgG secondary antibodies were used to detect the cell surface expression of CD20-CAR. However, as shown in Figure II-1B, all these anti-rat IgG antibodies could not detect CD20-CAR. Therefore, we decided to develop the monoclonal antibody against CD20-CAR.

To establish the monoclonal antibody against CD20-CAR, we immunized mice with CD20-CAR-expressing NIH-3T3 cells (Fig. II-1C). Hybridoma cells that produced antibodies against scFv-CD20 were selected by reactivity with anti-canine CD20 antibody by ELISA and flow cytometry (data not shown). And after hybridoma selection and cloning, a single hybridoma clone (1F6-11D-1F) was established. The subclass of 1F6-11D-1F was determined to be mouse IgG2b kappa by Mouse Immunoglobulin Isotyping kit. Non-transduced PBMCs and CAR-T cells were stained

with 1F6-11D-1F, and it was confirmed that 1F6-11D-1F detected only CAR-T cells, whereas 1F6-11D-1F did not detect PBMCs (Fig. II-1D). Among the technical approaches to assessing survival of infused CAR-T cells, the most common method is quantitative PCR using CAR-specific primers (Morgan, RA. *et al*., 2006, Kochenderfer, JN. *et al*., 2010). However, flow cytometric analysis using CAR-specific antibody is favorable because it allows additional evaluation such as multi-parameter analysis and cell sorting (Jena, B. *et al*., 2013). Our results indicate that 1F6-11D-1F can be useful tool to detect the infused CD20-CAR-T cells from blood sample of the infused animals.

1F6-11D-1F was raised against scFV-CD20, next, 1F6-11D-1F was assessed to determine whether it could be used to detect chimeric anti-canine CD20 therapeutic antibody by ELISA (Fig. II-2A). As shown in Figure II-2B, this ELISA assay could detect chimeric anti-canine CD20 antibody. This result indicates that 1F6-11D-1F can be used for measurement of blood concentration of therapeutic antibody during anti-CD20 antibody therapy. Pharmacokinetic study in antibody therapy is essential to determine the basis of individual variability. The pharmacokinetic studies of rituximab have revealed that there exists wide inter-individual variability, and high serum drug

concentrations appear to correlate with good clinical response (Berinstein, NL. *et al*., 1998, Jäger, U. *et al*., 2012). While rituximab serum levels in lymphoma patients were well validated, there are no information about pharmacokinetics of therapeutic anti-canine CD20 antibody. Therefore, using the antibody developed in this study, further investigation is needed to optimize the detection range of circulating therapeutic antibody.

In summary, we established a novel monoclonal antibody against scFv region of anti-canine CD20 antibody, 4E1-7, and demonstrated that this antibody can detect CD20-CAR-expressing cells in flow cytometry. This antibody has also potential to be applied for detecting therapeutic anti-canine CD20 antibody. This study will be helpful for further investigation of canine CAR-T cell therapy and antibody therapy.

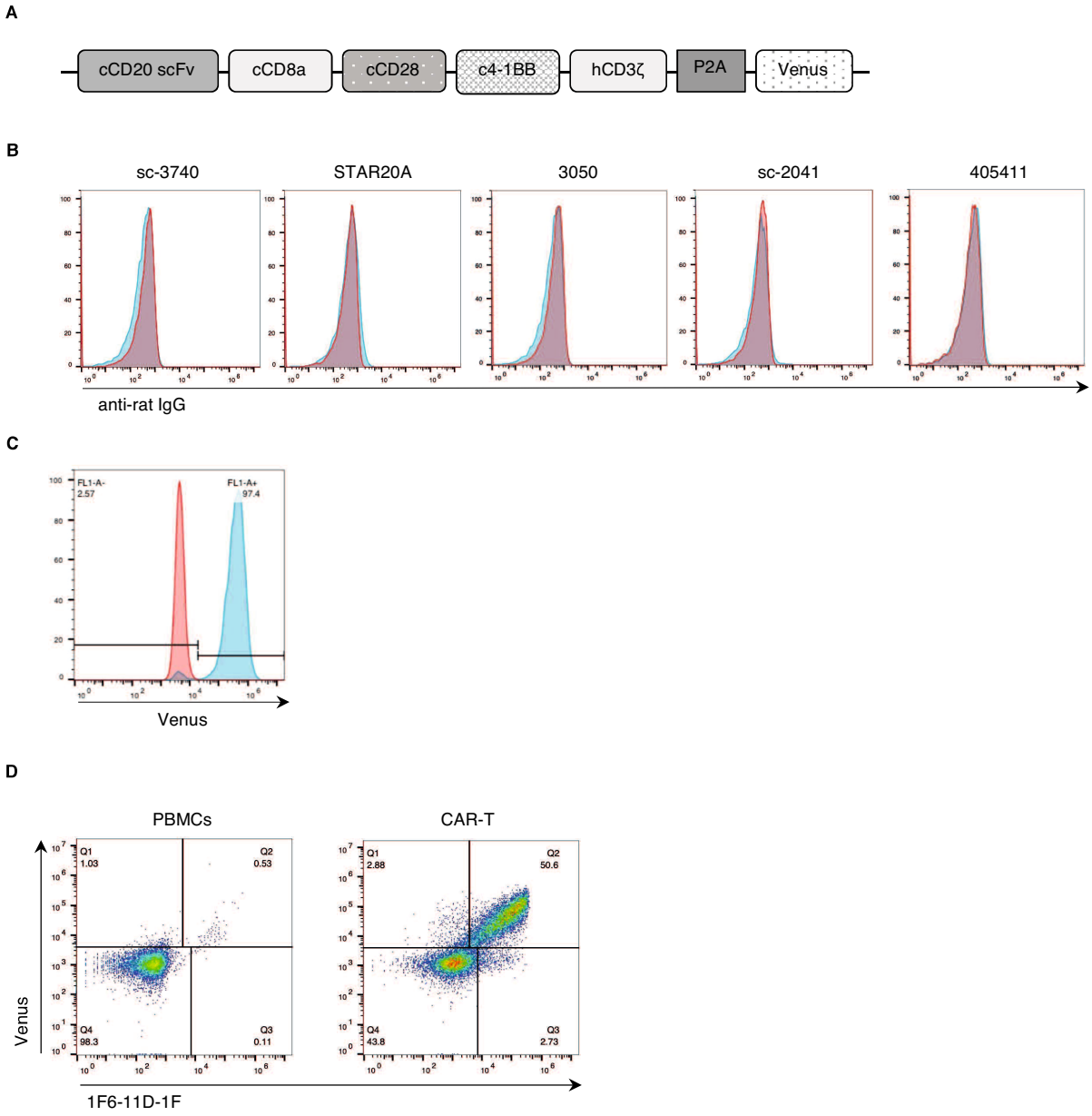

Fig. II-1. Generation of anti-CD20-CAR monoclonal antibody.

(A) Schematic diagram of the canine CD20-CAR-expressing construct. (B) Reactivity of commercially available anti-rat IgG secondary antibodies against CLC/CAR. CLC cells were retrovirally transduced with the CD20-CAR-expressing vector (CLC/CAR).

Wild-type CLC (CLC/WT, red) and CLC/CAR (blue) cells were stained with the following anti-rat IgG antibodies: goat anti-rat IgG-PE (sc-3740), rabbit F(ab')2 anti-rat IgG-RPE (STAR20A), goat anti-rat IgG(H+L)-PE (3050), goat anti-rat IgG-Biotin (sc-2041), or DyLight 649 goat anti-rat IgG (405411). Staining with sc-2041 was followed by incubation with streptavidin-PE. (C) Establishment of CD20-CAR-expressing murine cells. NIH-3T3 cells were retrovirally transduced with the CAR-expressing vector (NIH-3T3/CAR). Wild-type NIH-3T3 (NIH-3T3/WT, red) and NIH-3T3/CAR (blue) cells were assessed by Venus expression. (D) CD20-CAR detection using the established antibody. PBMCs (isolated from a healthy beagle, and stimulated by IL-2 and phytohemagglutinin) and CD20-CAR-T cells were stained with the established anti-CD20-CAR antibody (1F6-11D-1F). The dot plot shows Venus expression versus 1F6-11D-1F staining.

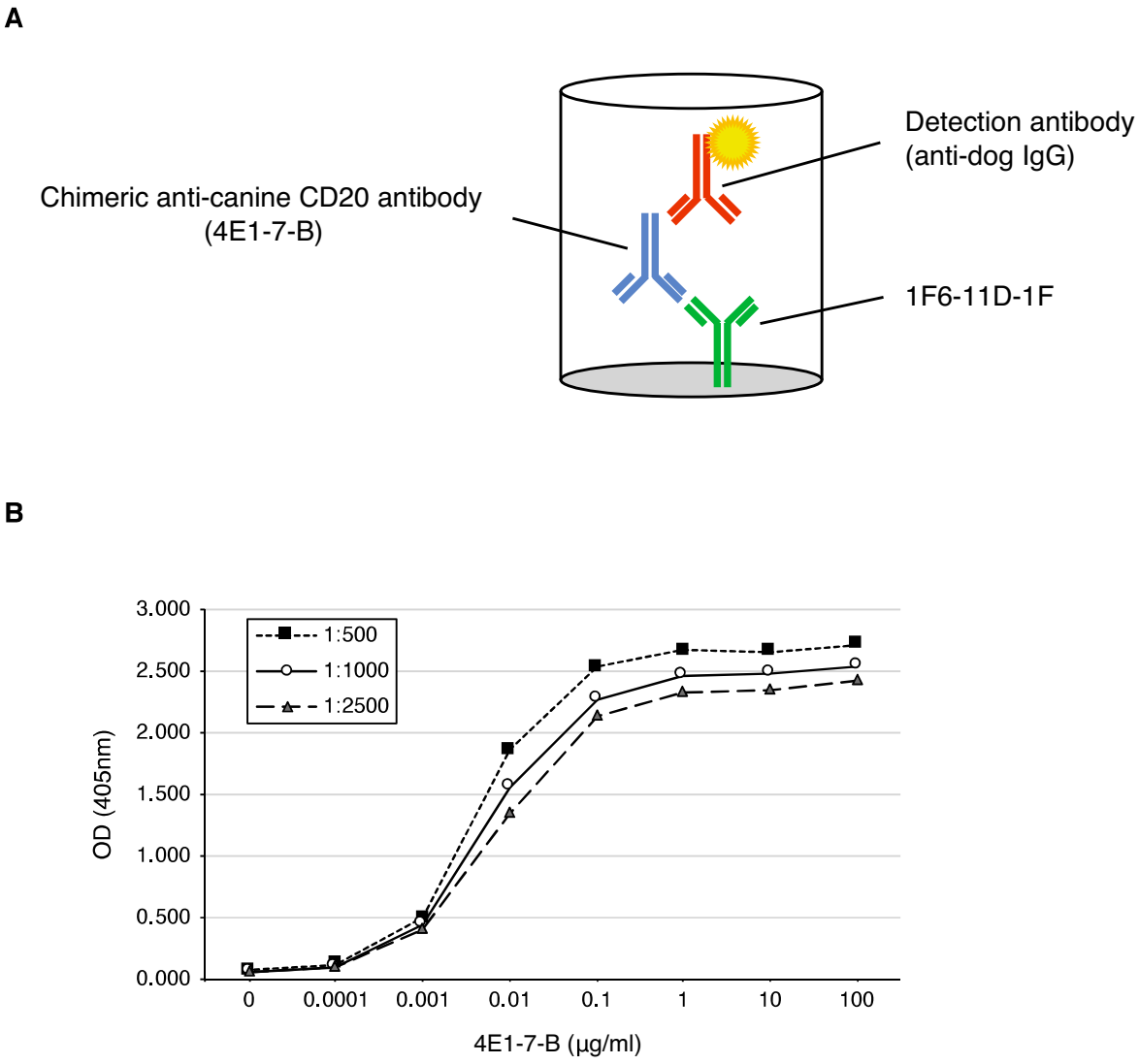

Fig. II-2. ELISA for the measurement of chimeric anti-canine CD20 antibody.

(A) Schematic diagram of ELISA. ELISA was conducted by coating the wells with 1F6-11D-1F, and the serially diluted chimeric anti-canine CD20 antibody was added and detected by HRP-labelled anti-dog IgG. (B) Plates were coated with 1F6-11D-1F (1 μg/ml), followed by incubation with serially diluted chimeric anti-canine CD20 antibody (4E1-7-B). Antibody binding was detected by HRP-conjugated anti-dog IgG

antibody (dilution 1:500, 1:1000, and 1:2500). Substrate solution was added and absorbance at 405 nm was measured.

Chapter 3

Establishment and characterization of monoclonal antibody

against canine CD8 alpha

SUMMARY

Understanding of the microenvironment of cancer plays a crucial role in cancer research. A tool is needed to evaluate the immune cells surrounding the cancer cells. This study establishes and evaluates a novel monoclonal antibody against canine CD8α. The antibody was produced by immunization of rats with canine CD8α-expressing cells. After establishment and selection of hybridoma cells, the clone F3-B2 was established. The reactivity of F3-B2 was confirmed using canine CD8α-overexpressing murine cells. Flow cytometric analysis also demonstrated that F3-B2 reacts with canine CD8α naturally expressed in canine peripheral blood mononuclear cells and a canine T-cell lymphoma cell line. The specimens of lymphoid tissue showed immunohistochemical staining for F3-B2. Moreover, we also found that F3-B2 exhibited reactivity against feline CD8. Thus, this antibody provides a good research tool to analyze CD8-positive cytotoxic lymphocytes in canine and feline tumors.

INTRODUCTION

Cancer is one of the main causes of death in older dogs. Some of the naturally occurring canine cancers have also received attention as an ideal model for human cancer. For instance, soft tissue sarcomas in dogs and humans have shown to share similar genetic complexity (Aguirre-Hernández, J. *et al*., 2009). In addition, dogs with osteosarcoma show similar biological behavior and response to treatment to humans (Withrow, SJ. and Wilkins, RM., 2010). Canine lymphoma also shares many characteristics, such as incidence, biological behavior, and genetic aberrations, with human lymphoma (Hansen, K. and Khanna, C., 2004). The value of dogs as a lymphoma model is also supported by previous study, in which dogs with spontaneous B cell non-Hodgkin lymphoma were enrolled in a clinical trial of Bruton tyrosine kinase (Btk) inhibitor (Honigberg, LA. *et al*., 2010). The evaluation of cancer immunotherapy in dogs offers particular advantages in some kind of tumor, because immunocompetent dogs have an immunosuppressive cancer microenvironment that enables evaluation of the interaction between cancer and immune cells. Several studies have demonstrated that, as with human cancers, the immunosuppressive cancer microenvironment, such as

regulatory T cells, tumor-associated macrophages, and myeloid-derived suppressor cells, exists and correlates with poor prognosis in canine patients with B cell lymphoma and mammary tumor (Mitchell, L. *et al*., 2012, Raposo, T. *et al*., 2014, Mucha, J. *et al*., 2014). Therefore, tools for evaluating canine immune cells are important. Several antibodies have been reported, however, antibodies which can detect canine CD8 via immunohistochemistry using formalin-fixed and paraffin-embedded (FFPE) samples are limited (Moore, PF. *et al*., 1992, Trompieri-Silveira, AC. *et al*., 2009, Partridge, BR. *et al*., 2020, Fisher, DJ. *et al*., 1995, Caniatti, M. *et al*., 1996). This study established a novel monoclonal antibody against canine CD8α (cCD8α), evaluated by flow cytometry and immunohistochemistry.

MATERIALS AND METHODS

Cells

Rat kidney cell line, NRK, murine fibroblast cell line, NIH-3T3, retroviral packaging cell lines, PLAT-GP and PLAT-E, and feline T cell lymphoma cell line, 3201, were cultured in D10 complete medium (Dulbecco's modified Eagle's medium supplemented with high glucose, 10% fetal bovine serum (FBS), 100 units/ml penicillin, 100 μg/ml streptomycin, and 55 μM 2-mercaptoethanol). Canine T cell lymphoma cell line, UL-1, was cultured in R10 complete medium (RPMI1640 supplemented with 10% FBS, 100 units/ml penicillin, 100 μg/ml streptomycin, and 55 μM 2-mercaptoethanol). Peripheral blood mononuclear cells (PBMCs) were isolated from a healthy dog and were stimulated by interleukin (IL)-2 and phytohemagglutinin.

NRK cells stably expressing chimeric antigen receptor (CAR) were established via retrovirus transduction, as previously described (Mizuno, T. *et al*., 2009, Nemoto, Y. *et al*., 2018). A third-generation CAR construct was used in this study. The CAR construct was comprised of the anti-CD20 scFv (Mizuno, T. *et al*., 2020) linked to the canine CD8α hinge and transmembrane domain, followed by the canine CD28 and

4-1BB co-stimulatory domain, and human CD3ζ signaling domain. For the co-expression of CARs together with fluorescent protein, the CAR construct was followed by a P2A peptide fused to Venus fragments. This CAR-P2A-Venus construct was ligated into pMx-IP retroviral vector. Retrovirus particles were generated by transient transfection of Plat-GP cells with the CAR-encoding retrovirus vector. Supernatants containing the retrovirus were collected after 48 hours, and used to transduce the NRK cells (NRK/CAR).

To obtain the cell line expressing the full length-cCD8α, the cCD8α gene was subcloned into a pMx-IP retroviral vector containing a puromycin resistance gene. Retrovirus particles were generated by transient transfection of PLAT-E cells with the cCD8α-encoding pMx-IP vector, and NIH-3T3 cells were transduced with supernatants containing cCD8α-expressing retrovirus, followed by puromycin selection (NIH-3T3/cCD8α). In parallel, NIH-3T3 cells were transduced with a retrovirus encoding the empty vector, as a control (NIH-3T3/emp).

CD8 knockout 3201 cells were generated using the CRISPR-Cas9 technology. Guide sequences targeting feline CD8 (5'-CACCGGTTCCGCTTATCGCCCGTGA-3'

and 5'-AAACTCACGGGCGATAAGCGGAACC-3') were cloned into a lentiCRISPRv2 plasmid (gift from Feng Zhang [Addgene Cambridge, MA, USA, plasmid #52961; http://n2t.net/addgene:52961; RRID:Addgene_52961]). CRISPR plasmid was co-transfected with packaging plasmids, p8.9QV and pCVSVG, into HEK293T cells. After transfection to HEK293T cells, supernatants including CRISPR lentivirus particles were harvested, and 3201 cells were infected with the concentrated viral supernatant, and cultured in the presence of puromycin (1 μg/ml) to select the stably transduced cells.

All cells were cultured in a humidified incubator at 37 °C and 5% CO_2.

Production of a rat monoclonal antibody

All animal studies were carried out in accordance with the Yamaguchi University Animal Care and Use Committee Regulations. A panel of antibodies against cCD8α was obtained by immunization with NRK/CAR cells, as previously described (Umeki, S. *et al*., 2011). In brief, 1×10^7 NRK/CAR cells in 500 μl of phosphate-buffered saline (PBS) were emulsified with an equal amount of Titer Max Gold (CytRx,

California, US), and injected intracutaneously into the hind footpads of 6-week-old Sprague-Dawley rats (SLC Japan, Shizuoka, Japan). Eight weeks after injection, cells were collected from popliteal lymph nodes and fused with P3U1 myeloma cells. Hybridoma cells that produced antibodies positive for cCD8α were identified by cell enzyme-linked immunosorbent assay and flow cytometry, and the resulting hybridoma cells were cloned by limiting dilution. After replacement of the culture media by serum-free media, the monoclonal antibody was purified using Protein G Sepharose 4 Fast Flow (GE Healthcare Japan, Tokyo, Japan).

Flow cytometry

Cells were collected and resuspended in FACS buffer (PBS containing 2% FBS and 0.1% NaN_3). A total of 2×10^5 cells was stained with each antibody for 30 min on ice. Cell surface expression of CD8α was detected by incubation with the established antibody, followed by incubation with DyLight 649-labeled anti-rat IgG antibody (BioLegend, San Diego, CA, USA). In addition to the established antibody, the following antibodies were used: rat anti-dog CD8α APC (clone YCATE55.9;

eBioscience, Inc. Vienna, Austria), rat anti-dog CD8α FITC (clone YCATE55.9; Bio-Rad Laboratories, Inc. Hercules, CA, USA), and corresponding isotype control antibodies. For isotyping analysis of established antibody, cCD8α-expressing cells were stained with established antibody, followed by biotin-labeled anti-rat Ig antibodies specific to each subclass (BioLegend), and detected using Dylight 649-labeled streptavidin (BioLegend). Samples were analyzed using an Accuri C6 (BD Biosciences, San Diego, CA, USA), and results were analyzed using FlowJo software (BD Biosciences).

Immunohistochemistry

FFPE sections from healthy dogs and cats were used for immunohistochemical staining, as described in our previous report (Shosu, K. *et al*., 2016). After dewaxing, antigen retrieval proceeded in citrate buffer (pH 6.0) at 125 °C for 30 s. In the case of feline sections, antigen retrieval was performed in citrate buffer (pH 9.0) at 125 °C for 10 min. Then the sections were washed in distilled water and rinsed with PBS. Endogenous peroxidase activity was blocked with 3% hydrogen

peroxide in methanol for 30 min at room temperature (RT). The sections were washed with distilled water, then rinsed with PBS. To block nonspecific protein activity, the sections were incubated for 30 min at RT with 5% skimmed milk and 5% bovine serum albumin (BSA) in PBS. After blocking nonspecific protein activity, the sections were rinsed with PBS, followed by incubation with primary antibody overnight at 4 °C. All primary antibodies were diluted with 2% BSA in PBS. Rat anti-human CD3 antibody (clone CD3-12: Serotec, Oxford, UK), rabbit anti-human Granzyme B (Spring Bioscience Corp, Pleasanton, CA), established antibody, and corresponding isotype control antibodies were used as primary antibody. Anti-human CD3 and anti-human Granzyme B antibodies were confirmed to cross-react with canine tissues in previous reports (Sisó, S. *et al*., 2017, Moore, PF. *et al*., 2013). The antibody-treated sections were rinsed with PBS, followed by treatment with horseradish peroxidase (HRP)-conjugated secondary antibodies (goat anti-rat IgG antibody for CD3 and established antibody; goat anti-rabbit IgG antibody for Granzyme B; Histofine Simple Stain MAX PO: Nichirei Corporation, Tokyo, Japan) for 30 min at RT. The sections were rinsed with PBS, and color was developed with the peroxidase stain 3’,3’-diaminobenzidine

(DAB Kit & Enhancer; Nacalai Tesque, Kyoto, Japan) for 5 min at RT. After the sections were washed in distilled water, they were counterstained for 5 min with Mayer's hematoxylin solution (Merck KGaA, Darmstadt, Germany), washed in distilled water, dehydrated in graded baths of ethanol, cleared in xylene, and mounted with a xylene-based mounting solution (Matsunami, Osaka, Japan).

RESULTS AND DISCUSSION

To establish the monoclonal antibody against canine CD8α, we immunized rats with cCD8α-expressing NRK cells. In our laboratory, in order to develop a novel cancer therapy for canine cancer, an immune cell therapy using CAR-expressing T (CAR-T) cells was previously developed (Sakai, O. *et al*., 2020). CAR-T cells were developed by transducing the CAR construct in order to have the antibody single-chain variable fragment (scFv) and canine CD8α as extracellular domains (Fig. III-1A), and this CD8α was considered useful for immunization to induce antibodies against CD8α. CAR-expressing cells were used for immunization of rats, because the original purpose of the study was to establish an antibody that could detect CAR. Since the CAR construct used has scFv and CD8α as an extracellular domain, there was a possibility that antibodies against these two molecules were produced. Therefore, in this study, we focused on the antibody against cCD8α. And after hybridoma selection and cloning, a single hybridoma clone (F3-B2) was established.

First, the NIH-3T3/emp and NIH-3T3/cCD8α cells were stained with F3-B2 and isotype control antibodies, and it was confirmed that F3-B2 detected only cCD8α-

expressing NIH-3T3 cells, whereas F3-B2 did not detect NIH-3T3/emp (Fig. III-1B). Next, antibody isotyping of F3-B2 was performed using flow cytometry, and the subclass of F3-B2 was determined to be IgG2a lambda (Fig. III-1C). To determine whether this antibody can detect endogenous CD8α expressed on canine cells, PBMCs and the canine T-cell lymphoma cell line UL-1 were stained with F3-B2 antibody. As shown in Figure III-1D, F3-B2 reacted with both PBMCs and UL-1 cells (bottom panels). Also, F3-B2 and the commercially available anti-cCD8α antibody (CD8α-APC) had almost the same reactivity (top panels). Double staining analysis by flow cytometry revealed that cells of the same population of canine PBMCs were stained positively with both F3-B2 and commercially available anti-cCD8α antibody (CD8α-FITC) (Fig. III-1E). These results indicate that the established monoclonal antibody, clone F3-B2, recognizes canine CD8α. In addition, F3-B2 showed almost the same reactivity as commercially available anti-canine CD8α antibody (Fig. III-1E). However, the double staining analysis showed that there was a cell population that became stained with both antibodies (Fig. III-1E). This result indicated that the epitopes of these antibodies did not overlap.

Next, F3-B2 was assessed to determine whether it could be used for immunohistochemistry. The results of the immunohistochemical staining are shown in Figure III-2. All lymphoid tissue specimens were positively stained by F3-B2 antibody. Many F3-B2-positive cells were detected in the lymph node and thymus, while only a few cells were positively stained in the spleen. The specimens were also positively stained for CD3 and Granzyme B. In lymph node specimens, staining patterns were similar, and mainly cells in the paracortical area were positive for CD3, Granzyme B, and CD8α (Fig. III-2A). From these results, F3-B2 was also shown to be adaptable for immunohistochemistry using paraffin-embedded tissues.

Finally, F3-B2 was also evaluated whether this antibody can detect feline CD8. As shown in Figure III-3A, lymph node tissue from healthy cats showed positive staining for F3-B2. Feline CD8 knockout 3201 cells (3201/fCD8ko) were established to confirm that F3-B2 specifically recognize feline CD8. FACS analysis revealed that F3-B2 can react with wild-type 3201 cells, whereas F3-B2 cannot react with 3201/fCD8ko cells (Fig. III-3B). These results suggest that F3-B2 can be used to detect feline CD8 in both immunohistochemical staining and flow cytometry.

In this study, we established a novel antibody against canine CD8α, and demonstrated that this antibody can be used in not only flow cytometry but also immunohistochemistry using FFPE sections. CD8 is the main marker of cytotoxic T lymphocytes, which play an important role in cancer regression. In addition, the significance of tumor-infiltrating lymphocytes as a prognostic factor has been reported in canine tumors (Porcellato, I. *et al*., 2020, Franzoni, MS. *et al*., 2019). Franzoni MS *et al*. evaluated tumor-infiltrated $CD8^+$ T lymphocytes in canine mammary-gland tumors using immunohistochemistry (Raposo, T. *et al*., 2014). However, they used freshly frozen samples because anti-CD8 antibodies that can be used in canine FFPE samples are limited. Antibody detectable in FFPE samples enables further analysis from archive samples.

In conclusion, we established the antibody against canine CD8α, and confirmed that this antibody can be used in immunohistochemistry using FFPE samples. The novel anti-canine CD8α antibody of the present study, clone F3-B2, enables a more precise evaluation of canine $CD8^+$ cells, providing a new method for determining the immune responses in dogs and cats.

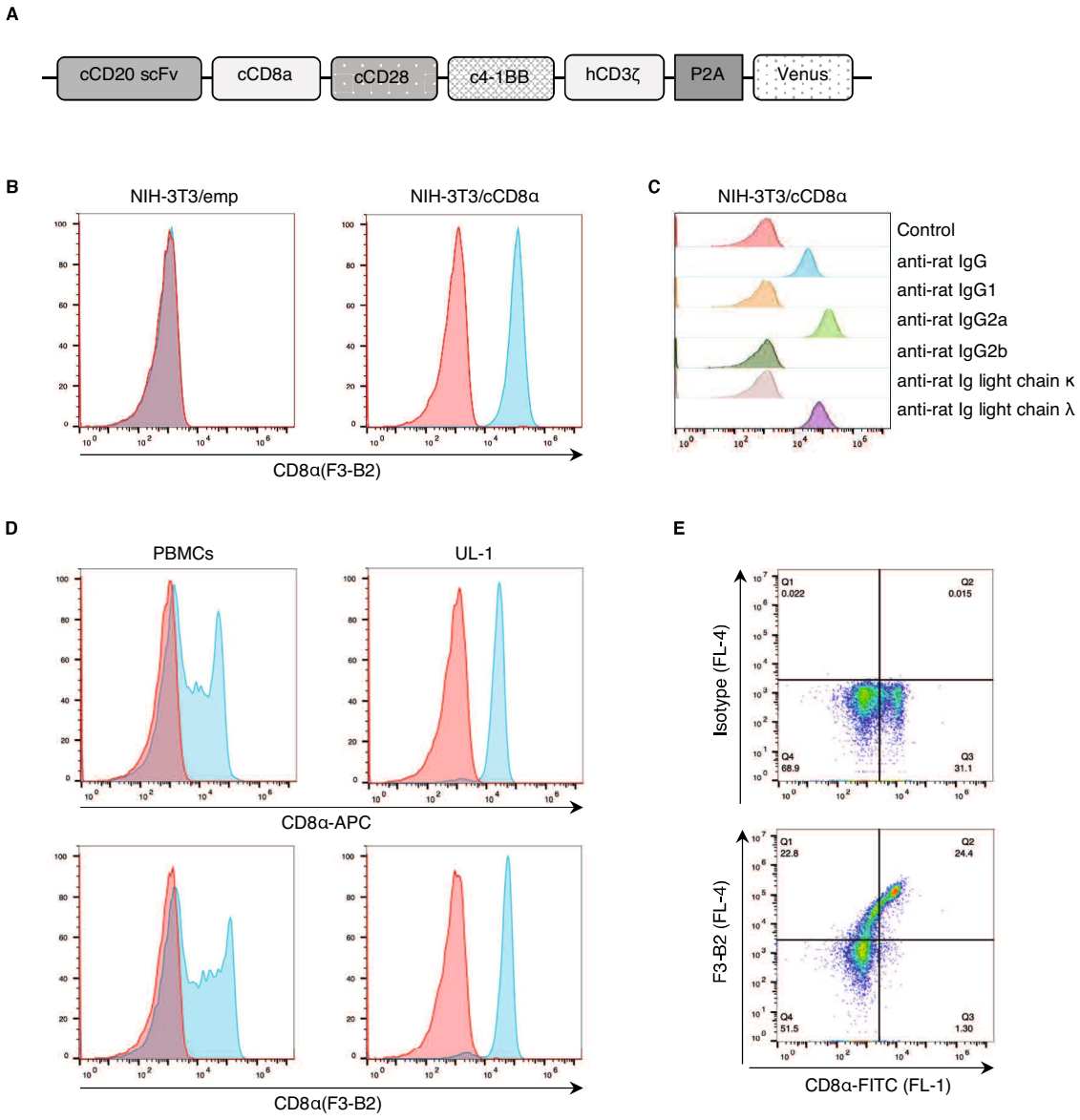

Fig. III-1. Generation and characterization of anti-canine CD8α antibody.

(A) Schematic diagram of the canine CAR-expressing construct. (B) NIH-3T3 cells were retrovirally transduced with a canine CD8α-expressing vector. NIH-3T3/emp (transduced with an empty vector) and NIH-3T3/cCD8α cells were stained with 10 μg/ml of isotype control antibody (red) or anti-canine CD8α antibody (F3-B2, blue),

followed by Dylight 649-labeled anti-rat IgG secondary antibody. (C) Isotyping analysis of anti-canine CD8α antibody. Canine CD8α-expressing NIH-3T3 cells were stained with 10 μg/ml of anti-canine CD8α antibody (F3-B2), followed by Dylight 649-labeled anti-rat IgG secondary antibody (blue, positive control). The cells were also stained with 10 μg/ml of F3-B2, followed by biotin-labeled anti-rat Ig antibodies specific to each subclass, and detection used Dylight 649-labeled streptavidin. (D) PBMCs (isolated from a healthy beagle, and stimulated by IL-2 and phytohemagglutinin) and UL-1 (canine T-cell lymphoma cell line) were stained with 10 μg/ml of isotype control antibody (red) or anti-canine CD8α antibody (blue), followed by Dylight 649-labeled anti-rat IgG secondary antibody. The top and bottom panels show the results of commercially available antibody (CD8α-APC) and F3-B2, respectively. (E) PBMCs were stained with 10 μg/ml of isotype control antibody or anti-canine CD8α antibody (F3-B2), followed by Dylight 649-labeled anti-rat IgG secondary antibody. The cells were additionally stained with commercially available FITC-labeled anti-canine CD8α antibody.

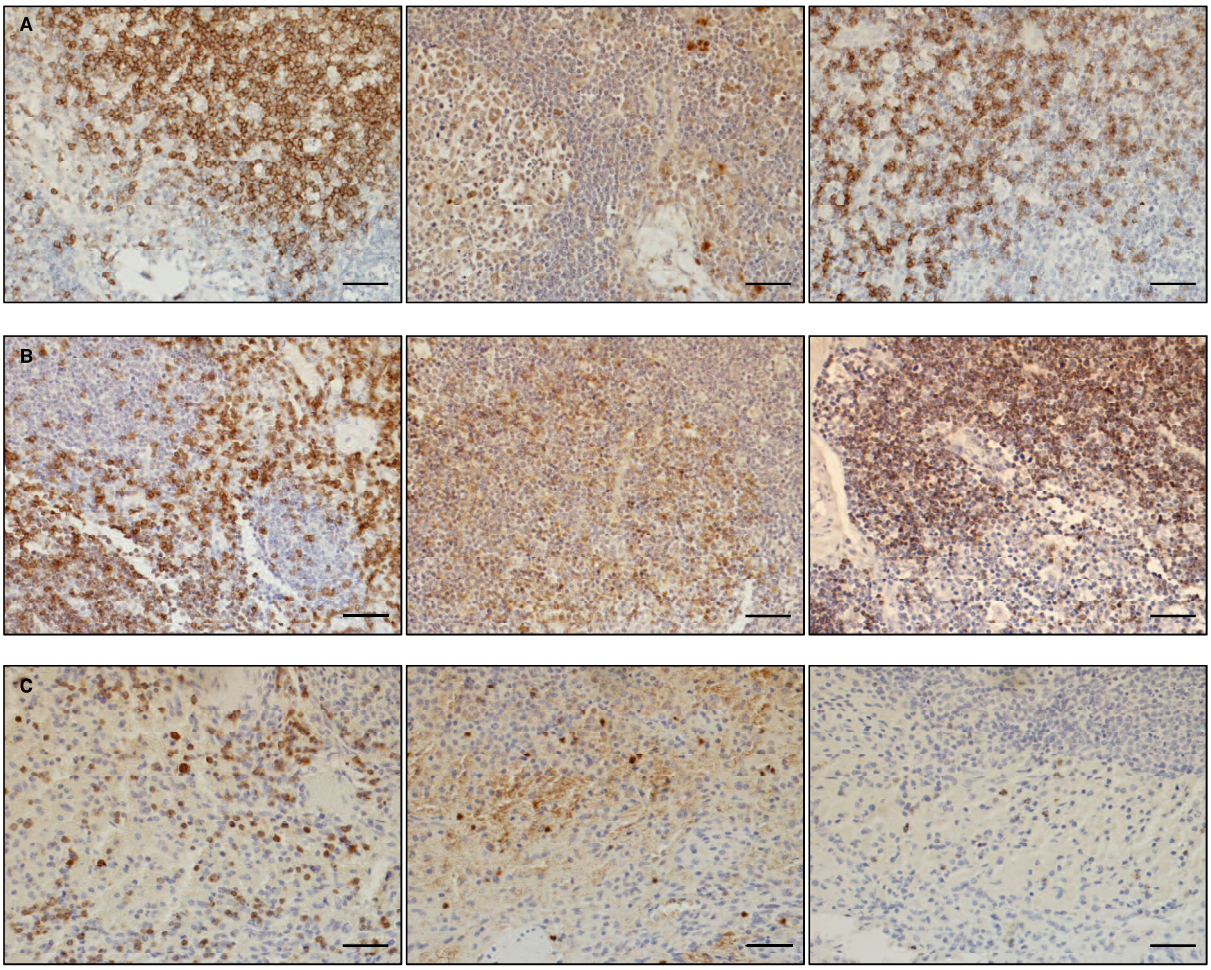

Fig. III-2. Immunohistochemical analysis using established anti-canine CD8α antibody. Tissue specimens from healthy dogs were stained immunohistochemically with anti-human CD3, anti-human Granzyme B, and anti-canine CD8α (F3-B2). Representative immunostaining of lymph node (A), thymus (B), and spleen (C) is shown. The left, middle, and right panels represent immunohistochemical staining of CD3, Granzyme B, and CD8α (F3-B2), respectively. The scale bar indicates 40 μm.

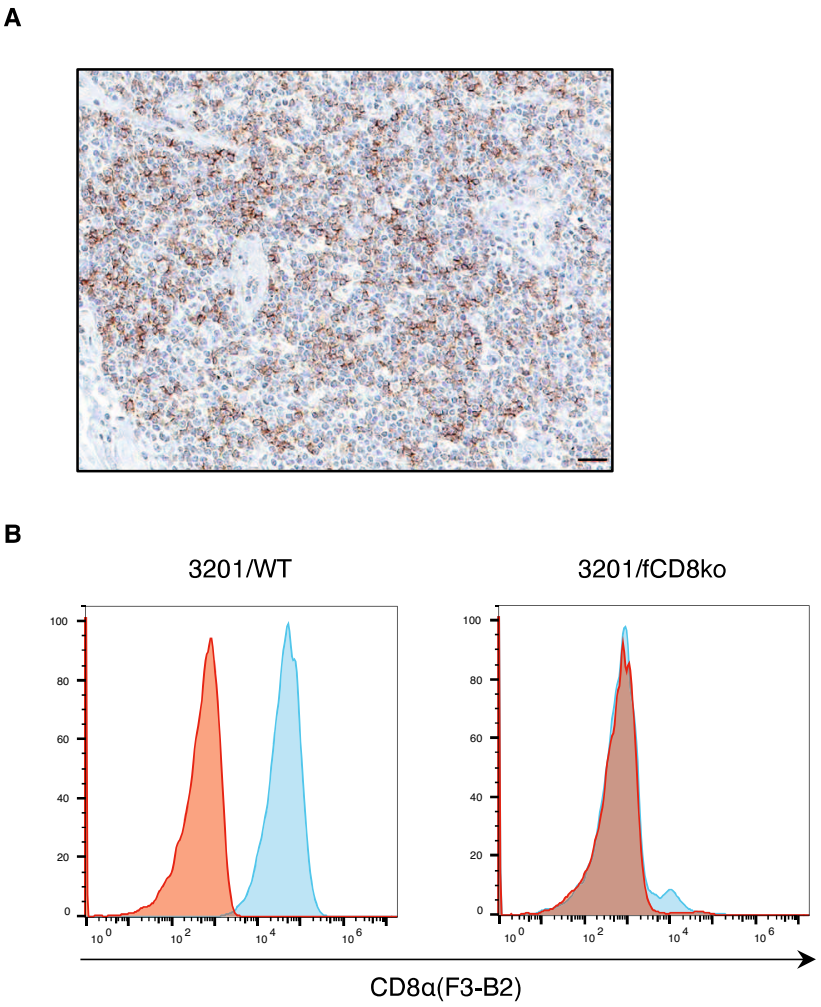

Fig. III-3. F3-B2 also shows reactivity against feline CD8.

(A) Representative immunostaining of lymph node from healthy cats. Tissue specimens were stained immunohistochemically with anti-canine CD8α antibody (F3-B2). The scale bar indicates 20 μm. (B) Wild-type 3201 (3201/WT) and feline CD8 knockout 3201 (3201/fCD8ko) cells were stained with 10 μg/ml of isotype control antibody (red) or anti-canine CD8α antibody (F3-B2, blue), followed by Dylight 649-labeled anti-rat IgG secondary antibody.

Chapter 4

Optimization of canine CD20 chimeric antigen receptor T cell manufacturing and *in vitro* and *in vivo* cytotoxic activity against B-cell lymphoma

SUMMARY

Canine B cell lymphoma is one of the most common hematopoietic neoplasms in veterinary medicine, and it is considered a relevant model for human diffuse large B cell lymphoma (DLBCL). Although the standard treatment consisting of multidrug chemotherapy is effective in most cases, treatment is often challenging because of relapse and drug resistance. The adoptive transfer of autologous T cells genetically modified to express a CD19-specific chimeric antigen receptor (CD19 CAR-T cells) has been shown to be highly effective in human B cell malignancies. However, there is no clinically available canine CAR-T cell therapy. We generated canine second-generation and third-generation CAR-T cells by retroviral gene transduction. Optimization was performed to investigate effective viral transduction protocols and favorable culture conditions for canine CAR-T cells. The RetroNectin-bound virus infection method resulted in more than 70% transduction efficiency. The effect of culture conditions on the phenotype of CAR-T cells was evaluated by the expression of surface markers. *In vitro* cytotoxicity assays of target cells cultured with CD20 CAR-transduced cells demonstrated that CD20 CAR-T cells exhibit cytotoxicity against CD20-expressing

canine B cell lymphoma cells and canine CD20-transduced murine cells, whereas no effect was observed against cells that lacked canine CD20 expression. Finally, *in vivo* antitumor activity was assessed using mice xenograft model as a preliminary experiment. Our study established virus-based canine CAR-T cell generation, providing fundamental data for a better understanding of canine adoptive T cell therapy.

INTRODUCTION

Monoclonal antibody therapy and adoptive cell therapy represent a novel therapeutic approach for cancer immunotherapy. The adoptive transfer of autologous T cells that are genetically modified to express a CD19-specific chimeric antigen receptor (CD19 CAR-T cells) has produced a high rate of complete remission in clinical trials for human B cell acute lymphoblastic leukemia (B-ALL), chronic lymphocytic leukemia (CLL), and non-Hodgkin lymphoma (NHL) (Geyer, MB. and Brentjens, RJ., 2016). In this approach, the patient's T cells are isolated, activated, and transduced to express chimeric antigen receptors (CARs) that recognize specific tumor-associated antigens. CARs are composed of an antigen recognition domain of a specific antibody connected to stimulating and intercellular signaling domains. First-generation CARs contained a single signaling domain derived from CD3. Second- and third-generation CARs have one and two additional co-stimulatory domains, respectively. Once CARs bind the corresponding antigen on tumor cells, CAR-T cells are activated and show cytotoxic functions causing tumor cell death.

Canine B cell lymphoma is one of the most common hematopoietic

neoplasms in veterinary medicine (Zandvliet, M., 2016). The standard treatment generally consists of a multidrug chemotherapy regimen, and it is effective in most cases. However, the treatment of canine lymphoma is often challenging because many dogs develop relapsed or refractory disease. Drug resistance is also very common, and there is a distinct need for novel therapeutic agents. In addition, canine B cell lymphoma is considered as an ideal model for non-Hodgkin's lymphoma in humans because the lymphomas of both species share similar clinical characteristics (Rowell, JL. *et al*., 2011). The evaluation of cancer immunotherapy in dogs with spontaneous cancers is thought to offer a further advantage (Park, JS. *et al*., 2016). because cancer xenograft models in immunocompromised mice may not fully substitute the immunosuppressive tumor microenvironment.

Although a few studies have been reported on canine CAR-T cell therapy, basic information of canine CAR-T cells is limited (Mata, M. *et al*., 2014, Smith, JB. *et al*., 2015, Mata, M. and Gottschalk, S., 2016, Panjwani, MK. *et al*., 2016, Yin, Y. *et al*., 2018). Electroporated autologous T cells expressing first-generation CARs were administered to a dog with spontaneous B cell lymphoma (Panjwani, MK. *et al*., 2016).

The treatment with CAR-T cells was well tolerated, although the antitumor effect was modest and transient. The authors concluded that limited antitumor activity, in part, was due to the CAR construct lacking a co-stimulatory domain, and transduction by electroporation leading to transient expression of CARs. The stable expression of CARs that enables efficient activation of transduced T cells is indispensable for an adequate antitumor effect. To develop CAR-T cell therapy for spontaneous osteosarcoma (OS) in dogs as preclinical models, canine CAR-T cells generated through retroviral transduction were also evaluated (Mata, M. *et al*., 2014). They developed expansion and transduction protocols for the generation of canine CAR-T cells, and demonstrated that canine T cells expressing a HER2-specific CARs showed cytotoxic activity against HER2-positive canine OS cell lines. In another study, which focused on the effectiveness of combination therapy of immune checkpoint blockade and CAR-T cells, the authors generated humanized interleukin-13 receptor α2 (IL-13Rα2) CAR-T cells, and showed that human IL-13Rα2 CAR-T cells recognized canine IL-13Rα2-expressing glioma, OS lung cancer, and leukemia cell lines (Yin, Y. *et al*., 2018). They also generated canine IL-13Rα2 CAR-T cells and tested *in vitro* and *in vivo* antitumor

activity.

In this study, we generated canine CAR-T cells that expressed CARs stably and showed high cytotoxic activity. We evaluated the optimized retroviral transduction protocol, and demonstrated that canine CD20 CAR-T cells were generated efficiently by retroviral transduction. To investigate the optimal culture conditions for adoptive T cell therapy, the effects of culture conditions on the characterization of CAR-T cells were assessed in various culture conditions. Furthermore, *in vitro* and *in vivo* antitumor activity of canine CD20 CAR-T cells was investigated using B cell lymphoma cells. This study provides fundamental information of CAR-T cell therapy in veterinary medicine.

MATERIALS AND METHODS

Cell line validation statement and culture

Six cell lines were used in this study, and all cell lines were previously established and validated. Plat-E was kindly provided from Dr. Kitamura (Institute of Medical Science, University of Tokyo, Tokyo, Japan), and EL4 was obtained from Tohoku University (Sendai, Japan) (Morita, S. *et al*., 2000, GORER, PA., 1950). PG13 and CTAC were obtained from the American Type Culture Collection (Manassas, VA, USA) and Riken Cell Bank (Tsukuba, Japan), respectively (Miller, AD. *et al*., 1991, KASZA, L., 1964). CLBL-1 was previously established and validated by Rütgen BC et al (Rütgen, BC. *et al*., 2010). CLC was established and characterized in our laboratory, as previously described (Umeki, S. *et al*., 2013).

Retroviral packaging cell lines, Plat-E and PG13, were cultured in D10 complete medium (Dulbecco's modified Eagle's medium supplemented with high glucose, 10% fetal bovine serum (FBS), 100 units/ml penicillin and 100 μg/ml streptomycin, and 55 μM 2-mercaptoethanol). Canine thyroid adenocarcinoma cell lines, CTAC, canine B cell lymphoma cell line, CLBL-1, canine T cell lymphoma cell

line, CLC, and murine T cell lymphoma cell line, EL4, were cultured in R10 complete medium (RPMI1640 supplemented with 10% FBS, 100 units/ml penicillin and 100 μg/ml streptomycin, and 55 μM 2-mercaptoethanol).

To obtain cell-based artificial antigen presenting cells (aAPCs), CTAC were retrovirally transduced with canine CD80, canine CD83, canine CD86, and human CD137L.

Luciferase (luc)-expressing target cells, CLBL-1/luc, CLC/luc, and EL4/luc, were described in our study (Mizuno, T. *et al*., 2020).

All cell lines were tested for mycoplasma contamination by e-Myco^{TM} Plus Mycoplasma PCR detection kit (iNtRON Biotechnology, Inc., Burlingon, MA, USA) in our laboratory, and cultured in a humidified incubator at 37 °C and 5% CO_2, unless otherwise noted.

CRISPR-Cas9 editing of cell lines

CD20 knockout CLBL-1/luc cells were generated using the CRISPR-Cas9 technology. Guide sequences targeting canine CD20 (5'-

CACCGGGGCTTTTCATAGGATCTAC-3’ and 5’-AAACGTAGATCCTATGAAAAGCCCC-3’) were cloned into a lentiCRISPRv2 plasmid (gift from Feng Zhang [Addgene Cambridge, MA, USA, plasmid #52961; http://n2t.net/addgene:52961; RRID:Addgene_52961]). CRISPR plasmid was co-transfected with packaging plasmids, p8.9QV and pCVSVG, into HEK293T cells. After transfection to HEK293T cells, supernatants including CRISPR lentivirus particles were harvested, and CLBL-1/luc cells were infected with the concentrated viral supernatant, and cultured in the presence of hygromycin (300 μg/ml) to select for stably transduced cells, followed by limiting dilution to isolate individual clones.

CAR construction and retrovirus production

A third-generation CAR construct was mainly used in this study. The anti-canine CD20 scFv sequence was derived from the variable region of an anti-CD20 monoclonal antibody developed in our laboratory (Mizuno, T. *et al*., 2020). The CAR construct was comprised of the anti-CD20 scFv linked to the canine CD8α hinge and transmembrane domain, followed by the canine CD28 and 4-1BB co-stimulatory

domain, and human CD3ζ signaling domain. For the co-expression of CARs together with fluorescent protein, the CAR construct was followed by a P2A peptide fused to Venus fragments. This CAR-P2A-Venus construct was ligated into the PacI and HincII site of the MSGV Hu Acceptor PGK-NGFR (Addgene). Two second-generation CAR constructs, with either CD28 or 4-1BB as a co-stimulatory domain, were generated for comparison with the third-generation CARs.

To obtain a PG13 cell line stably producing viruses, retrovirus particles were generated by transient transfection of Plat-E cells with the CAR-encoding retrovirus vector. Supernatants containing the retrovirus were collected after 48 hours, and used to transduce the PG13 for the production of retrovirus for T cell transduction.

Retrovirus production from the PG13 producer cell line was conducted as follows. First, 3×10^6 transduced PG13 cells were seeded in T75 flasks and cultured in a CO_2 incubator at 32 °C or 37 °C. Twenty-four hours later, the culture media was changed to fresh DMEM containing 10% FBS, 100 units/ml penicillin, 100 μg/ml streptomycin, and 5 mM sodium butyrate and incubated for 24 hours. The retrovirus-containing supernatants were filtered through 0.45 μm filters and stored at -80 °C until

use.

Cell stimulation, transduction, and expansion of CAR-T cells

All blood samples were obtained from healthy beagle dogs kept as blood donors for Yamaguchi University Animal Medical Center. Peripheral blood mononuclear cells (PBMCs) were isolated using Lymphoprep (Axis-Shield, Oslo, Norway) gradient centrifugation and then stimulated in the presence of 200 U/ml of recombinant human IL-2 (Proleukin; Novartis, Basel, Switzerland) for 72 hours. Cells were stimulated with: phytohemagglutinin (PHA) (condition #1), anti-CD3 plus anti CD28 antibodies (condition #2), cell-based aAPCs (condition #3), or IL-15 and IL-21 (condition #4). CAR-T cells generated through condition #1 were compared with those from condition #2, #3, and #4.

In condition #1, cells were stimulated with 5 μg/ml PHA (Sigma, St. Louis, MO, USA). In condition #2, anti-CD3 (clone CA17.2A12; Bio-Rad Laboratories, Inc. Hercules, CA, USA) and anti-CD28 (clone 1C6; eBioscience, Inc. Vienna, Austria) antibodies were used. Cells were stimulated on culture plates coated with anti-CD3 (5

μg/ml) alone, or anti-CD3 (5 μg/ml) and anti-CD28 (5 μg/ml) antibodies. In condition #3, CTAC cells expressing co-stimulatory molecules (CD80, CD83, CD86, and CD137L) were used as aAPCs. CTAC cells were treated with mitomycin-c (50 μg/ml) for 45 min and co-cultured with primary PBMCs. In condition #4, 10 IU/ml recombinant human IL-15 (Pepro Tech, Inc. Rocky Hill, NJ, USA) and/or 10 ng/ml recombinant canine IL-21 (Sino Biological, Inc. Beijing, China) were added to cultures together with 5 μg/ml PHA.

Retroviral transduction was performed after initial stimulation using recombinant human fibronectin fragment (RetroNectin; TaKaRa Bio, Shiga, Japan). Non-treated 24-well culture plates were coated with 0.5 ml of RetroNectin solution (10 μg/ml or 20 μg/ml) diluted with PBS for 2 hours at room temperature in accordance with the manufacturer's instructions. After removal of the RetroNectin solution, plates were washed with PBS. Then, 0.5 ml of retrovirus-containing supernatants were added to the RetroNectin-coated plate, and preparation of a virus-bound plate was performed using shaking or centrifugation methods. Plates were incubated on a plate shaker (set to 100 rpm) for 16 hours at 4 °C or centrifuged at 2000 × g for 2 hours at 4 °C. A total of

2.5×10^5 stimulated T cells was added to the virus-bound plates and incubated in a 37 °C, 5% CO_2 incubator for 24 hours, followed by the second virus infection in the same manner. To promote contact between T cells and viral particles, plates were centrifuged at 500 × g for 1 min after second infection.

After retroviral transduction, CAR-T cells were subsequently expanded with 200 U/ml IL-2 for 6 days. In condition #4, IL-15 and IL-21 were added during expansion. Non-transduced T cells, used as controls, were stimulated with 5 μg/ml PHA and expanded in parallel in the presence of 200 U/ml IL-2. A portion of CAR-T cells was cryopreserved using cell freezing medium (Bambanker; Lymphotec, Tokyo, Japan) to evaluate phenotypic and functional characteristics of cryopreserved CAR-T cells compared with fresh cells.

Flow cytometry

CAR-T cells were collected and washed with PBS, followed by incubation with Fixable Viability Dye eFluor 780 (eBioscience, Inc. Vienna, Austria) for 30 min on ice. Then, cells were resuspended in FACS buffer (PBS containing 2% FBS and 0.1%

NaN_3). A total of 2×10^5 cells were stained with each antibody for 30 min on ice. After incubation, cells were washed and fixed in 1% paraformaldehyde and stored until analysis. For T cell phenotyping, the following antibodies were used: mouse anti-dog CD3 (clone CA17.2A12; dilution 1:500), mouse anti-dog CD21 RPE (clone CA2.1D6; dilution 1:20) and mouse anti-human CD62L RPE (clone FMC46; Bio-Rad Laboratories, Inc. Hercules, CA, USA; dilution 1:20); rat anti-dog CD8a APC (clone YCATE55.9; eBioscience; dilution 1:20); mouse anti-dog CD4 (clone CA13.1E4; dilution 1:4), and mouse anti-dog CD45RA (clone CA21.4B3; undiluted) kindly provided by P.F. Moore (University of California, Davis). Anti-human CD62L antibody was confirmed to cross-react with canine cells in previous report (Withers, SS. *et al*., 2018). For analysis of PD-1 and PD-L1 expression on CAR-T cells, anti-cPD-1 (clone 4F12-E6; concentration 10 μg/ml) and anti-cPD-L1 (clone G11-6; concentration 10 μg/ml) antibodies prepared in our laboratory were used (Nemoto, Y. *et al*., 2018). Purified rat IgG2a antibody (clone RTK2758; BioLegend, San Diego, CA, USA; concentration 10 μg/ml) was used as isotype control for anti-cPD-1 and anti-cPD-L1 antibodies.

Samples were analyzed using an Accuri C6 (BD Biosciences, San Diego, CA, USA), and results were analyzed using FlowJo software (BD Biosciences).

Cytotoxicity assay

The cytotoxic activity of T cells transduced with CARs was assessed using a luciferase-based assay. Target (T) cells (CLBL-1/luc, CLBL-1/luc/cCD20ko, CLC/luc, EL4/luc, or EL4/luc/cCD20 cells) were co-cultured with effector (E) cells (CAR-T cells or non-transduced T cells) at the indicated E/T ratio in 96-well plates. After incubation for 4 hours in a 5% CO_2 air incubator at 37 °C, the luciferase activities of viable cells were assessed for luminescence using ONE-Glo™ Luciferase Assay reagent (Promega Corporation, Madison, WI, USA). Specific lysis was determined using the luminescence of target cells alone, and NP-40 lysed target cells, corresponding to 0% lysis and 100% lysis respectively.

Cytokine production by CAR-T cells

In 96-well plates, CAR-T cells or non-transduced control T cells were co-

cultured with target tumor cells CLBL-1/luc. After 4 hours, the culture supernatant was collected and the production of IFN-γ was quantified using an enzyme-linked immunosorbent assay (R&D Systems, Minneapolis, MN, USA).

Mouse study

All animal studies were carried out in accordance with the Yamaguchi University Animal Care and Use Committee Regulations. CAR-T cell used in this experiment was third-generation CAR-T prepared with PHA stimulation (condition #1), and retroviral transduction was conducted by centrifugation method using 10 μg/ml of RetroNectin solution and virus supernatant prepared at 37 °C. Control PBMCs were stimulated and cultured in parallel without CAR transduction. Cells were cryopreserved at -80 °C, and thawed two days before injection. Fifteen NOD/SCID mice (KBT Oriental Co., Ltd., Saga, Japan), pretreated with intraperitoneal injection of cyclophosphamide (200 mg/kg), were intraperitoneally inoculated with 1×10^6 CLBL-1/luc cells 48 hours after pretreatment (day 0). The tumor-bearing mice were randomized to three groups, and receive one of the following intravenous injections on

day 12, 16, and 20: sterile PBS, 5×10^6 non-transduced T cells in sterile PBS, and 5×10^6 CAR-T cells in sterile PBS. From day 24 to day 27, mice were examined at the time of death, and the remaining mice surviving on day 27 were euthanized. All mice were examined at necropsy and their tissues were fixed in buffered formaldehyde and embedded in paraffin. Sections were prepared for H&E staining and immunohistochemical staining.

Immunohistochemistry

Spleen of tumor-bearing mice was immunohistochemically stained for canine CD3 (injected CAR-T cells) and canine CD79a (injected CLBL-1/luc cells), as described in our previous report (Shosu, K. *et al*., 2016). After dewaxing, antigen retrieval proceeded in citrate buffer (pH 6.0) at 125 °C for 30 s. Then the sections were washed in distilled water and rinsed with PBS. Endogenous peroxidase activity was blocked with 3% hydrogen peroxide in methanol for 30 min at room temperature (RT). The sections were washed with distilled water, then rinsed with PBS. To block nonspecific protein activity, the sections were incubated for 30 min (CD3) or 1 hour

(CD79a) at RT with 5% skimmed milk and 5% bovine serum albumin (BSA) in PBS. After blocking nonspecific protein activity, the sections were rinsed with PBS, followed by incubation with primary antibody overnight at 4 °C. All primary antibodies were diluted with 2% BSA in PBS. Rat anti-human CD3 antibody (clone CD3-12: Serotec, Oxford, UK), mouse anti-human CD79a antibody (clone HM57: Serotec), and corresponding isotype control antibodies were used as primary antibody. The antibody-treated sections were rinsed with PBS, followed by treatment with horseradish peroxidase (HRP)-conjugated secondary antibodies (goat anti-rat IgG antibody for CD3; goat anti-mouse IgG antibody for CD79a; Histofine Simple Stain MAX PO: Nichirei Corporation, Tokyo, Japan) for 30 min at RT. The sections were rinsed with PBS, and color was developed with the peroxidase stain 3',3'-diaminobenzidine (DAB Kit & Enhancer; Nacalai Tesque, Kyoto, Japan) for 5 min at RT. After the sections were washed in distilled water, they were counterstained for 5 min with Mayer's hematoxylin solution (Merck KGaA, Darmstadt, Germany), washed in distilled water, dehydrated in graded baths of ethanol, cleared in xylene, and mounted with a xylene-based mounting solution (Matsunami, Osaka, Japan).

Statistical analysis

Statistical analysis was performed using JMP14.0 software (JMP Japan, Tokyo, Japan). The assumption of normality was performed by using Shapiro-Wilk test. Two-tailed Student's t test and one-way ANOVA followed by Tukey–Kramer multiple comparison test were used for comparison of two groups or more than two groups, respectively. A P value of less than 0.05 was considered as statistically significant.

RESULTS

Generation of canine CD20 CAR-T cells

To generate and evaluate genetically modified CAR-expressing canine T cells, vectors encoding second-generation (either of CD28 or 4-1BB) and third-generation CARs were used (Fig. IV-1A). Canine PBMCs were activated, and retrovirally transduced on days 3 and 4 (Fig. IV-1B). The optimization of transduction efficiency was evaluated with the expression of Venus fluorescent protein. At first, virus transduction efficiency was compared with the methods of shaking or centrifugation, and the transduction temperature of 32 °C or 37 °C. Compared with the shaking method, the preparation of RetroNectin-coated plates using the centrifugation method obviously improved the transduction efficiency (3.15% in the shaking method vs 61.1% in the centrifugation method, using retrovirus produced at 37 °C), whereas the effect of the temperature difference was extremely modest (4.39% vs 3.15% in the shaking method, and 60.0% vs 61.1% in the centrifugation method) (Fig. IV-1C). We also examined the effect of the concentration of RetroNectin and found that a lower concentration of RetroNectin (10 μg/ml) resulted in almost the same transduction

efficiency as the higher concentration (20 μg/ml) (Fig. IV-1D). Based on these results, RetroNectin-coated plates were prepared with 10 μg/ml RetroNectin, and the centrifugation method using retrovirus produced at 37 °C was used in subsequent experiments.

Phenotypic analysis of second- and third-generation canine CAR-T cells

Phenotypic characterization of generated canine CAR-T cells was evaluated using flow cytometry for surface markers. Gating strategy to identify each phenotypic marker of CAR-T cells was described in Fig. IV-2A. Firstly, we evaluated the CD4/CD8 phenotype of CAR-T cells, and no significant difference was observed between the three CAR constructs, two second-generation and one third-generation (Fig. IV-2B). There was a certain amount of CD4-CD8- population, most of which was CD3+ T cells. To evaluate the T cell differentiation status, we assessed the expression of CD45RA and CD62L, and CAR-T cells were classified into four differentiation subsets: stem cell memory T cells (Tscm, CD45RA+CD62L+), central memory T cells (Tcm, CD45RA-CD62L+), effector memory T cells (Tem, CD45RA-CD62L-), and effector T cells (Teff,

CD45RA+CD62L-). Generated CAR-T cells were composed mainly of the effector T cell subset, followed by Tem and Tscm, but there were few Tcm cells. Furthermore, there were no significant differences in the proportion of each subset between second- and third-generation CAR constructs (Fig. IV-2C). We also assessed PD-1 and PD-L1 expression to evaluate one of the exhausted markers of T cells. Half of CAR-T cells expressed PD-1, and the second- and third-generation CAR-T cells showed almost same level of PD-1 and PD-L1 expression (Fig. IV-2D).

Effect of the T cell stimulation conditions on phenotypic changes in CAR-T cells

Next, we evaluated the effect of the condition of T cell stimulation on phenotypical changes in CAR-T cells. Cell stimulation with an anti-CD3 antibody (Fig. IV-1B, condition #2) resulted in an increase in the CD8+ subset, and this was more obvious when the cells were stimulated by both anti-CD3 and anti-CD28 antibodies (Fig. IV-3A). Since the results are varied in each donor, individual data from three dogs are shown in Fig. IV-3B and IV-3C. Regarding the T cell differentiation status, two out of three donors (donor #2 and #3) showed an increase in the effector T cell subset and

decreased PD-L1 expression by stimulation of CD3 alone, and the same result was observed when the cells were stimulated using CD3 plus CD28 (Fig. IV-3B, IV-C). However, the effect of stimulation of CD3 on PD-1 expression differed in each donor.

To evaluate the effect of costimulatory molecules, in addition to PHA stimulation, mitomycin-C-treated CTAC cells expressing co-stimulatory molecules (CD80, CD83, CD86, and CD137L) were used as aAPCs (Fig. IV-1B, condition #3), when stimulating PBMCs. Since the results are varied in each donor, individual data from three dogs are shown in Fig. IV-4B. CAR-T cells stimulated by PHA and aAPCs increased the CD8+ subset (Fig. IV-4A). Although the percentage of the Tscm subset varied between the donors, stimulation by aAPCs had a tendency to increase the Teff subset (Fig. IV-4B). There was also a tendency that stimulation by aAPCs decreased the expression of PD-1 and PD-L1, and PD-L1 expression was significantly decreased by aAPC stimulation (Fig. IV-4C).

To evaluate the influence of interleukins, IL-15 and IL-21 were used in addition to the base conditions (condition #1: PHA and IL-2). We used IL-15 and/or IL-21 during cell stimulation (day 0–3) and cell expansion (day 4–10) (Fig. IV-1B,

condition #4). As shown in Fig. IV-5, the additional treatments of IL-15 and/or IL-21 influenced no significant differences in CD4/CD8 phenotype, memory phenotype, and PD-1 and PD-L1 expression.

Canine CAR-T cells show CD20 specific cytotoxicity against canine lymphoma cell lines

To demonstrate the cytotoxic activity of canine CD20 CAR-T cells, a canine B cell lymphoma cell line, CLBL-1, was used as a target cell line. We also used cCD20 knockout CLBL-1 cells, cCD20 non-expressing canine T cell lymphoma cell line (CLC), and cCD20 transduced murine T cell lymphoma cell line (EL4/cCD20) to evaluate the target specificity of CAR-T cells. All cell lines were transduced to express luciferase, and the cell surface expression of cCD20 was verified prior to the cytotoxicity assay (Fig. IV-6A).

First, the cytotoxic activity of second- and third-generation canine CAR-T cells was assessed (Fig. IV-6B). These CAR-T cells showed high *in vitro* cytotoxic activity against cCD20-expressing target cells, whereas non-transduced control T cells

did not show cytotoxic activity, and there was no significant difference between the generation of vectors. To determine whether canine CAR-T cells become activated and acquired effector cell function, we also performed ELISA assays to detect IFN-γ production. ELISA assays revealed that canine CAR-T cells released IFN-γ in an E/T ratio dependent manner when co-cultured with CLBL-1/luc cells (Fig. IV-6C). We also found that IFN-γ production from second-generation CAR-T cells with the CD28 co-stimulatory domain was significantly higher than that of third-generation CAR-T cells.

Target specificity was evaluated using third-generation CAR-T cells (Fig. IV-6D-F). CAR-T cells did not exhibit cytotoxicity against cCD20 knockout CLBL-1 cells (Fig. IV-6D) or CLC cells, a canine T cell lymphoma cell line originally lacking the expression of cCD20 (Fig. IV-6E). The cytotoxicity assay using EL4 cells revealed that cCD20 CAR-T cells exhibit cytotoxicity against EL4 cells transduced to express cCD20, whereas no effect was observed against parental EL4 cells that lack cCD20 expression (Fig. IV-6F). These results indicated that the cytotoxicity of canine CD20 CAR-T cells depended on the surface expression of cCD20.

Next, we assessed whether the various conditions of cell stimulation

influenced the cytotoxic activity of CAR-T cells (Fig. IV-6G-I). All canine CAR-T cells generated through conditions #1, #2, #3, and #4 exhibited cytotoxic activity against CLBL-1/luc cells. CAR-T cells generated using condition #2 (stimulated by CD3 alone, or CD3 and CD28) showed significantly higher cytotoxicity than those with condition #1 (PHA alone) (Fig. IV-6G), and this was consistent with an increased Teff subset in condition #2 (Donor #3 in Fig. IV-3B). Meanwhile, stimulation by aAPC (condition #3) and addition of IL-15 and IL-21 (condition #4) did not affect the cytotoxic activity of CAR-T cells (Fig. IV-6H and IV-I).

Finally, we assessed the CAR-T cell expansion capacity of each stimulation. As shown in Fig. IV-7, cell expansion capacity was variable between 10 to 40-fold increase, and those were quite variable between each time and each dog. Especially, the expansion capacity was varied greatly in second-generation CAR-T cells and stimulation with CD3 antibody. In contrast, stimulation with aAPCs resulted in consistently high expansion rate.

Phenotype and function of cryopreserved CAR-T cells

To evaluate whether cryopreserved CAR-T cells sustained their phenotypic and functional characteristics, we examined cryopreserved cells compared with fresh cells. First, we assessed the phenotypic characteristics of fresh and cryopreserved CAR-T cells (Fig. IV-8A). We did not observe any differences in CD4/CD8 expression and memory T cell subset, although an increase of PD-1-expressing cells was observed in cryopreserved cells. We also evaluated the cytotoxic function of cryopreserved CAR-T cells and found that cytotoxic function was limited on the day of thawing, but the cytotoxic function recovered to the same degree as that of fresh cells by 2 days after thawing (Fig. IV-8B). We evaluated the cells at 2 days after thawing, and confirmed cytokine production from cryopreserved CAR-T cells (Fig. IV-8C).

In vivo antitumor activity of CD20 CAR-T in mouse model

The *in vivo* experiments were carried out in intraperitoneal injection model of CLBL-1/luc cells. Our preliminary experiments revealed that enlargement of the spleen was observed in almost all cases in this model, and the other organs showed no big changes except occasional enlargement of abdominal lymph nodes. Therefore, spleen of

tumor-bearing mice was evaluated to determine the antitumor effect of CD20 CAR-T cells. As shown in Figure IV-9A, the spleen weight at the endpoint was significantly lower in mice treated with CAR-T cells compared to that in mice treated with non-transduced control PBMCs. H&E staining of spleen revealed the infiltration of CLBL-1/luc cells into the whole area of spleen in all three groups (Fig. IV-9B). Necrosis was observed in all three groups, however, necrotic areas were larger in CAR-T cells-treated group than other two groups. The infiltration of CLBL-1/luc cells was also evaluated by CD79a staining (Fig. IV-9C). Cells positively stained for CD79a were observed in whole area of spleen, and the CD79a-negative area was larger in CAR-treated group, compared to other two groups. To determine whether CAR-T cells infiltrate into tumor-bearing spleen, the T cell marker CD3 was stained by immunohistochemistry. As shown in Figure IV-9D, the area positively stained with CD3 was observed only in CAR-T cells-treated group.

DISCUSSION

The purpose of this study was to generate and evaluate canine CD20-specific CAR-T cells. We also focused on the optimal protocol for the generation of canine CAR-T cells. Previous studies on canine CAR-T cells have investigated the expansion and transduction methodology that enables the generation of sufficient numbers of canine CAR-T cells (Mata, M. *et al*., 2014, Panjwani, MK. *et al*., 2016). However, detailed investigations on the generation protocol of canine CAR-T cells are still lacking. Therefore, we examined the optimal methods for viral transduction, and the effect of cell stimulating conditions on T cell phenotype.

Regarding the transduction efficiency of the virus, the temperature at 37 °C during collection of the virus, and use of a virus-bound RetroNectin method was found to be the most efficient method (maximum 72.8% transduction efficiency) in this study. Meta *et al*. investigated the optimal retroviral transduction of canine CAR-T cells, and achieved a maximum 34.9% transduction efficiency using RetroNectin (Mata, M. *et al*., 2014). Our method greatly improved the retroviral transduction efficiency of canine T cells.

Analyzing the subsets of CAR-T cells is crucial because of the heterogeneity of CAR-T cells administered to individual patients, which has effects on efficacy, toxicity, and sustainability after *in vivo* transfusion. The different subsets of T cells and their role in CAR-T cell therapy have been investigated in many human studies (Golubovskaya, V. and Wu, L., 2016). However, there are no studies that have focused on subset changes in canine CAR-T cells. In this study, we focused on the CD4 and CD8 subsets, memory and effector T cell subsets, and some of exhausted markers on CAR-T cells. To obtain CAR-T cells with ideal phenotypes, we compared several conditions, such as second-generation vs third-generation vectors, T cell stimulation conditions, CAR-T culturing conditions (with/without IL-15 and IL-21). Unfortunately, none of the conditions tested generated notable differences in CD4/CD8 ratio, Tscm/Tcm populations, or exhausted marker (PD-1 and PD-L1) expression levels. Among these, Teff/Tscm/Tcm ratios are considered important, because central memory cells in CAR-T production correlated with the duration of persistence (Louis, CU. *et al*., 2011, Wang, X. *et al*., 2016), and cells with stem cell-like properties of self-renewal and multi-potency (Tscm) were shown to correlate with CAR-T cell expansion in lymphoma

patients (Xu, Y. *et al*., 2014, Gattinoni, L. *et al*., 2012). The upregulation of co-inhibitory receptors, such as PD-1, Tim-3, and Lag-3, was associated with CAR-T cell activation, and PD-1 expression on CAR-T cells was not desirable because PD-1/PD-L1 interactions inhibited CAR-T cell function (Zolov, SN. *et al*., 2018). Based on the results of human CAR-T cell therapy, the characteristics of an effective CAR-T cell product are presumed to be adequate numbers of memory subset cells and lower expression of exhaustion markers, such as PD-1. However, PD-1/PD-L1 expression is not absolute marker of exhausted T cells. Therefore, the functional analysis such as IFN-γ production or proliferation assay may be needed for appropriate evaluation of exhaust status of CAR-T cells. In this study, we were unable to find any conditions that increased the subset with stem cell-like properties (Tscm and Tcm). Canine CAR-T cells in this study were mainly composed of the effector T cell subset, which had a high expression level of PD-1. This suggested that the stimulation used in this study was consistently too strong, so that T cells differentiated into an effector subset and became excessively activated. Therefore, our CAR-T cells might not be ideal because there is a possibility that they lack long-lasting antitumor effects in lymphoma patients. There is a

need to further examine the stimulation protocol to generate adequate numbers of memory subset cells. However, based on the result that stimulation using anti-CD3/CD28 or aAPCs had a tendency to lead to lower expression levels of PD-L1, we inferred that more physiological stimulation is favorable for the ideal phenotype of canine CAR-T cells. We have also evaluated the expansion capacity of canine PBMCs under each condition. Canine CAR-T cells expanded efficiently, however, the expansion capacity of non-transduced PBMCs and CAR-T cells was almost same. There is a possibility that CAR-specific stimulation results in further expansion of CAR-T cells. The results also indicated that cell expansion capacity was variable between each condition and each donor. The stimulation using aAPCs showed consistently high fold expansion, indicating that specific stimulating condition may provide the uniform expansion kinetics in individual patients. Efficient expansion of CAR-T cells is crucial, especially in actual patients who have been heavily pretreated with chemotherapy. Therefore, further investigation is needed to achieve efficient cell expansion.

Although the cell culturing conditions to induce the ideal cell surface phenotypes need to be considered as discussed above, our canine CD20 CAR-T cells

exhibited high *in vitro* cytotoxic activity irrespective of the culture conditions, suggesting the potential of canine third-generation CAR-T cells. In addition, we demonstrated that cryopreserved CAR-T cells maintained their cytotoxic functions. The functions and immunophenotypes of cryopreserved CAR-T cells were evaluated previously (Lee, SY. *et al*., 2018). It was concluded that, in agreement with our findings, the cryopreservation of human CAR-T cells did not result in any significant changes in function or immunophenotype. Unfortunately, we have not evaluated the expansion kinetics of cryopreserved cells, but it showed almost same viability and CAR-expression as those without cryopreserved. Use of cryopreserved cells has several advantages because it allows scheduling flexibility for the infusion timing or enables large-scale culture and stocking of CAR-T cells. So, it may be favorable for canine CAR-T cell therapy that cryopreserved cells were shown to sustain their function.

We also evaluated the *in vivo* antitumor activity in xenograft model. The spleen weight of CAR-T-treated mice was significantly lower than that of PBMC-treated mice, however, the antitumor activity observed in this study was mild, and significant difference was not determined between the PBS-treated mice and the CAR-

T-treated mice. This may be due to, in part, the xenograft model used in this study. Our intraperitoneal injection model forms the tumor lesion in spleen, and this may behave like a solid tumor. Although the reasons are not fully understood, previous study have shown that CAR-T cell therapy for solid tumors is not so effective as for hematological tumors (Martinez, M. and Moon, EK., 2019). Therefore, many studies adopted the intravenous injection model, and the antitumor activity was measured using *in vivo* imaging system (Tsukahara, T. *et al*., 2013). Because we could not use the *in vivo* imaging system, we firstly attempted to establish a mouse xenograft model which enables the macroscopic evaluation of antitumor activity (data not shown). However, our preliminary experiments revealed that, intravenous injection of CLBL-1/luc cells did not form any macroscopic tumor foci. Subcutaneous injection resulted in macroscopic tumor development, however, antitumor activity of CAR-T cells was not observed. Our intraperitoneal injection model seems to be suitable for macroscopic evaluation of CAR-T cells to same extent. In addition, results of immunohistochemistry indicate that CAR-T cells infiltrate the tumor site to some extent, and killed the lymphoma cells.

In summary, we first generated canine CD20 CAR-T cells expressing CARs stably. Phenotypic analysis was performed to investigate suitable culture conditions for adoptive T cell therapy. We also demonstrated that our CAR-T cells exhibited high *in vitro* CD20-specific cytotoxic activity against canine B cell lymphoma cells. Companion dogs have drawn attention as a cancer model (Park, JS. *et al*., 2016), and our study provides fundamental data for a better understanding of canine CAR-T cell therapy.

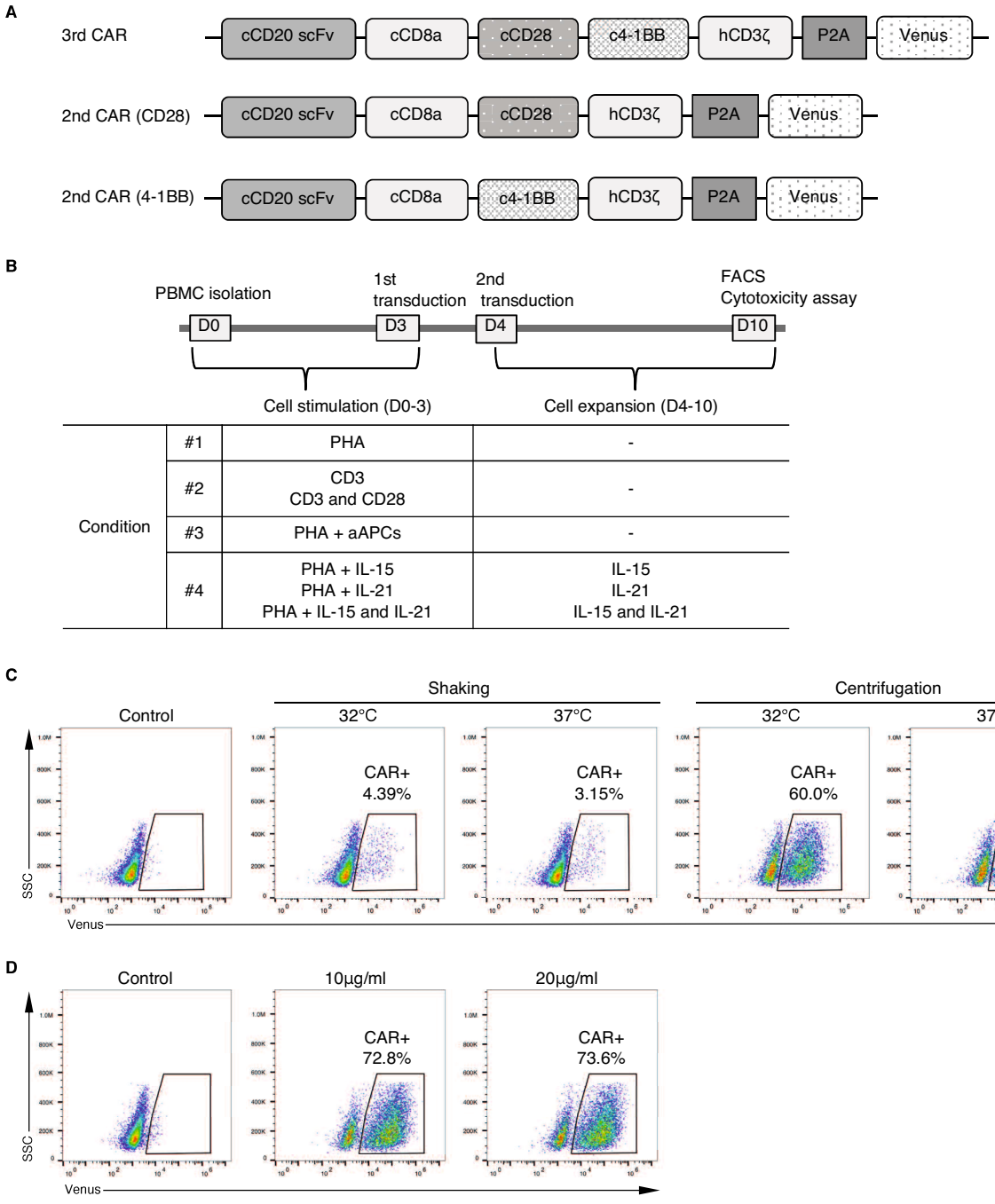

Fig. IV-1. Generation of canine CAR-T cells by retroviral transduction and optimization of transduction conditions.

(A) Schematic diagram of the canine CAR-expressing vector. (B) Protocol for the generation of canine CAR-T cells. Four conditions (conditions #1, #2, #3, and #4) were

used for cell stimulation and expansion. PBMCs from healthy dogs were isolated on day 0 (D0), and stimulated by indicated conditions until day 3 (D3). After stimulation, cells were retrovirally transduced on day 3 and 4 (D3 and D4). Transduced cells were expanded and evaluated on day 10 (D10). In condition #4, IL-15 and/or IL-21 were added during cell expansion (D4-D10). (C) Optimization of retroviral transduction using RetroNectin. Transduction efficiency was assessed by Venus expression using flow cytometry. Retrovirus production from a PG13 producer cell line was conducted at 32 °C or 37 °C, and virus-bound plates were prepared by shaking or centrifugation methods. RetroNectin-coated plates were prepared using 20 μg/ml RetroNectin solution. PBMCs were stimulated and expanded using condition #1, and non-transduced cells treated in the same manner were used as a control. This experiment was performed only once. (D) The effect of RetroNectin concentration on transduction efficiency. PBMCs were stimulated using condition #1, and transduced by retrovirus produced at 37 °C. RetroNectin-coated plates were prepared using 10 μg/ml or 20 μg/ml RetroNectin solution, and virus-binding was performed using a centrifugation method. This experiment was performed only once.

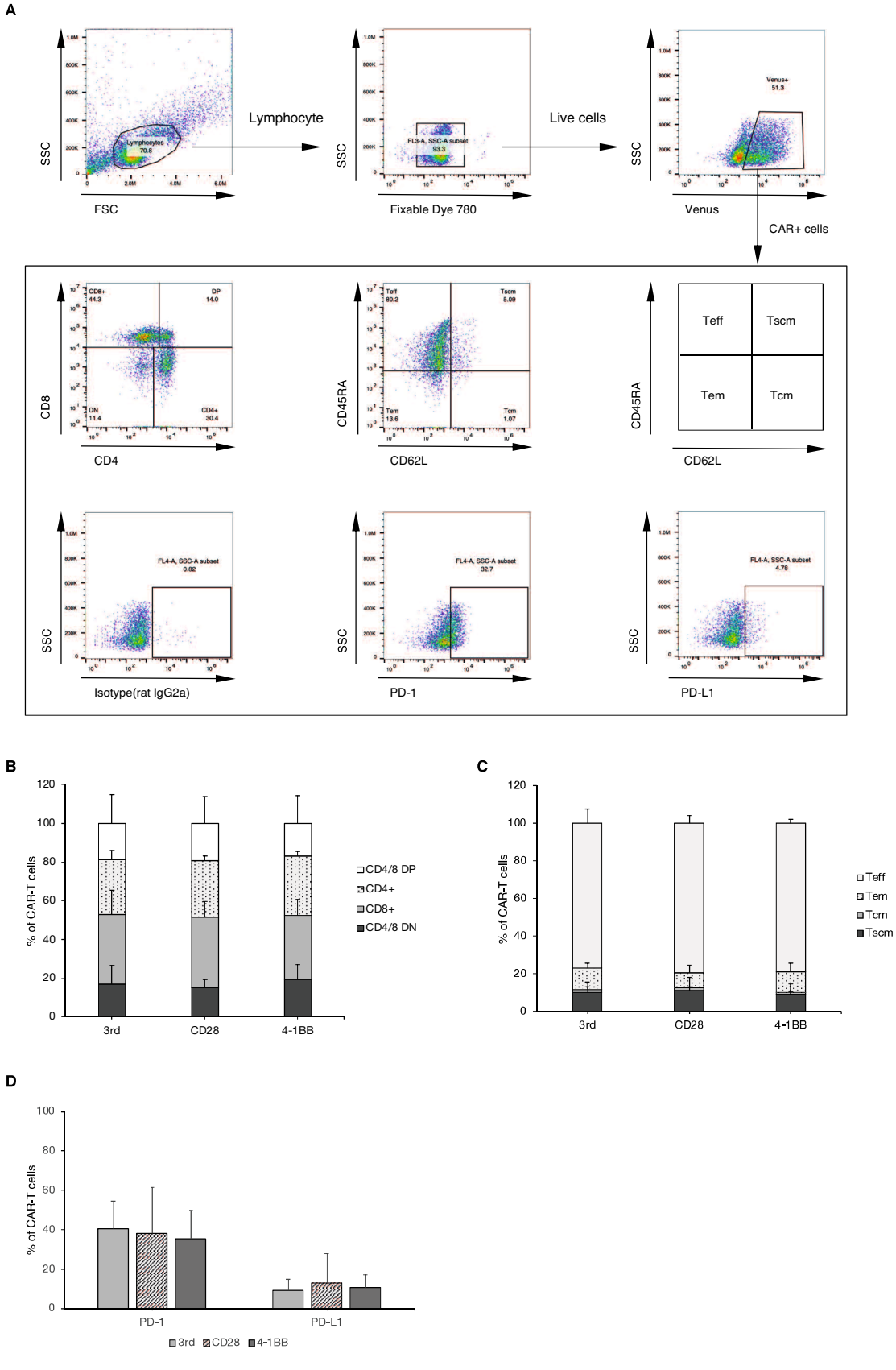
A
SSC
FSC
Lymphocytes
70.8
Lymphocyte
SSC
Fixable Dye 780
FL3-A, SSC-A subset
93.3
Live cells
SSC
Venus
Venus+
51.3
CAR+ cells
CD8
CD4
CD8+
44.3
DP
14.0
DN
11.4
CD4+
30.4
CD45RA
CD62L
Teff
80.2
Tscm
5.09
Tem
13.6
Tcm
1.07
CD45RA
CD62L
Teff
Tscm
Tem
Tcm
SSC
Isotype(rat IgG2a)
FL4-A, SSC-A subset
0.82
SSC
PD-1
FL4-A, SSC-A subset
32.7
SSC
PD-L1
FL4-A, SSC-A subset
4.78
B
% of CAR-T cells
120
100
80
60
40
20
0
3rd
CD28
4-1BB
CD4/8 DP
CD4+
CD8+
CD4/8 DN
C
% of CAR-T cells
120
100
80
60
40
20
0
3rd
CD28
4-1BB
Teff
Tem
Tcm
Tscm
D
% of CAR-T cells
100
80
60
40
20
0
PD-1
PD-L1
3rd
CD28
4-1BB

Fig. IV-2. Phenotypic evaluation of second- and third-generation canine CAR-T cells. PBMCs were stimulated using condition #1 and transduced with second- and third-generation CARs. CAR-expressing cells were stained and analyzed by flow cytometry. Each experiment was independently performed using three healthy dogs. Data are shown as the average of three dogs, and error bars indicate standard deviation. (A) Fluorescence-activated cell sorting (FACS) gating strategy for phenotypic evaluation of CAR-expressing cells. Representative FACS plots of CAR-transduced cells are shown. Lymphocytes are first gated in SSC/FSC dot plot, followed by exclusion of dead cells by Fixable Dye 780 staining. CAR-expressing cells were gated by Venus expression, and phenotypic characteristics were evaluated. (B) Frequency of $CD4^+$ and $CD8^+$ cells. DP: double positive, DN: double negative. (C) T cell memory subset analysis based on CD45RA and CD62L expression. (D) Expression levels of PD-1 and PD-L1 in CAR-T cells.

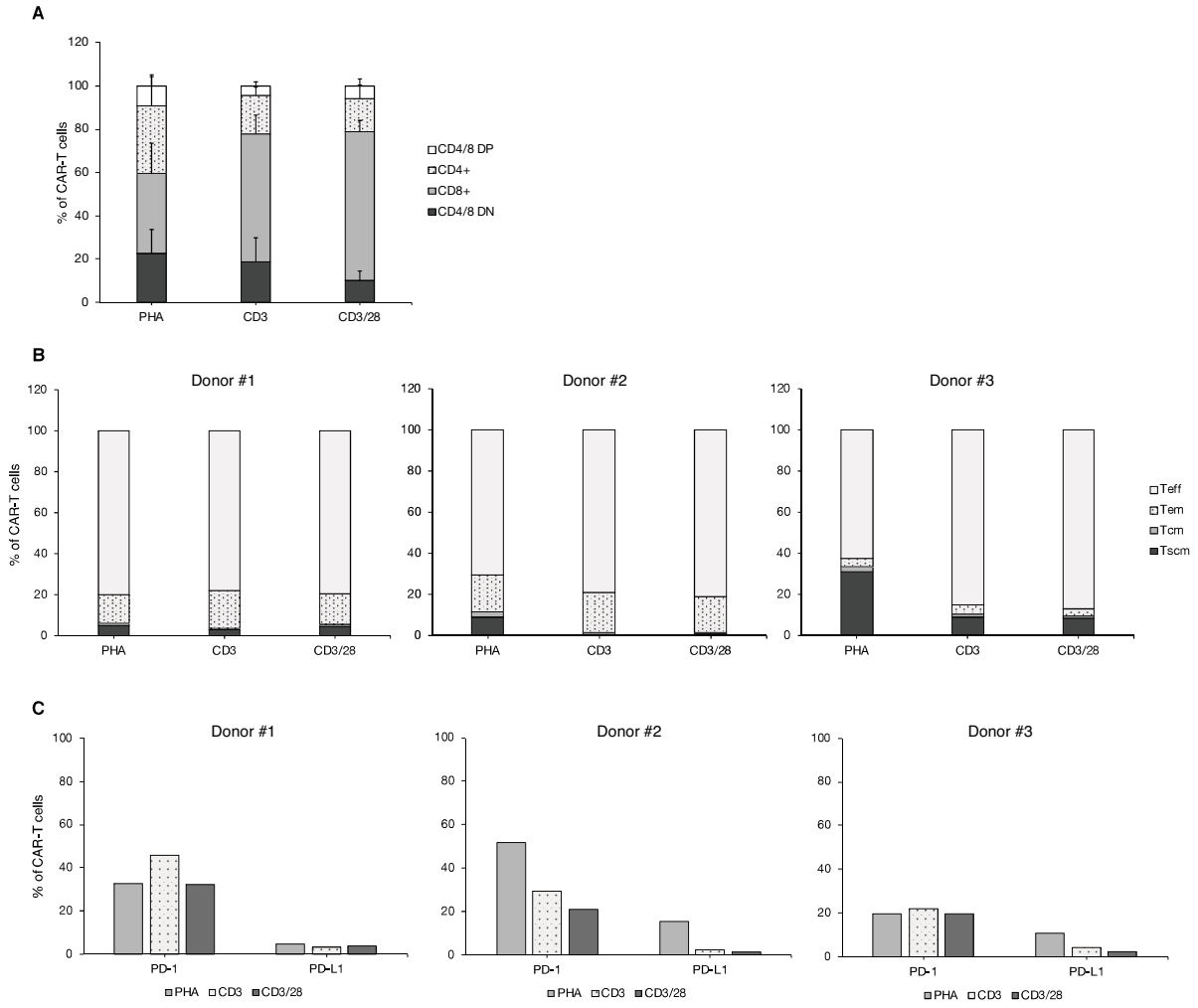

Fig. IV-3. T cell stimulation with CD3/CD28 and its phenotypic effect on CAR-T cells. PBMCs were stimulated by condition #1 (PHA) or condition #2 (CD3 and/or CD28), and transduced with third-generation CARs. CAR-expressing cells were stained and analyzed by flow cytometry. Each experiment was independently performed using three healthy dogs. Data are shown as the average of three dogs, and error bars indicate standard deviation of the results from three dog (A). The results from each dog were shown in each separated graph in B and C. (A) Frequency of $CD4^+$ and $CD8^+$ cells. (B)

T cell memory subset analysis based on CD45RA and CD62L expression. (C) Expression levels of PD-1 and PD-L1 in CAR-T cells.

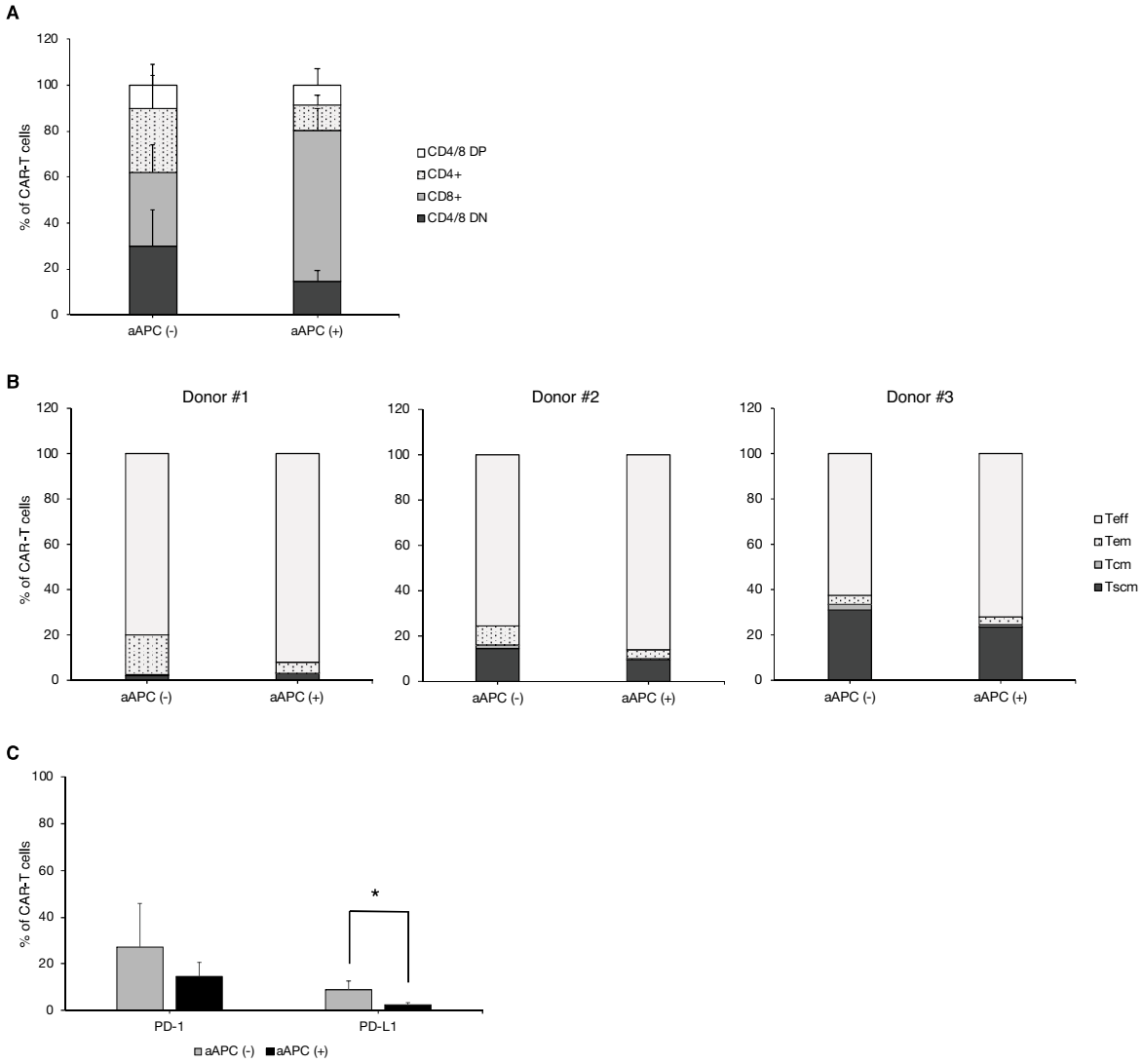

Fig. IV-4. T cell stimulation by artificial antigen presenting cells.

PBMCs were stimulated using condition #1 (PHA) or condition #3 (PHA plus aAPC), and transduced with third-generation CARs. CAR-expressing cells were stained and analyzed by flow cytometry. Data are shown as the average of three dogs, and error bars indicate standard deviation of the results from three dog (A and C). The results from each dog were shown in each separated graph in B. (A) Frequency of $CD4^+$ and $CD8^+$ cells.

(B) T cell memory subset analysis based on CD45RA and CD62L expression. (C) Expression of PD-1 and PD-L1 in CAR-T cells. * indicates $p<0.05$.

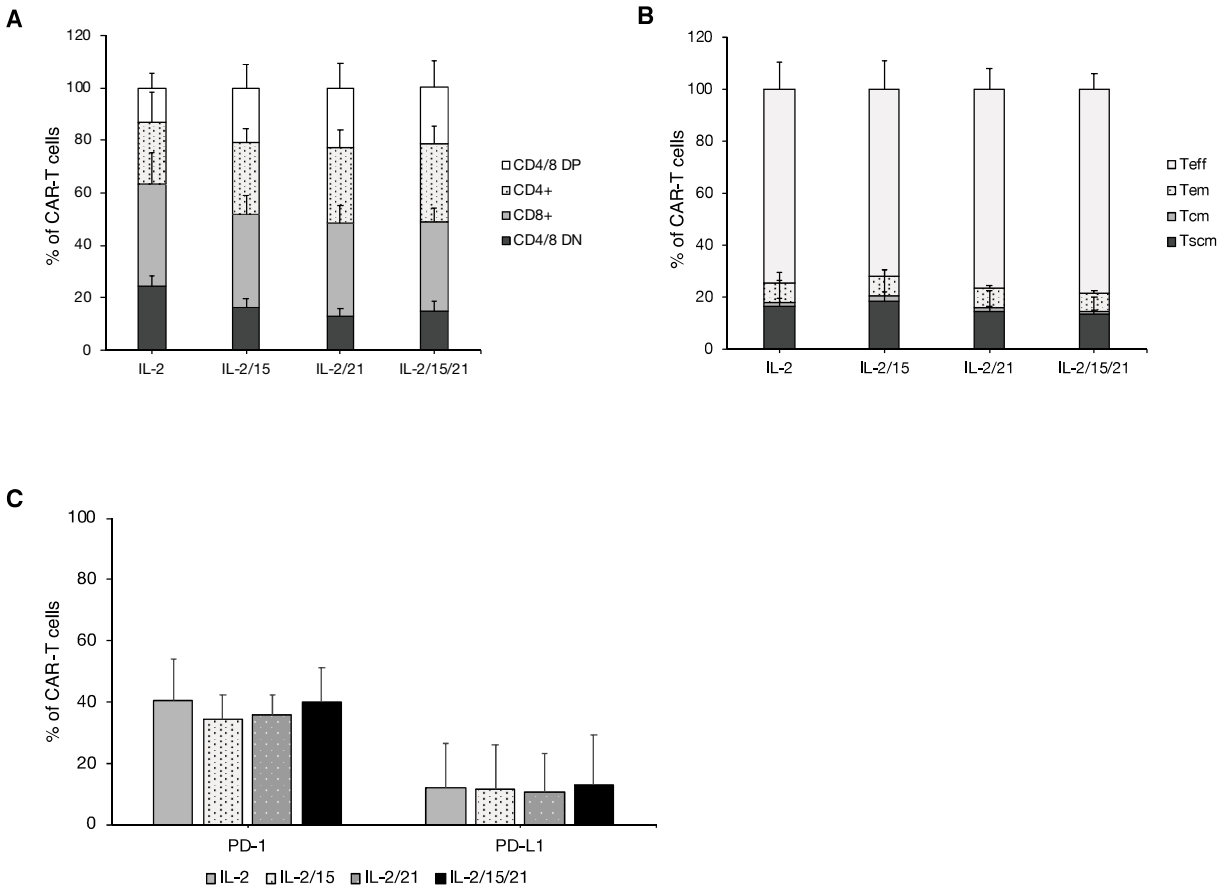

Fig. IV-5. Effect of cytokine modulation in culture conditions.

PBMCs were stimulated using condition #1 or condition #4, and transduced with third-generation CARs. In all conditions, IL-2 was used during cell stimulation and cell expansion. In addition to IL-2, IL-15, and/or IL-21 were used in condition #4. Each experiment was independently performed using three healthy dogs. Data are shown as the average of three dogs, and error bars indicate standard deviation. (A) Frequency of $CD4^+$ and $CD8^+$ cells. (B) T cell memory subset analysis based on CD45RA and CD62L expression. (C) Expression levels of PD-1 and PD-L1 in CAR-T cells.

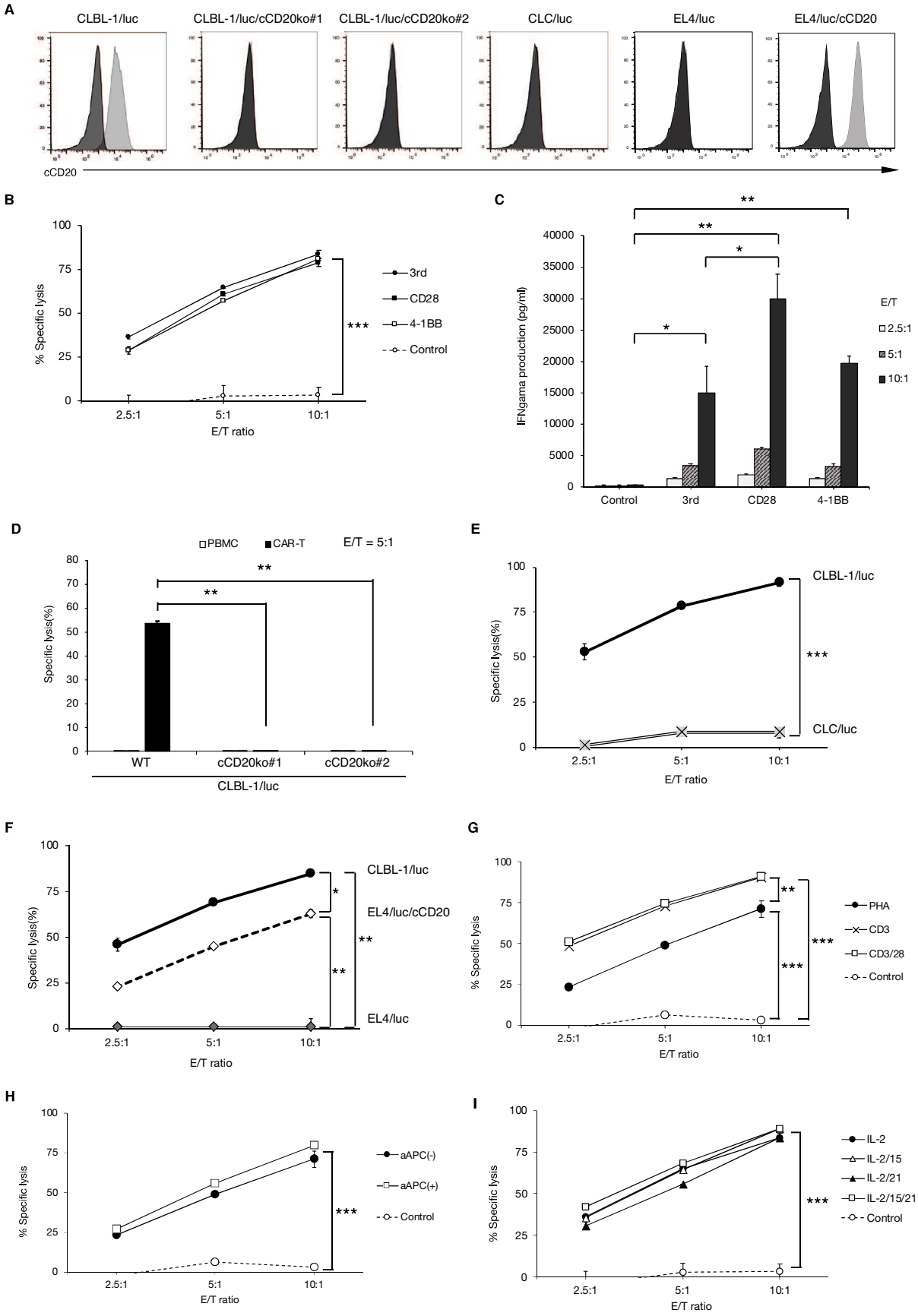
A
CLBL-1/luc
CLBL-1/luc/cCD20ko#1
CLBL-1/luc/cCD20ko#2
CLC/luc
EL4/luc
EL4/luc/cCD20
cCD20
B
% Specific lysis
E/T ratio
2.5:1
5:1
10:1
3rd
CD28
4-1BB
Control
***
C
IFNgama production (pg/ml)
E/T
2.5:1
5:1
10:1
Control
3rd
CD28
4-1BB
D
PBMC
CAR-T
E/T = 5:1
Specific lysis(%)
WT
cCD20ko#1
cCD20ko#2
CLBL-1/luc
E
Specific lysis(%)
CLBL-1/luc
CLC/luc
E/T ratio
F
Specific lysis(%)
CLBL-1/luc
EL4/luc/cCD20
EL4/luc
E/T ratio
G
% Specific lysis
PHA
CD3
CD3/28
Control
E/T ratio
H
% Specific lysis
aAPC(-)
aAPC(+)
Control
E/T ratio
I
% Specific lysis
IL-2
IL-2/15
IL-2/21
IL-2/15/21
Control
E/T ratio

Fig. IV-6. Cytotoxic activity and target specificity of canine CD20 CAR-T cells.

(A) Surface expression of cCD20 on target cell lines. Cells were stained with an anti-canine CD20 monoclonal antibody, and analyzed by flow cytometry. Anti-cCD20 staining (gray histograms) overlaid with control (black histograms). All data except CLBL-1/luc was performed only once, but a representative result from several experiments is shown in the case of CLBL-1/luc cells. (B and C) Cytotoxic activity and IFN-γ production of canine CAR-T cells. Canine second- (CD28 or 4-1BB) and third-generation (3rd) CD20 CAR-T cells were generated using condition #1, and cultured with CLBL-1/luc cells at the indicated E/T ratio. Specific lysis (B) was measured after 4 hours, and IFN-γ (C) was quantified by ELISA. Non-transduced T cells were used as a control. (D, E and F) Target specificity of canine CD20 CAR-T cells. Canine T cells were stimulated using condition #1, and transduced with third-generation CARs. CAR-T cells were cultured with wild-type CLBL-1/luc cells (WT), cCD20 knock-out CLBL-1/luc cells (cCD20ko #1 and #2) (D), CLC/luc cells (E), EL4/luc cells, and EL4/luc/cCD20 cells (F) at the indicated E/T ratio. (G, H and I) PBMCs were stimulated using condition #1 (stimulation with PHA), condition #2 (stimulation with CD3 and/or CD28) (G), condition #3 (stimulation with aAPC) (H), or condition #4 (addition of IL-15 and/or IL-21) (I), and transduced with third-generation CARs. CAR-T cells were cultured with CLBL-1/luc cells and specific lysis was measured after 4 hours. Each experiment was independently performed using three healthy dogs in duplicate, and a representative result from three experiments is shown in (B), (G), (H),

and (I). The ELISA was performed in duplicate, and the result from one experiment with no replicate is shown in (C). The cytotoxic experiments were performed in duplicate in (D), (E), and (F), and the result from one experiment with no replicate is shown. All error bars indicate standard deviation between experimental replicates. *, **, and *** indicate $p<0.05$, $p<0.01$, and $p<0.001$, respectively.

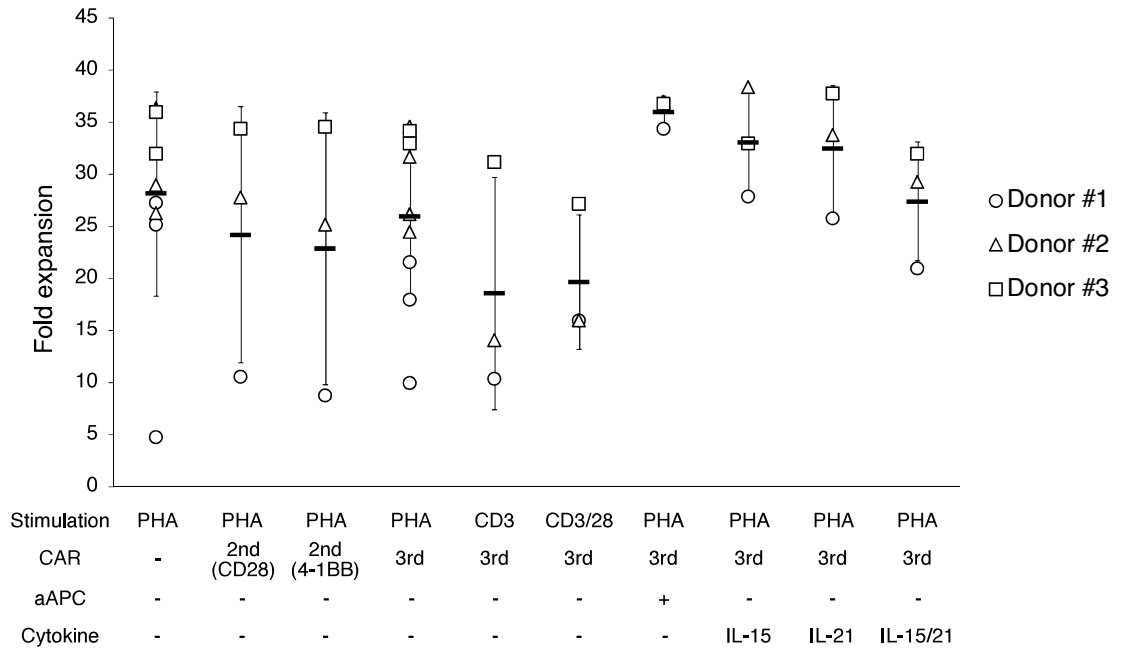

Fig. IV-7. CAR-T cells expansion capacity by various treatment.

Fold expansion during cell expansion period. The total cell numbers of Day 10 was compared with those of Day 3. The results of non-transduced PBMCs, condition #1 (PHA), condition #2 (CD3 and CD3/28), condition #3 (aAPCs), and condition #4 (IL-15, Il-21, and IL-15/21) are shown. The results of second-generation CAR are also shown (CD28 and 4-1BB). Each condition is shown below the figure. PHA: stimulation with PHA, CD3 and CD3/28: stimulation with CD3 and/or CD28 antibodies, CAR: CAR construct (second- and third-generation). CAR(-) means non-transduced control T cells expanded in parallel, aAPC: stimulation with aAPCs, Cytokine: stimulation with indicated interleukins. Bars indicate average, and error bars indicate standard deviation.

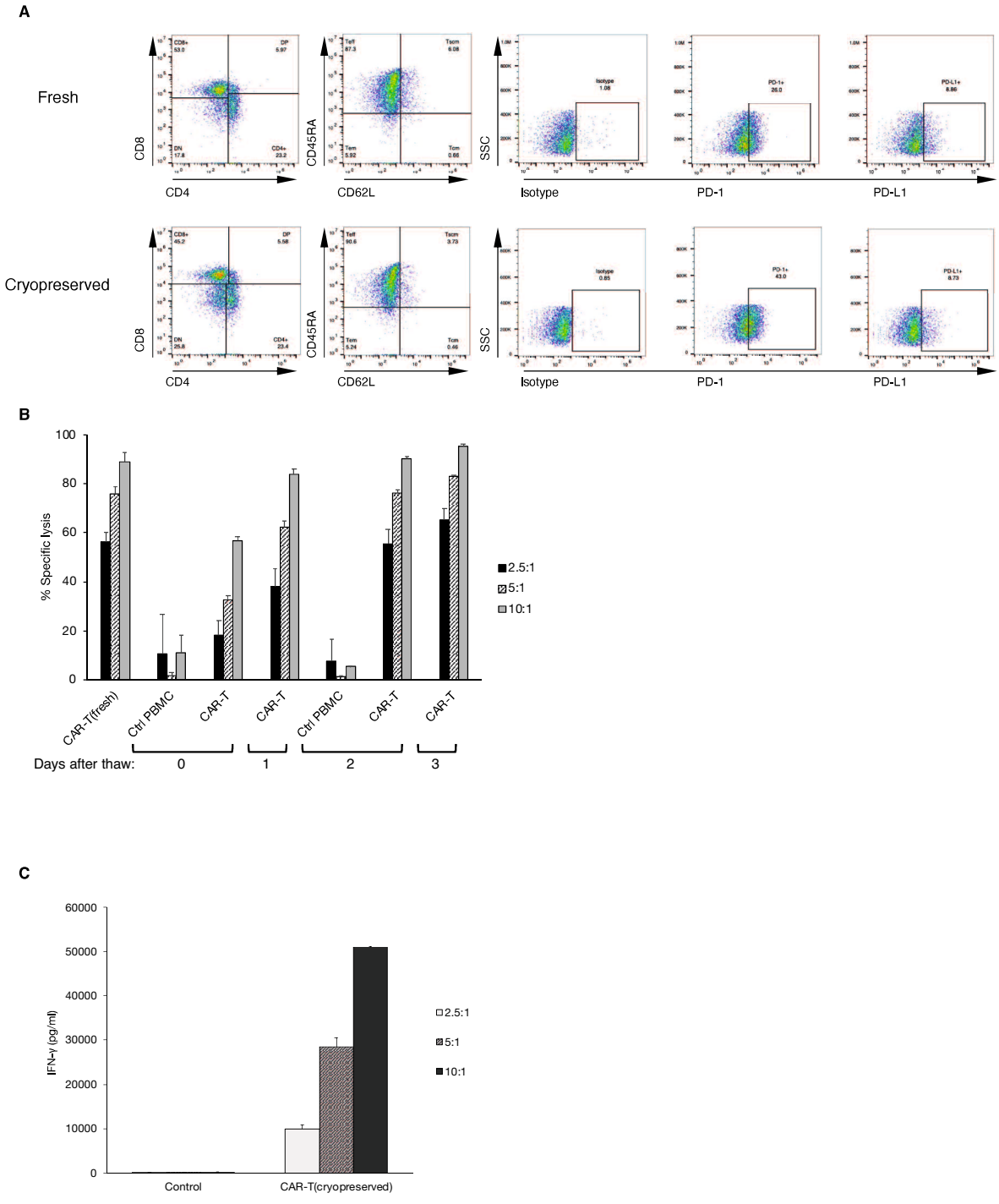

Fig. IV-8. Phenotypic and functional analysis of cryopreserved canine CAR-T cells. PBMCs were stimulated using condition #1 and transduced with third-generation CARs. Cells were expanded until day 10, and then either kept in culture (fresh) or

cryopreserved at -80 °C. Cryopreserved cells were thawed and evaluated. Error bars indicate standard deviation between experimental replicates. (A) Fresh cells on day 12 and cryopreserved cells 2 days after thawing were evaluated by flow cytometry for the indicated surface markers. One representative of two independent experiments is shown. (B) Fresh or cryopreserved cells were cultured with CLBL-1/luc cells at the indicated E/T ratio. Cytotoxic activity of fresh CAR-T cells on day 10 and cryopreserved cells at 0, 1, 2, or 3 days after thawing were measured. The experiment was performed in duplicate, and representative data from two independent experiments are shown. (C) IFN-γ production of cryopreserved CAR-T cells. Cryopreserved cells at 2 days after thawing were cultured with CLBL-1/luc cells at the indicated E/T ratio, and 4 hours later, supernatants were harvested and IFN-γ was measured using an ELISA. The ELISA was performed in duplicate, and the result from one experiment with no replicate is shown.

A

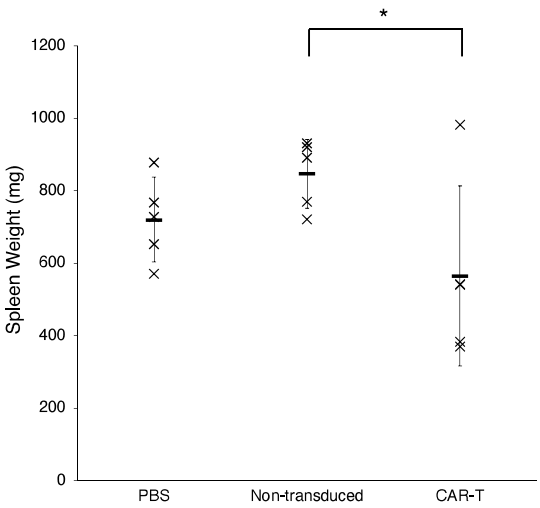
*
1200
1000
800
600
400
200
0
Spleen Weight (mg)
PBS
Non-transduced
CAR-T

B

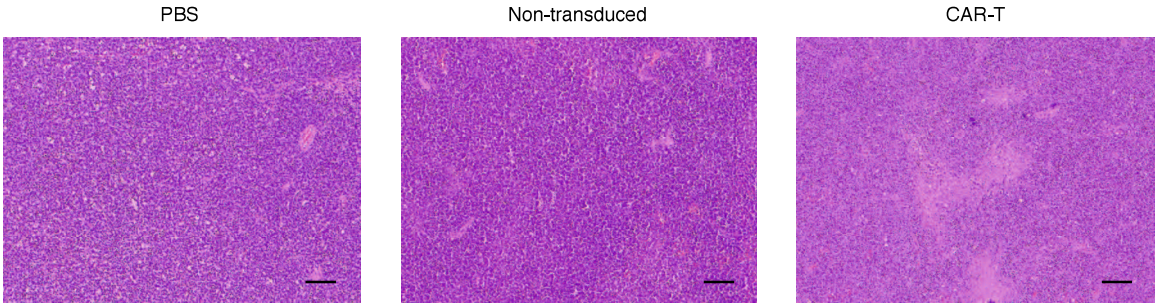
PBS
Non-transduced
CAR-T

C

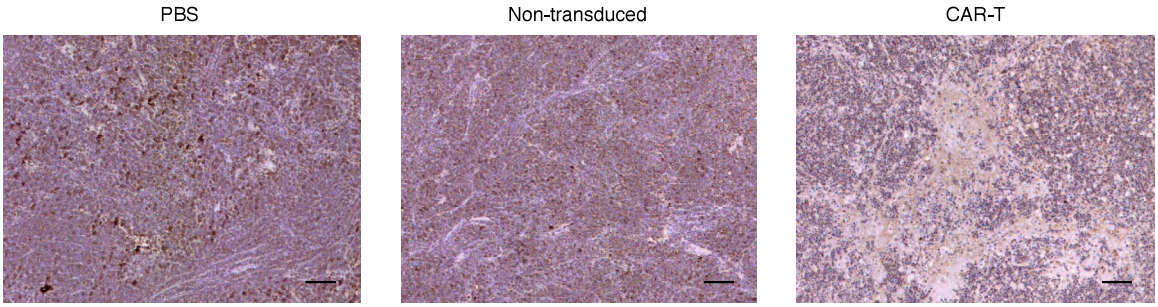
PBS
Non-transduced
CAR-T

D

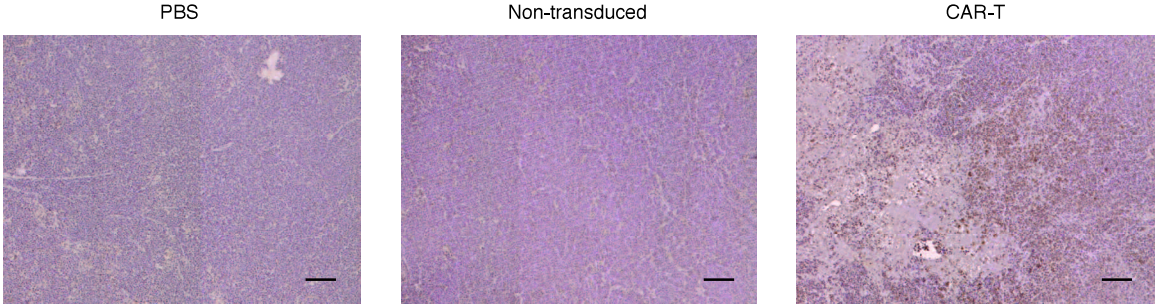
PBS
Non-transduced
CAR-T

Fig. IV-9. *In vivo* antitumor activity of CD20 CAR-T cells.

NOD/SCID mice pretreated with intraperitoneal injection of cyclophosphamide, and 48 hours after pretreatment, CLBL-1/luc cells were intraperitoneally inoculated (day 0). The tumor-bearing mice were received one of the following treatments on day 12, 16, and 20: PBS, non-transduced T cells, and CAR-T cells. (A) Spleen weight of tumor-bearing mice. Bars indicate average, and error bars indicate standard deviation. * indicates $p<0.05$. (B) H&E staining of spleen from representative mice. (C and D) Representative images of immunohistochemical staining. Spleens from tumor-bearing mice were stained for CD79a (C) and CD3 (D). Scale bar indicates 100 μm.

Chapter 5

Optimization of the culture condition for generation of canine CD20-CAR-T cells for adoptive immunotherapy

SUMMARY

Chimeric antigen receptor (CAR) T cell therapy targeting CD20 has a potential to be a promising new treatment for canine B cell lymphoid malignancy. There are many factors which influence the efficacy of infused CAR-T cells, however, optimal approach for producing potent CAR-T cells with favorable phenotype for dogs remains unknown. In this study, we tried several culture conditions, and evaluated its phenotypic effect on CAR-T cells. In the comparison of several kinds of mitogens, stimulation with phytohemagglutinin (PHA) showed high transduction efficacy, while stimulation with concanavalin A (ConA) is superior in memory T cell formation. Akt inhibition at the initial stage of CAR-T production showed a tendency to enhance the transduction efficiency and memory T cell formation. Serum-free media, widely used for *ex vivo* expansion of human T cells for adoptive immunotherapy, turned out to be not suitable for canine CAR-T cell culture. This study provides the fundamental information for understanding *ex vivo* expansion of canine T cells in adoptive immunotherapy.

INTRODUCTION

Canine cancer is clinically important, and attracts attention as relevant model for human cancer. The similarity of human and canine cancer has been reported in some of types of cancer, such as soft tissue sarcoma, osteosarcoma, and lymphoma (Aguirre-Hernández, J. *et al*., 2009, Withrow, SJ. and Wilkins, RM., 2010, Hansen, K. and Khanna, C., 2004). Canine cancer is useful as relevant model especially in the field of immunotherapy, because immunocompetent dogs have an immunosuppressive cancer microenvironment that enables evaluation of the interaction between cancer and immune cells.

Canine B cell lymphoma is one of the most common hematopoietic neoplasms in veterinary medicine. Multi-drug chemotherapy as standard treatment is effective in most cases, however, treatment is often challenging because of relapsed or refractory disease, and drug resistance. Therefore, a novel therapeutic agent is distinctly desired. As with human medicine, the novel immunotherapy, such as adoptive immunotherapy and monoclonal antibody therapy, have been developed in canine medicine (Panjwani, MK. *et al*., 2016, Mizuno, T. *et al*., 2020).

The adoptive transfer of CAR-T cells is a novel cancer immunotherapy which can redirect a patient's T cell to attack cancer cells. CD19-redirected CAR-T cell therapy is a promising strategy for children and adults with B cell malignancies (Turtle, CJ. *et al*., 2016, Neelapu, SS. *et al*., 2017, Curran, KJ. *et al*., 2019, Abramson, JS., 2020), and CD20-redirected CAR-T cell therapy is considered new approach for canine B cell lymphoma (Panjwani, MK. *et al*., 2016). The efficacy of infused CAR-T cells is associated with many factors, such as CAR-positive expression rate, proliferative response, and the persistence of infused cells *in vivo* (Golubovskaya, V. and Wu, L., 2016, McLellan, AD. and Ali Hosseini Rad, SM., 2019). Manufacturing of CAR-T cells is complicated process that involves *ex vivo* cell activation, gene modification and expansion, where many factors influence the quality of final products. Studies indicate that less-differentiated T cells with memory phenotype correlate with *in vivo* proliferation and persistence of CAR-T cells, leading to good clinical outcomes (Xu, Y. *et al*., 2014, Kalos, M. *et al.*, 2011).

Many studies have investigated the strategies to maintain memory phenotype of CAR-T cells (Golubovskaya, V. and Wu, L., 2016, McLellan, AD. and Ali Hosseini

Rad, SM., 2019). These include cytokine modulation, small molecule inhibitors that regulate transcription or metabolic transformation, immune checkpoint blockade, epigenetic modification, or costimulatory domain modification. Several small molecules identified to arrest T cells at the memory T cell stage, and recent studies have highlighted the importance of the Akt pathway in the regulation of T cell differentiation and memory formation (McLellan, AD. and Ali Hosseini Rad, SM., 2019, Mousset, CM. *et al*., 2018). In addition, protocols for generation of CAR-T cells using selective Akt inhibitors have been reported (Urak, R. *et al*., 2017, Zhang, Q. *et al*., 2019).

There are other factors that influence *ex vivo* culture of T cells, such as mitogens for cell stimulation and culture media. Mitogens are widely used to stimulate lymphocytes in culture. M Kazim Panjwani *et al.* used ConA stimulation to prepare canine CAR-T cells, however, its effects on T cell phenotype remain unknown (Panjwani, MK. *et al*., 2016). Generally, culture medium is complemented with serum to support cell growth. Serum provides factors that sustain cell expansion and proliferation, however, in the setting of adoptive immunotherapy, the use of serum is associated with concerns about the risk of contamination and immunogenicity.

Therefore, serum-free medium optimized for expansion of human T cells has developed, and used to expand CAR-T cells (Alnabhan, R. *et al*., 2018). Studies also demonstrated that serum-free media improve memory subset formation and *in vivo* antitumor function (Smith, C. *et al*., 2015, Medvec, AR. *et al*., 2017).

This study evaluated the phenotypic effects in following culture conditions: mitogens modulation, Akt inhibition at the initial stage of T cell stimulation, and use of serum-free media. The effects of culture conditions were assessed by transduction efficiency, memory subset formation, and the expression of activation/exhaustion markers. Our results provide supporting information on canine T cell culturing for adoptive immunotherapy.

MATERIALS AND METHODS

Cells

Retroviral packaging cell lines, Plat-E and PG13, were cultured in D10 complete medium (Dulbecco's modified Eagle's medium supplemented with high glucose, 10% fetal bovine serum (FBS), 100 units/ml penicillin and 100 μg/ml streptomycin, and 55 μM 2-mercaptoethanol). All cell lines were tested for mycoplasma contamination by e-Myco^{TM} Plus Mycoplasma PCR detection kit (iNtRON Biotechnology, Inc., Burlington, MA, USA) in our laboratory, and cultured in a humidified incubator at 37 °C and 5% CO_2.

CAR construction and retrovirus production

A third-generation CAR construct was used in this study (Sakai, O. *et al*., 2020). The anti-canine CD20 single-chain variable fragment (scFv) sequence was derived from the variable region of an anti-CD20 monoclonal antibody developed in our laboratory (Mizuno, T. *et al*., 2020). The CAR construct was comprised of the anti-CD20 scFv linked to the canine CD8α hinge and transmembrane domain, followed by

the canine CD28 and 4-1BB co-stimulatory domain, and human CD3ζ signaling domain. For the co-expression of CARs together with fluorescent protein, the CAR construct was followed by a P2A peptide fused to Venus fragments. This CAR-P2A-Venus construct was ligated into the PacI and HincII site of the MSGV Hu Acceptor PGK-NGFR (Addgene).

To obtain a PG13 cell line stably producing viruses, retrovirus particles were generated by transient transfection of Plat-E cells with the CAR-encoding retrovirus vector. Supernatants containing the retrovirus were collected after 48 hours, and used to transduce the PG13 for the retroviral production for T cell transduction.

Retroviral production from the PG13 producer cell line was conducted as follows. First, 3×10^6 transduced PG13 cells were seeded in T75 flasks and cultured in a CO_2 incubator at 37 °C. Twenty-four hours later, the culture media was changed to fresh DMEM containing 10% FBS, 100 units/ml penicillin, 100 μg/ml streptomycin, and 5 mM sodium butyrate and incubated for 24 hours. The retrovirus-containing supernatants were filtered through 0.45 μm filters and stored at -80 °C until use.

Cell stimulation, transduction, and expansion of CAR-T cells

All blood samples were obtained from healthy beagle dogs kept as blood donors for Yamaguchi University Animal Medical Center. Peripheral blood mononuclear cells (PBMCs) were isolated using Lymphoprep (Axis-Shield, Oslo, Norway) gradient centrifugation and then stimulated described below in the presence of 200 U/ml of recombinant human IL-2 (Proleukin; Novartis, Basel, Switzerland) for 72 hours.

To evaluate the phenotypic effect, various conditions were tested during CAR-T manufacturing as follows: mitogens (condition #1), Akt inhibitors (condition #2), and culture media (condition #3). Culture conditions used in this study are summarized in Table V-1. In condition #1, cells were stimulated with phytohemagglutinin (PHA, 5 μg/ml; Sigma, St. Louis, MO, USA), concanavalin A (ConA, 5 μg/ml; Calbiochem, San Diego, CA, USA), or phorbol myristate acetate (PMA, 25 ng/ml; Calbiochem) plus ionomycin (Iono, 1 μg/ml; Calbiochem) for first 72 hours. In condition #2, cells were stimulated with PHA or ConA, and Akt inhibitors were added for first 120 hours: Akt Inhibitor VIII (12 μM; Cayman Chemical, Ann Arbor, MI, USA) or GDC-0068 (1 or 10

μM; Cayman Chemical). R10 complete medium (RPMI1640 supplemented with 10% FBS, 100 units/ml penicillin and 100 μg/ml streptomycin, and 55 μM 2-mercaptoethanol) was used for culture of PBMCs in condition #1 and #2. In condition #3, in addition to R10 complete medium, two serum-free medium, LymphoONE T-cell Expansion Xeno-Free Medium (LymphoONE; TaKaRa Bio, Shiga, Japan) and CTS OpTmizer T-cell Expansion SFM (OpTmizer; Thermo Fisher Scientific, Waltham, MA, USA), were also used according to manufacturer's instructions. CTS Immune Cell Serum Replacement (SR; 2 or 5%; Thermo Fisher Scientific) was added to the OpTmizer as indicated.

Retroviral transduction was performed after initial stimulation using recombinant human fibronectin fragment (RetroNectin; TaKaRa Bio, Shiga, Japan). Non-treated 24-well culture plates were coated with 0.5 ml of RetroNectin solution (10 μg/ml) diluted with PBS for 2 hours at room temperature in accordance with the manufacturer's instructions. After removal of the RetroNectin solution, plates were washed with PBS. Then, 0.5 ml of retrovirus-containing supernatants were added to the RetroNectin-coated plate, and preparation of a virus-bound plate was performed using

centrifugation methods (2000 × g for 2 hours at 4 °C). A total of 2.5×10^5 stimulated T cells was added to the virus-bound plates and incubated in a 37 °C, 5% CO_2 incubator for 24 hours, followed by the second virus infection in the same manner. To promote contact between T cells and viral particles, plates were centrifuged at 500 × g for 1 min after second infection.

After retroviral transduction, CAR-T cells were subsequently expanded with 200 U/ml IL-2 for 6 days. Non-transduced T cells, used as controls, were stimulated with PHA or ConA and expanded in parallel in the presence of 200 U/ml IL-2.

Flow cytometry

CAR-T cells were collected and washed with PBS, followed by incubation with Fixable Viability Dye eFluor 780 (eBioscience, Inc. Vienna, Austria) for 30 min on ice. Then, cells were resuspended in FACS buffer (PBS containing 2% FBS and 0.1% NaN_3). A total of 2×10^5 cells was stained with each antibody for 30 min on ice. After incubation, cells were washed and fixed in 1% paraformaldehyde and stored until analysis. For T cell phenotyping, the following antibodies were used: mouse anti-dog

CD3 (clone CA17.2A12; dilution 1:500), mouse anti-dog CD21 RPE (clone CA2.1D6; dilution 1:20) and mouse anti-human CD62L RPE (clone FMC46; Bio-Rad Laboratories, Inc. Hercules, CA, USA; dilution 1:20); rat anti-dog CD8α APC (clone YCATE55.9; eBioscience; dilution 1:20); mouse anti-dog CD4 (clone CA13.1E4; dilution 1:4), and mouse anti-dog CD45RA (clone CA21.4B3; undiluted) kindly provided by P.F. Moore (University of California, Davis). Anti-human CD62L antibody was confirmed to cross-react with canine cells in previous report (Withers, SS. *et al*., 2018). For analysis of PD-1 and PD-L1 expression on CAR-T cells, anti-cPD-1 (clone 4F12-E6; concentration 10 μg/ml) and anti-cPD-L1 (clone G11-6; concentration 10 μg/ml) antibodies prepared in our laboratory were used (Nemoto, Y. *et al*., 2018). Purified rat IgG2a antibody (clone RTK2758; BioLegend, San Diego, CA, USA; concentration 10 μg/ml) was used as isotype control for anti-cPD-1 and anti-cPD-L1 antibodies.

Samples were analyzed using an Accuri C6 (BD Biosciences, San Diego, CA, USA), and results were analyzed using FlowJo software (BD Biosciences).

RESULTS AND DISCUSSION

We have previously reported the basic optimization of CAR-T generation (Sakai, O. *et al*., 2020 and chapter 4). Although the previous study revealed optimal transduction protocol to generate CAR-expressing canine T cells, culture conditions and cell stimulation protocol which can produce potent CAR-T cells with favorable phenotype for adoptive immunotherapy remain elusive. In this chapter, we further investigated the following points: mitogens, small molecule inhibitors, and serum-free medium (Table V-1). The phenotypic effects of these factors were assessed by transduction efficiency, differentiation status of T cells, and T cell exhaustion. Transduction efficiency was assessed by the expression of Venus fluorescent protein. To evaluate the T cell differentiation status, we assessed the expression of CD45RA and CD62L, and CAR-T cells were classified into four differentiation subsets: stem cell memory T cells (Tscm, CD45RA+CD62L+), central memory T cells (Tcm, CD45RA-CD62L+), effector memory T cells (Tem, CD45RA-CD62L-), and effector T cells (Teff, CD45RA+CD62L-). We also assessed PD-1 and PD-L1 expression to evaluate one of the exhausted markers of T cells.

Firstly, we evaluated the effect of mitogens on phenotypic changes in CAR-T cells (condition #1). As shown in Figure V-1, similar results were obtained from two healthy donors. As shown in Figure V-1A, stimulation with PHA resulted in the highest gene transduction rate (67.2% in donor #1 and 32.8% in donor #2), followed by stimulation with ConA (49.1% in donor #1 and 28.4% in donor #2) and PMA plus ionomycin (26.2% in donor #1 and 10.6% in donor #2). Phenotypic analysis of CAR-T cells revealed that CAR-T cells generated by ConA stimulation showed the highest number of Tscm subset, followed by PMA plus ionomycin stimulation and PHA stimulation (Fig. V-1B). Stimulation with ConA and PMA plus ionomycin resulted in decreased PD-1 expression in both donors, while decreased PD-L1 expression was observed only in ConA-stimulated cells from donor #1 (Fig. V-1C). These mitogens are widely used to stimulate lymphocytes, however, there are no studies that compare the effects of these mitogens. Although there is one report which describes the activating effects of these mitogens on canine B and T lymphocytes, the effects on transduction efficiency and cell phenotype are still unclear (Krakowka, S. and Ringler, SS., 1986). Our results indicate that the effects of transduction efficiency and cell phenotype vary

depends on each mitogen, and stimulation with ConA enhances memory T cell formation.

Next, we assessed how Akt inhibition influenced the phenotype of canine CAR-T cells (condition #2). In this experiment, PBMCs from five donors were used: PBMCs from two donors were stimulated with PHA, and the remaining were stimulated with ConA. Since two results from PHA-stimulated PBMCs and two of three results from ConA-stimulated PBMCs showed similar patterns, the representative data from three donors are shown in Figure V-2. In all samples from five donors, irrelevant of stimulation, Akt inhibition improved CAR-expression rate (Fig. V-2A). As shown in Figure V-2B, Akt inhibition by Akt inhibitor VIII resulted in increased number of Tscm subset in both two samples from PHA-stimulated PBMCs, and one of three samples from ConA-stimulated PBMCs (donor #1). Meanwhile, increment of Tscm subset by Akt inhibition was not observed in two of three samples from ConA-stimulated PBMCs (Fig. V-2B, donor #2). Decreased expression of PD-1 by Akt inhibition was observed in both two samples from PHA-stimulated PBMCs, and one of three samples from ConA-stimulated PBMCs (Fig. V-2C, PHA and donor #1). Akt inhibition by Akt inhibitor VIII

showed greater decrease in PD-1 expression than GDC-0068. In two of three samples from ConA-stimulated PBMCs, decreased expression of PD-1 and PD-L1 by Akt inhibition was not observed (Fig. V-2C, donor #2). The changes observed in this study, such as the increase of transduction efficiency and memory subset and the decrease of PD-1 expression, are considered to contribute clinical efficacy in CAR-T cell therapy. Qing Zhang et al. have also reported that Akt inhibition enhanced CAR-expression rate and memory phenotype (Zhang, Q. *et al*., 2019). The same results were observed, however, our results indicate that, especially in ConA-stimulated PBMCs, the effects of Akt inhibition are different between individuals. In addition, further studies are needed to whether Akt inhibition actually contributes to clinical efficacy of canine CAR-T cell therapy.

Finally, we examined whether the serum-free media could be used for canine CAR-T generation (condition #3). Instead of using R10 complete medium, two serum-free media, LymphoONE and OpTmizer, were used. Serum replacement was added to OpTmizer to evaluate the effect on canine T cells. As a result, PBMCs from three of four donors could expand in LymphoONE medium, while almost no cell growth was

observed in OpTmizer medium (Fig. V-3A). Moreover, PBMCs from two donors showed superior cell expansion in LymphoONE medium, compared to that in R10 complete medium (Fig. V-3A, donor #2 and #4). However, FACS analysis of collected cells revealed that the CAR-expression levels were low in serum-free conditions, especially in LymphoONE medium (Fig. V-3B). Moreover, the results from samples cultured in OpTmizer medium demonstrated that addition of serum replacement resulted in decreased CAR-expression levels. These results indicate that these serum-free media and serum replacement, optimized for human cell culture, are not suitable for preparation of canine CAR-T cells. However, there is still possibility that LymphoONE medium can be used for other adoptive cell therapy. Canine cell culture using serum-free medium is reported in cell line and mesenchymal stem cells (MSCs), however, information about culturing of canine PBMCs using serum-free medium is still lacking (Huang, D. *et al*., 2015, Devireddy, LR. *et al*., 2019). Development of novel serum-free medium which is optimized to expand canine PBMCs may help in producing more effective canine CAR-T cells.

In this study, we revealed effects of each mitogen on CAR-T cell phenotype.

We also demonstrated that Akt inhibition enhances the CAR-expression rate and memory phenotype. These results provide useful information in not only CAR-T cell therapy, but also other adoptive immunotherapy for canine cancer.

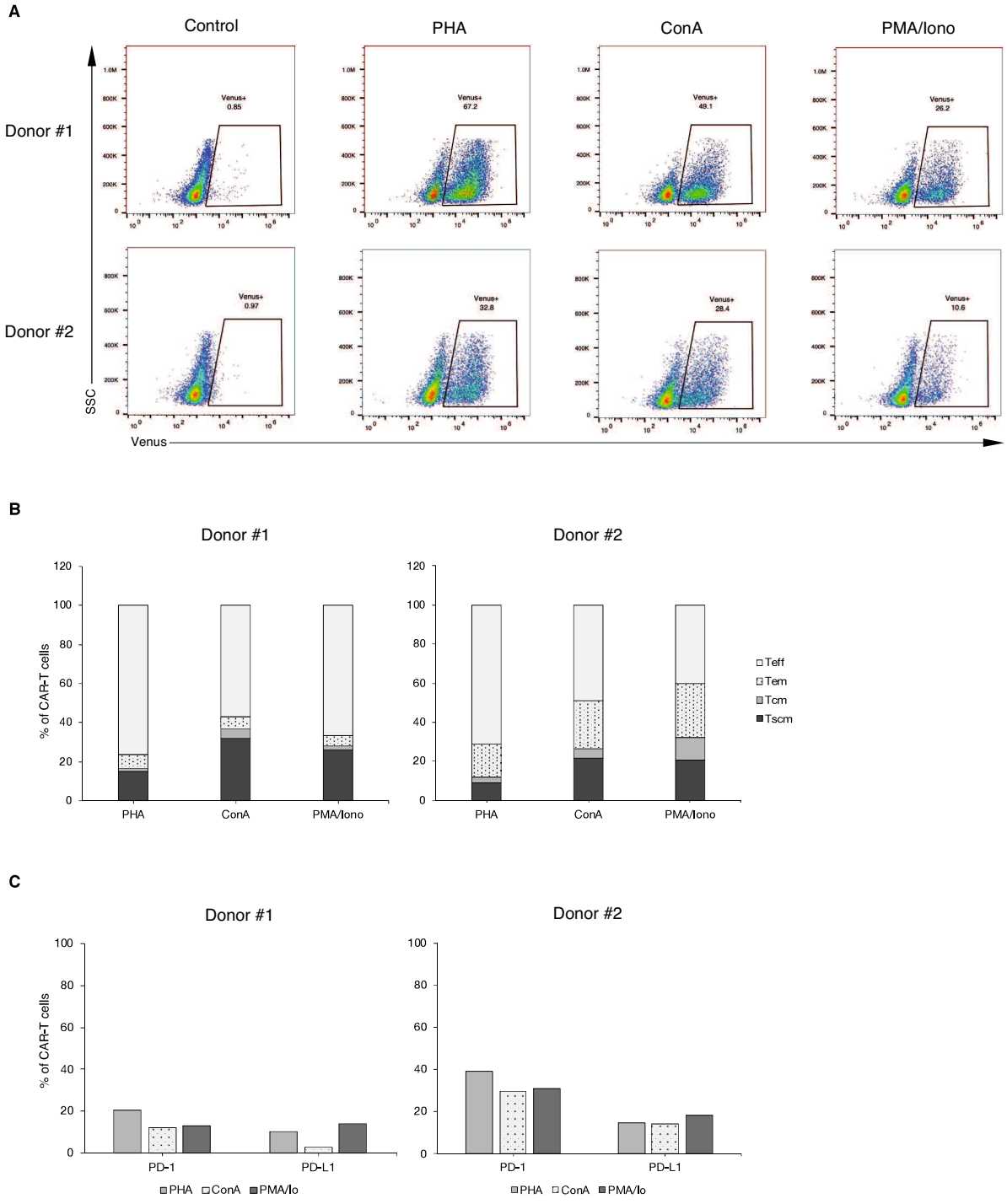

Fig. V-1. T cell stimulation with three mitogens and its effect on CAR-T cells.

PBMCs were stimulated using either of three mitogens and transduced with third-generation CAR construct. Control cells were stimulated with PHA and expanded in

parallel without transduction. Transduction efficiency was assessed by Venus expression using flow cytometry. CAR-expressing cells were stained and analyzed by flow cytometry. Each experiment was independently performed using two healthy dogs. (A) Transduction efficiency of CAR. (B) T cell memory subset analysis based on CD45RA and CD62L expression. (C) Expression levels of PD-1 and PD-L1 in CAR-T cells. CAR-T, chimeric antigen receptor T cells; PHA, phytohemagglutinin; ConA, concanavalin A; PMA, phorbol myristate acetate; Iono, ionomycin; Teff, effector T cells; Tem, effector memory T cells; Tcm, central memory T cells; Tscm, stem cell memory T cells

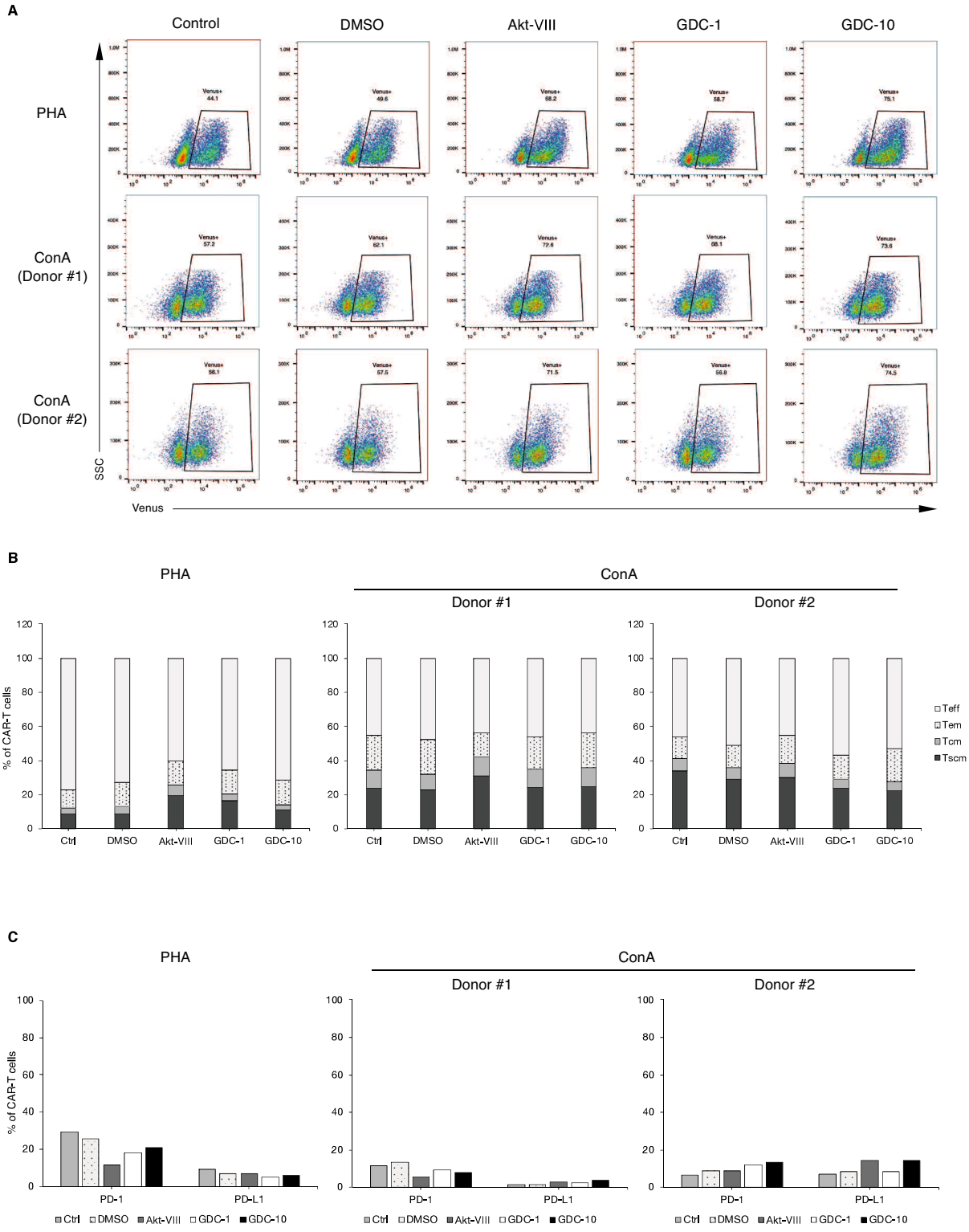
A
Control
DMSO
Akt-VIII
GDC-1
GDC-10
PHA
ConA (Donor #1)
ConA (Donor #2)
SSC
Venus
B
PHA
ConA
Donor #1
Donor #2
% of CAR-T cells
Ctrl
DMSO
Akt-VIII
GDC-1
GDC-10
Teff
Tem
Tcm
Tscm
C
PHA
ConA
Donor #1
Donor #2
% of CAR-T cells
PD-1
PD-L1
Ctrl
DMSO
Akt-VIII
GDC-1
GDC-10

Fig. V-2. Effect of Akt inhibition during T cell stimulation.

PBMCs were stimulated using PHA or ConA, and transduced with third-generation CAR. Akt inhibitors were added to culture medium for first 120 hours during CAR-T cell manufacturing; Akt Inhibitor VIII (12 μM) or GDC-0068 (1 or 10 μM). No-addition control (control) and vehicle control (0.05% DMSO) were stimulated and transduced in parallel. Transduction efficiency was assessed by Venus expression using flow cytometry. CAR-expressing cells were stained and analyzed by flow cytometry. Each experiment was independently performed using five healthy dogs (PHA, n=2; ConA, n=3), and representative data are shown. (A) Transduction efficiency of CAR. (B) T cell memory subset analysis based on CD45RA and CD62L expression. (C) Expression levels of PD-1 and PD-L1 in CAR-T cells. CAR-T, chimeric antigen receptor T cells; PHA, phytohemagglutinin; ConA, concanavalin A; Akt-VIII, Akt Inhibitor VIII; GDC-1, 1 μM GDC-0068; GDC-10, 10 μM GDC-0068; Teff, effector T cells; Tem, effector memory T cells; Tcm, central memory T cells; Tscm, stem cell memory T cells

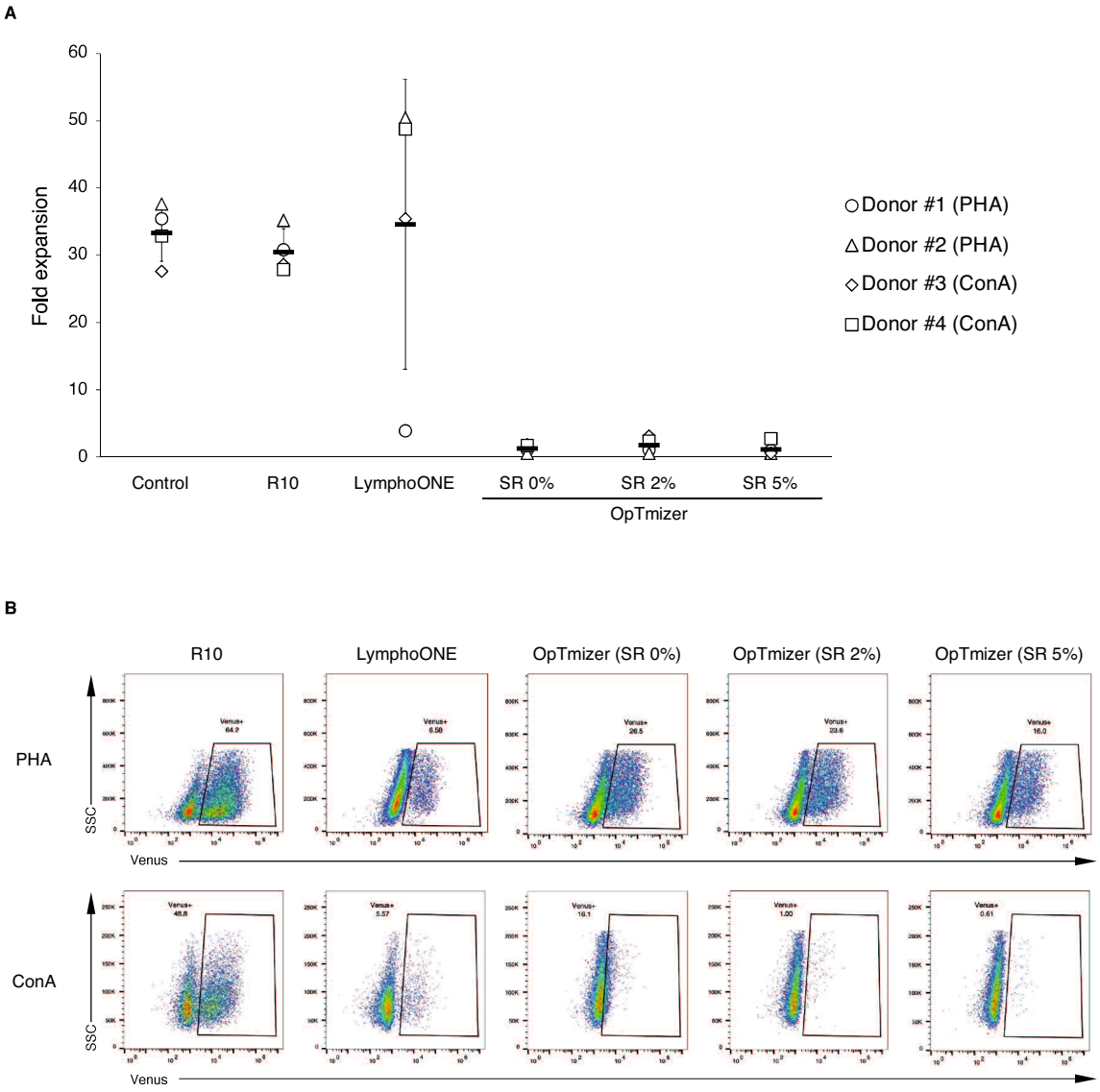

Fig. V-3. CAR-T cell production using serum-free media.

PBMCs were stimulated using PHA or ConA, and transduced with third-generation CAR. R10 complete medium or two serum-free media were used during all culture period, and serum replacement (2 or 5%) was added to the OpTmizer medium. (A) Fold expansion during cell expansion period. The total cell numbers of Day 10 was compared with those of Day 3. Control shows the results of non-transduced PBMCs. Bars indicate average, and error bars indicate standard deviation. (B) Transduction

efficiency was assessed by Venus expression using flow cytometry. Each experiment was independently performed using two healthy dogs, and representative data are shown. PHA, phytohemagglutinin; ConA, concanavalin A; R10, R10 complete medium; LymphoONE, LymphoONE T-cell Expansion Xeno-Free Medium; OpTmizer, CTS OpTmizer T-cell Expansion SFM; SR, CTS Immune Cell Serum Replacement

Table V-1. Culture conditions for the generation of CAR-T cells.

Condition	Cell stimulation	Akt inhibitor	Culture medium	Number of donors*
#1	PHA ConA PMA/Iono	-	R10	2
#2	PHA	- DMSO Akt-inhibitor VIII GDC-0068 (1 µg/ml) GDC-0068 (10 µg/ml)	R10	2
	ConA	- DMSO Akt-inhibitor VIII GDC-0068 (1 µg/ml) GDC-0068 (10 µg/ml)	R10	3
#3	PHA	-	R10 LymphoONE OpTmizer (SR 0%) OpTmizer (SR 2%) OpTmizer (SR 5%)	2
	ConA	-	R10 LymphoONE OpTmizer (SR 0%) OpTmizer (SR 2%) OpTmizer (SR 5%)	2

* Each donor was used once for each experimental condition.
Abbreviations: PHA, phytohemagglutinin; ConA, concanavalin A; PMA, phorbol myristate acetate; Iono, ionomycin; SR, serum replacement.

GENERAL DISCUSSION

In chapter 1, the expression of WT1 protein in canine tissue was investigated by immunohistochemistry. The results revealed that WT1 expression was detected in all of the canine lymphoma tissues used in this study. This indicates that, as same as in human cancer, high levels of wild-type WT1 are expressed in canine cancer. WT1 is one of the most characterized TAAs which is ranked as a high priority antigen target for therapeutic cancer vaccines by the National Cancer Institute (Cheever, MA. *et al*., 2009). Recently, one report has been published in which cell block tube sections of cavitary effusions from dogs and cats were immunostained with panel antibodies including WT1 (Marcos, R. *et al*., 2019). However, an extensive expression profile of WT1 and its oncogenic role in canine cancer is not fully elucidated. Further investigation is needed to understand the potential of cWT1 as target for cancer immunotherapy. Another significance of this study is the validation of antibody specificity. In many veterinary researches, antibodies specific for human antigen are widely used. Therefore, prudent interpretation is needed in its use for other species. In this study, we verified the antibody specificity by western blotting using over-expressing cells, showing exemplary method for detection of canine antigens.

Next, based on the recent developments in cancer immunotherapy, I focused on canine CAR-T cell therapy targeting CD20. In human CAR-T cell therapy, CD19 is the most frequently targeted antigen in clinical trials for hematological malignancies (Hartmann, J. *et al*., 2017, Sha, HH. *et al*., 2017). On the other hand, the expression of

CD20 is well established in canine lymphocytes and lymphoma cells, compared to that of CD19 (Kano, R. *et al*., 2005, Jubala, CM. *et al*., 2005). Therefore, to date, CD20 is mainly used as target molecule for canine CAR-T cell therapy and monoclonal antibody therapy. To establish the antibody which can detect CD20-CAR, immunization was conducted using CD20-CAR-expressing cells, and it resulted in production of two monoclonal antibodies, as described in chapter 2 and 3. It was demonstrated that monoclonal antibody specific to CD20-CAR can be used not only to detect the surface expression of CAR, but also to detect the therapeutic anti-canine CD20 antibody. Antibody therapy is the closest to clinical application in novel approach for canine B cell lymphoma, and this antibody will help to determine the *in vivo* kinetics of therapeutic antibody. The monoclonal antibody against canine CD8 was assessed whether it can be used in immunohistochemistry, because antibodies which can be used in immunohistochemistry using FFPE tissues from dogs and cats are very scarce. This antibody also will be good tool for cancer research.

As described in chapter 4 and 5, the establishment and characterization of canine CAR-T cell are the most important part of my PhD thesis. I generated two second-generation and one third-generation CAR-T cells. All of these CAR-T cells showed high *in vitro* cytotoxic activity against canine B cell lymphoma, however, the detailed difference between generations is unclear. Ramos CA *et al*. reported that, in patients with relapsed or refractory non-Hodgkin lymphoma, third-generation CD19-

CAR-T cells showed superior expansion and longer persistence than second-generation CD19-CAR-T cells (Ramos, CA. *et al*., 2018). Their results suggest that *in vivo* setting is needed to evaluate the difference between second-generation and third-generation CAR-T cells. The phenotypic change of CAR-T cells under various culture conditions is also assessed, mainly focused on memory T cell subset, because cells with memory phenotype in CAR-T product correlate with the clinical efficacy. Unfortunately, the culture conditions used in chapter 4 were turned out not to increase the memory subset. In chapter 5, it is demonstrated that ConA stimulation and Akt inhibition resulted in increased memory subset. However, the phenotypic change was not so drastic, and further optimization is needed to obtain more potent canine CAR-T cells. As a more fundamental problem, there exists a concern about the validation of classification criteria of memory lymphocyte subsets in dogs. Based on the previous report that evaluated age-related changes in memory subset in dogs, I assessed the expression of CD45RA and CD62L, and classified cells into each subset (Withers, SS. *et al*., 2018). In addition to CD45RA and CD62L, many surface markers have been identified for classification of T cell subsets in human and mouse, such as CD45RO, CCR7, CD127, CD27, and CD28 (Busch, DH. *et al*., 2016). Moreover, as reviewed by Jameson SC and Masopust D, the distinction of memory T cell populations is still challenging, because there coexist functionally and phenotypically distinction, and these criteria are not completely overlapped (Jameson, SC. and Masopust, D., 2018). The functional

characterization of canine memory T cell populations, as well as the identification of surface “memory” markers, is indispensable for generating cell products with optimal efficacy and safety profile.

In the course of my studies, I revealed that WT1, one of the most promising TAAs in human cancer, is highly expressed in canine lymphoma tissues. I also established two monoclonal antibodies against CAR and canine CD8, which can be used as diagnostic tools. And finally, I demonstrated the therapeutic potential of canine CD20-CAR-T cells. However, further investigations, such as quality-control assays including check of pathogenic contamination and residual replication competent retrovirus (RCR) and *in vivo* evaluation of kinetics and adverse effects, are necessary for clinical application. In human CAR-T cell therapy, new strategies are still discussed to address emerging issues, such as the limited efficacy against solid tumors, antigen loss relapse, and on-target/off-tumor toxicity (Wang, Z. *et al*., 2017). Large animal models, such as porcine and canine cancer models, can mimic the complexities of human disease, providing good platforms for investigation of therapeutic agent delivery and safety profile. The establishment of canine model for evaluating CAR-T cell therapy may help human patients as well as canine patients. I hope that future studies will unveil these issues, and CAR-T cell therapy will be new treatment option for canine patients with B cell lymphoma.

ACKNOWLEDGMENTS

I would like to express my sincere gratitude and appreciation to *Prof. Takuya Mizuno* for being a truly ideal supervisor and for kindly guiding me all steps of the way. I am highly indebted to him for his stimulating suggestions and encouragement that helped me in all the time of research and writing of this thesis.

I would like to appreciate to *Assis. Prof. Yuki Nemoto* and *Assis. Prof. Masaya Igase* for assisting me with my experiments. Their meticulous comments were an enormous help to me.

I am grateful to *Prof. Yasuyuki Endo* (*Laboratory of Veterinary Internal Medicine, Joint Faculty of Veterinary Medicine, Kagoshima University*), *Prof. Masaru Okuda* (*Laboratory of Veterinary Internal Medicine, Joint Faculty of Veterinary Medicine, Yamaguchi University*), *Prof. Masahiro Morimoto* (*Laboratory of Veterinary Pathology, Joint Faculty of Veterinary Medicine, Yamaguchi University*), *Assoc. Prof. Kenji Baba* (*Laboratory of Veterinary Internal Medicine, Joint Faculty of Veterinary Medicine, Yamaguchi University*), *Assis. Prof. Masashi Sakurai* (*Laboratory of Veterinary Pathology, Joint Faculty of Veterinary Medicine, Yamaguchi University*), *Assis. Prof. Yusuke Sakai* (*Laboratory of Veterinary Pathology, Joint Faculty of Veterinary Medicine, Yamaguchi University*), *Assis. Prof. Satoshi Kambayashi*

(*Laboratory of Veterinary Internal Medicine, Joint Faculty of Veterinary Medicine, Yamaguchi University*), and *Dr. Hwang Chung Chew* (*AstraZeneca Japan*) for all their help and kindness.

I wish to thank *Saori Umeki*, *Takuma Yanase, Gaku Suyama, Arisa Kaji*, *Haruka Tokuda, Hiroka Yamamoto*, and all the lab. members for supporting me with my doctorial life.

Finally, I would like to give my thanks to my family and friends for the supports in everything I do.

REFERENCES

Abramson JS. Anti-CD19 CAR T-Cell Therapy for B-Cell Non-Hodgkin Lymphoma. Transfus Med Rev. 2020 Jan;34(1):29-33.

Aguirre-Hernández J, Milne BS, Queen C, O'Brien PC, Hoather T, Haugland S, Ferguson-Smith MA, Dobson JM, Sargan DR. Disruption of chromosome 11 in canine fibrosarcomas highlights an unusual variability of CDKN2B in dogs. BMC Vet Res. 2009 Jul 31;5:27.

Alnabhan R, Gaballa A, Mörk LM, Mattsson J, Uhlin M, Magalhaes I. Media evaluation for production and expansion of anti-CD19 chimeric antigen receptor T cells. Cytotherapy. 2018 Jul;20(7):941-951.

Berinstein NL, Grillo-López AJ, White CA, Bence-Bruckler I, Maloney D, Czuczman M, Green D, Rosenberg J, McLaughlin P, Shen D. Association of serum Rituximab (IDEC-C2B8) concentration and anti-tumor response in the treatment of recurrent low-grade or follicular non-Hodgkin's lymphoma. Ann Oncol. 1998 Sep;9(9):995-1001.

Brayer J, Lancet JE, Powers J, List A, Balducci L, Komrokji R, Pinilla-Ibarz J. WT1 vaccination in AML and MDS: A pilot trial with synthetic analog peptides. Am J Hematol. 2015 Jul;90(7):602-7.

Busch DH, Fräßle SP, Sommermeyer D, Buchholz VR, Riddell SR. Role of memory T cell subsets for adoptive immunotherapy. Semin Immunol. 2016 Feb;28(1):28-34.

Call KM, Glaser T, Ito CY, Buckler AJ, Pelletier J, Haber DA, Rose EA, Kral A, Yeger H, Lewis WH, et al. Isolation and characterization of a zinc finger polypeptide gene at the human chromosome 11 Wilms' tumor locus. Cell. 1990 Feb 9;60(3):509-20.

Caniatti M, Roccabianca P, Scanziani E, Paltrinieri S, Moore PF. Canine lymphoma: immunocytochemical analysis of fine-needle aspiration biopsy. Vet Pathol. 1996 Mar;33(2):204-12.

Chavez JC, Locke FL. CAR T cell therapy for B-cell lymphomas. Best Pract Res Clin Haematol. 2018 Jun;31(2):135-146.

Cheever MA, Allison JP, Ferris AS, Finn OJ, Hastings BM, Hecht TT, Mellman I, Prindiville SA, Viner JL, Weiner LM, Matrisian LM. The prioritization of cancer antigens: a national cancer institute pilot project for the acceleration of translational

research. Clin Cancer Res. 2009 Sep 1;15(17):5323-37.

Curran KJ, Margossian SP, Kernan NA, Silverman LB, Williams DA, Shukla N, Kobos R, Forlenza CJ, Steinherz P, Prockop S, Boulad F, Spitzer B, Cancio MI, Boelens JJ, Kung AL, Khakoo Y, Szenes V, Park JH, Sauter CS, Heller G, Wang X, Senechal B, O'Reilly RJ, Riviere I, Sadelain M, Brentjens RJ. Toxicity and response after CD19-specific CAR T-cell therapy in pediatric/young adult relapsed/refractory B-ALL. Blood. 2019 Dec 26;134(26):2361-2368.

Devireddy LR, Myers M, Screven R, Liu Z, Boxer L. A serum-free medium formulation efficiently supports isolation and propagation of canine adipose-derived mesenchymal stem/stromal cells. PLoS One. 2019 Feb 27;14(2):e0210250.

Drakos E, Rassidakis GZ, Tsioli P, Lai R, Jones D, Medeiros LJ. Differential expression of WT1 gene product in non-Hodgkin lymphomas. Appl Immunohistochem Mol Morphol. 2005 Jun;13(2):132-7.

Fisher DJ, Naydan D, Werner LL, Moore PF. Immunophenotyping lymphomas in dogs: a comparison of results from fine needle aspirate and needle biopsy samples. Vet Clin Pathol. 1995;24(4):118-123.

Franzoni MS, Brandi A, de Oliveira Matos Prado JK, Elias F, Dalmolin F, de Faria Lainetti P, Prado MCM, Leis-Filho AF, Fonseca-Alves CE. Tumor-infiltrating CD4+and CD8+ lymphocytes and macrophages are associated with prognostic factors in triple-negative canine mammary complex type carcinoma. Res Vet Sci. 2019 Oct;126:29-36.

Gardner HL, Fenger JM, London CA. Dogs as a Model for Cancer. Annu Rev Anim Biosci. 2016;4:199-222.

Gattinoni L, Klebanoff CA, Restifo NP. Paths to stemness: building the ultimate antitumour T cell. Nat Rev Cancer. 2012 Oct;12(10):671-84.

Gessler M, Poustka A, Cavenee W, Neve RL, Orkin SH, Bruns GA. Homozygous deletion in Wilms tumours of a zinc-finger gene identified by chromosome jumping. Nature. 1990 Feb 22;343(6260):774-8.

Geyer MB, Brentjens RJ. Review: Current clinical applications of chimeric antigen receptor (CAR) modified T cells. Cytotherapy. 2016 Nov;18(11):1393-1409.

Golubovskaya V, Wu L. Different Subsets of T Cells, Memory, Effector Functions, and

CAR-T Immunotherapy. Cancers (Basel). 2016 Mar 15;8(3):36.

GORER PA. Studies in antibody response of mice to tumour inoculation. Br J Cancer. 1950 Dec;4(4):372-9.

Guedan S, Posey AD Jr, Shaw C, Wing A, Da T, Patel PR, McGettigan SE, Casado-Medrano V, Kawalekar OU, Uribe-Herranz M, Song D, Melenhorst JJ, Lacey SF, Scholler J, Keith B, Young RM, June CH. Enhancing CAR T cell persistence through ICOS and 4-1BB costimulation. JCI Insight. 2018 Jan 11;3(1):e96976.

Hansen K, Khanna C. Spontaneous and genetically engineered animal models; use in preclinical cancer drug development. Eur J Cancer. 2004 Apr;40(6):858-80.

Hartmann J, Schüßler-Lenz M, Bondanza A, Buchholz CJ. Clinical development of CAR T cells-challenges and opportunities in translating innovative treatment concepts. EMBO Mol Med. 2017 Sep;9(9):1183-1197.

Honigberg LA, Smith AM, Sirisawad M, Verner E, Loury D, Chang B, Li S, Pan Z, Thamm DH, Miller RA, Buggy JJ. The Bruton tyrosine kinase inhibitor PCI-32765 blocks B-cell activation and is efficacious in models of autoimmune disease and B-cell malignancy. Proc Natl Acad Sci U S A. 2010 Jul 20;107(29):13075-80.

Huang B, Pi L, Chen C, Yuan F, Zhou Q, Teng J, Jiang T. WT1 and Pax2 re-expression is required for epithelial-mesenchymal transition in 5/6 nephrectomized rats and cultured kidney tubular epithelial cells. Cells Tissues Organs. 2012;195(4):296-312.

Huang D, Peng WJ, Ye Q, Liu XP, Zhao L, Fan L, Xia-Hou K, Jia HJ, Luo J, Zhou LT, Li BB, Wang SL, Xu WT, Chen Z, Tan WS. Serum-Free Suspension Culture of MDCK Cells for Production of Influenza H1N1 Vaccines. PLoS One. 2015 Nov 5;10(11):e0141686.

Ichimura R, Shibutani M, Mizukami S, Suzuki T, Shimada Y, Mitsumori K. A case report of an uncommon sex-cord stromal tumor consisted of luteal and sertoli cells in a spayed bitch. J Vet Med Sci. 2010 Feb;72(2):229-34.

Igase M, Nemoto Y, Itamoto K, Tani K, Nakaichi M, Sakurai M, Sakai Y, Noguchi S, Kato M, Tsukui T, Mizuno T. A pilot clinical study of the therapeutic antibody against canine PD-1 for advanced spontaneous cancers in dogs. Sci Rep. 2020 Oct 27;10(1):18311.

Ito D, Brewer S, Modiano JF, Beall MJ. Development of a novel anti-canine CD20 monoclonal antibody with diagnostic and therapeutic potential. Leuk Lymphoma. 2015 Jan;56(1):219-25.

Ito D, Frantz AM, Modiano JF. Canine lymphoma as a comparative model for human non-Hodgkin lymphoma: recent progress and applications. Vet Immunol Immunopathol. 2014 Jun 15;159(3-4):192-201.

Jäger U, Fridrik M, Zeitlinger M, Heintel D, Hopfinger G, Burgstaller S, Mannhalter C, Oberaigner W, Porpaczy E, Skrabs C, Einberger C, Drach J, Raderer M, Gaiger A, Putman M, Greil R; Arbeitsgemeinschaft Medikamentöse Tumortherapie (AGMT) Investigators. Rituximab serum concentrations during immuno-chemotherapy of follicular lymphoma correlate with patient gender, bone marrow infiltration and clinical response. Haematologica. 2012 Sep;97(9):1431-8.

Jain S, Aresu L, Comazzi S, Shi J, Worrall E, Clayton J, Humphries W, Hemmington S, Davis P, Murray E, Limeneh AA, Ball K, Ruckova E, Muller P, Vojtesek B, Fahraeus R, Argyle D, Hupp TR. The Development of a Recombinant scFv Monoclonal Antibody Targeting Canine CD20 for Use in Comparative Medicine. PLoS One. 2016 Feb 19;11(2):e0148366.

Jameson SC, Masopust D. Understanding Subset Diversity in T Cell Memory. Immunity. 2018 Feb 20;48(2):214-226.

Jena B, Maiti S, Huls H, Singh H, Lee DA, Champlin RE, Cooper LJ. Chimeric antigen receptor (CAR)-specific monoclonal antibody to detect CD19-specific T cells in clinical trials. PLoS One. 2013;8(3):e57838.

Jubala CM, Wojcieszyn JW, Valli VE, Getzy DM, Fosmire SP, Coffey D, Bellgrau D, Modiano JF. CD20 expression in normal canine B cells and in canine non-Hodgkin lymphoma. Vet Pathol. 2005 Jul;42(4):468-76.

Kalos M, Levine BL, Porter DL, Katz S, Grupp SA, Bagg A, June CH. T cells with chimeric antigen receptors have potent antitumor effects and can establish memory in patients with advanced leukemia. Sci Transl Med. 2011 Aug 10;3(95):95ra73.

Kano R, Inoiue C, Okano H, Yamazaki J, Takahashi T, Watari T, Tokuriki M, Hasegawa A. Canine CD20 gene. Vet Immunol Immunopathol. 2005 Dec 15;108(3-4):265-8.

KASZA L. ESTABLISHMENT AND CHARACTERIZATION OF CANINE

THYROID ADENOCARCINOMA AND CANINE MELANOMA CELL LINES. Am J Vet Res. 1964 Jul;25:1178-85.

Kochenderfer JN, Wilson WH, Janik JE, Dudley ME, Stetler-Stevenson M, Feldman SA, Maric I, Raffeld M, Nathan DA, Lanier BJ, Morgan RA, Rosenberg SA. Eradication of B-lineage cells and regression of lymphoma in a patient treated with autologous T cells genetically engineered to recognize CD19. Blood. 2010 Nov 18;116(20):4099-102.

Kothapalli K, Kirkness E, Pujar S, Van Wormer R, Meyers-Wallen VN. Exclusion of candidate genes for canine SRY-negative XX sex reversal. J Hered. 2005;96(7):759-63.

Krakowka S, Ringler SS. Activation specificity of commonly employed mitogens for canine B- and T-lymphocytes. Vet Immunol Immunopathol. 1986 Mar;11(3):281-9.

Krug LM, Dao T, Brown AB, Maslak P, Travis W, Bekele S, Korontsvit T, Zakhaleva V, Wolchok J, Yuan J, Li H, Tyson L, Scheinberg DA. WT1 peptide vaccinations induce CD4 and CD8 T cell immune responses in patients with mesothelioma and non-small cell lung cancer. Cancer Immunol Immunother. 2010 Oct;59(10):1467-79.

Lee SY, Olsen P, Lee DH, Kenoyer AL, Budde LE, O'Steen S, Green DJ, Heimfeld S, Jensen MC, Riddell SR, Press OW, Till BG. Preclinical Optimization of a CD20-specific Chimeric Antigen Receptor Vector and Culture Conditions. J Immunother. 2018 Jan;41(1):19-31.

Liao JC, Gregor P, Wolchok JD, Orlandi F, Craft D, Leung C, Houghton AN, Bergman PJ. Vaccination with human tyrosinase DNA induces antibody responses in dogs with advanced melanoma. Cancer Immun. 2006 Apr 21;6:8.

Louis CU, Savoldo B, Dotti G, Pule M, Yvon E, Myers GD, Rossig C, Russell HV, Diouf O, Liu E, Liu H, Wu MF, Gee AP, Mei Z, Rooney CM, Heslop HE, Brenner MK. Antitumor activity and long-term fate of chimeric antigen receptor-positive T cells in patients with neuroblastoma. Blood. 2011 Dec 1;118(23):6050-6.

Marcos R, Marrinhas C, Malhão F, Canadas A, Santos M, Caniatti M. The cell tube block technique and an immunohistochemistry panel including Wilms tumor 1 to assist in diagnosing cavitary effusions in dogs and cats. Vet Clin Pathol. 2019 Mar;48(1):50-60.

Martinez M, Moon EK. CAR T Cells for Solid Tumors: New Strategies for Finding,

Infiltrating, and Surviving in the Tumor Microenvironment. Front Immunol. 2019 Feb 5;10:128.

Mata M, Gottschalk S. Man's Best Friend: Utilizing Naturally Occurring Tumors in Dogs to Improve Chimeric Antigen Receptor T-cell Therapy for Human Cancers. Mol Ther. 2016 Sep;24(9):1511-2.

Mata M, Vera JF, Gerken C, Rooney CM, Miller T, Pfent C, Wang LL, Wilson-Robles HM, Gottschalk S. Toward immunotherapy with redirected T cells in a large animal model: ex vivo activation, expansion, and genetic modification of canine T cells. J Immunother. 2014 Oct;37(8):407-15.

McLellan AD, Ali Hosseini Rad SM. Chimeric antigen receptor T cell persistence and memory cell formation. Immunol Cell Biol. 2019 Aug;97(7):664-674.

Medvec AR, Ecker C, Kong H, Winters EA, Glover J, Varela-Rohena A, Riley JL. Improved Expansion and In Vivo Function of Patient T Cells by a Serum-free Medium. Mol Ther Methods Clin Dev. 2017 Nov 7;8:65-74.

Menke AL, van der Eb AJ, Jochemsen AG. The Wilms' tumor 1 gene: oncogene or tumor suppressor gene? Int Rev Cytol. 1998;181:151-212.

Miller AD, Garcia JV, von Suhr N, Lynch CM, Wilson C, Eiden MV. Construction and properties of retrovirus packaging cells based on gibbon ape leukemia virus. J Virol. 1991 May;65(5):2220-4.

Mitchell L, Dow SW, Slansky JE, Biller BJ. Induction of remission results in spontaneous enhancement of anti-tumor cytotoxic T-lymphocyte activity in dogs with B cell lymphoma. Vet Immunol Immunopathol. 2012 Feb 15;145(3-4):597-603.

Mizuno T, Kato Y, Kaneko MK, Sakai Y, Shiga T, Kato M, Tsukui T, Takemoto H, Tokimasa A, Baba K, Nemoto Y, Sakai O, Igase M. Generation of a canine anti-canine CD20 antibody for canine lymphoma treatment. Sci Rep. 2020 Jul 10;10(1):11476.

Mizuno T, Suzuki R, Umeki S, Okuda M. Crossreactivity of antibodies to canine CD25 and Foxp3 and identification of canine CD4+CD25 +Foxp3+ cells in canine peripheral blood. J Vet Med Sci. 2009 Dec;71(12):1561-8.

Moore PF, Affolter VK, Keller SM. Canine inflamed nonepitheliotropic cutaneous T-cell lymphoma: a diagnostic conundrum. Vet Dermatol. 2013 Feb;24(1):204-11.e44-5.

Moore PF, Rossitto PV, Danilenko DM, Wielenga JJ, Raff RF, Severns E. Monoclonal antibodies specific for canine CD4 and CD8 define functional T-lymphocyte subsets and high-density expression of CD4 by canine neutrophils. Tissue Antigens. 1992 Aug;40(2):75-85.

Morgan RA, Dudley ME, Wunderlich JR, Hughes MS, Yang JC, Sherry RM, Royal RE, Topalian SL, Kammula US, Restifo NP, Zheng Z, Nahvi A, de Vries CR, Rogers-Freezer LJ, Mavroukakis SA, Rosenberg SA. Cancer regression in patients after transfer of genetically engineered lymphocytes. Science. 2006 Oct 6;314(5796):126-9.

Morita S, Kojima T, Kitamura T. Plat-E: an efficient and stable system for transient packaging of retroviruses. Gene Ther. 2000 Jun;7(12):1063-6.

Mousset CM, Hobo W, Ji Y, Fredrix H, De Giorgi V, Allison RD, Kester MGD, Falkenburg JHF, Schaap NPM, Jansen JH, Gattinoni L, Dolstra H, van der Waart AB. Ex vivo AKT-inhibition facilitates generation of polyfunctional stem cell memory-like CD8+T cells for adoptive immunotherapy. Oncoimmunology. 2018 Aug 6;7(10):e1488565.

Mucha J, Majchrzak K, Taciak B, Hellmén E, Król M. MDSCs mediate angiogenesis and predispose canine mammary tumor cells for metastasis via IL-28/IL-28RA (IFN-λ) signaling. PLoS One. 2014 Jul 30;9(7):e103249.

Narita M, Masuko M, Kurasaki T, Kitajima T, Takenouchi S, Saitoh A, Watanabe N, Furukawa T, Toba K, Fuse I, Aizawa Y, Kawakami M, Oka Y, Sugiyama H, Takahashi M. WT1 peptide vaccination in combination with imatinib therapy for a patient with CML in the chronic phase. Int J Med Sci. 2010 Apr 20;7(2):72-81.

Neelapu SS, Locke FL, Bartlett NL, Lekakis LJ, Miklos DB, Jacobson CA, Braunschweig I, Oluwole OO, Siddiqi T, Lin Y, Timmerman JM, Stiff PJ, Friedberg JW, Flinn IW, Goy A, Hill BT, Smith MR, Deol A, Farooq U, McSweeney P, Munoz J, Avivi I, Castro JE, Westin JR, Chavez JC, Ghobadi A, Komanduri KV, Levy R, Jacobsen ED, Witzig TE, Reagan P, Bot A, Rossi J, Navale L, Jiang Y, Aycock J, Elias M, Chang D, Wiezorek J, Go WY. Axicabtagene Ciloleucel CAR T-Cell Therapy in Refractory Large B-Cell Lymphoma. N Engl J Med. 2017 Dec 28;377(26):2531-2544.

Nemoto Y, Shosu K, Okuda M, Noguchi S, Mizuno T. Development and characterization of monoclonal antibodies against canine PD-1 and PD-L1. Vet Immunol Immunopathol. 2018 Apr;198:19-25.

Oji Y, Oka Y, Nishida S, Tsuboi A, Kawakami M, Shirakata T, Takahashi K, Murao A, Nakajima H, Narita M, Takahashi M, Morita S, Sakamoto J, Tanaka T, Kawase I, Hosen N, Sugiyama H. WT1 peptide vaccine induces reduction in minimal residual disease in an Imatinib-treated CML patient. Eur J Haematol. 2010 Oct;85(4):358-60.

Oka Y, Tsuboi A, Taguchi T, Osaki T, Kyo T, Nakajima H, Elisseeva OA, Oji Y, Kawakami M, Ikegame K, Hosen N, Yoshihara S, Wu F, Fujiki F, Murakami M, Masuda T, Nishida S, Shirakata T, Nakatsuka S, Sasaki A, Udaka K, Dohy H, Aozasa K, Noguchi S, Kawase I, Sugiyama H. Induction of WT1 (Wilms' tumor gene)-specific cytotoxic T lymphocytes by WT1 peptide vaccine and the resultant cancer regression. Proc Natl Acad Sci U S A. 2004 Sep 21;101(38):13885-90.

Oka Y, Udaka K, Tsuboi A, Elisseeva OA, Ogawa H, Aozasa K, Kishimoto T, Sugiyama H. Cancer immunotherapy targeting Wilms' tumor gene WT1 product. J Immunol. 2000 Feb 15;164(4):1873-80.

Okawa T, Kurio Y, Morimoto M, Hayashi T, Nakagawa T, Sasaki N, Okuda M, Mizuno T. Calreticulin expression in neoplastic versus normal dog mammary glands: a cDNA subtraction-based study. Res Vet Sci. 2012 Feb;92(1):80-91.

Panjwani MK, Atherton MJ, MaloneyHuss MA, Haran KP, Xiong A, Gupta M, Kulikovsaya I, Lacey SF, Mason NJ. Establishing a model system for evaluating CAR T cell therapy using dogs with spontaneous diffuse large B cell lymphoma. Oncoimmunology. 2019 Oct 23;9(1):1676615.

Panjwani MK, Smith JB, Schutsky K, Gnanandarajah J, O'Connor CM, Powell DJ Jr, Mason NJ. Feasibility and Safety of RNA-transfected CD20-specific Chimeric Antigen Receptor T Cells in Dogs with Spontaneous B Cell Lymphoma. Mol Ther. 2016 Sep;24(9):1602-14.

Park JS, Withers SS, Modiano JF, Kent MS, Chen M, Luna JI, Culp WTN, Sparger EE, Rebhun RB, Monjazeb AM, Murphy WJ, Canter RJ. Canine cancer immunotherapy studies: linking mouse and human. J Immunother Cancer. 2016 Dec 20;4:97.

Partridge BR, O'Brien TJ, Lorenzo MF, Coutermarsh-Ott SL, Barry SL, Stadler K, Muro N, Meyerhoeffer M, Allen IC, Davalos RV, Dervisis NG. High-Frequency Irreversible Electroporation for Treatment of Primary Liver Cancer: A Proof-of-Principle Study in Canine Hepatocellular Carcinoma. J Vasc Interv Radiol. 2020 Mar;31(3):482-491.e4.

Pearson GR, Gregory SP, Charles AK. Immunohistochemical demonstration of Wilms tumour gene product WT1 in a canine "neuroepithelioma" providing evidence for its classification as an extrarenal nephroblastoma. J Comp Pathol. 1997 Apr;116(3):321-7.

Peruzzi D, Gavazza A, Mesiti G, Lubas G, Scarselli E, Conforti A, Bendtsen C, Ciliberto G, La Monica N, Aurisicchio L. A vaccine targeting telomerase enhances survival of dogs affected by B-cell lymphoma. Mol Ther. 2010 Aug;18(8):1559-67.

Porcellato I, Silvestri S, Menchetti L, Recupero F, Mechelli L, Sforna M, Iussich S, Bongiovanni L, Lepri E, Brachelente C. Tumour-infiltrating lymphocytes in canine melanocytic tumours: An investigation on the prognostic role of CD3+ and CD20+lymphocytic populations. Vet Comp Oncol. 2020 Sep;18(3):370-380.

Rafiq S, Hackett CS, Brentjens RJ. Engineering strategies to overcome the current roadblocks in CAR T cell therapy. Nat Rev Clin Oncol. 2020 Mar;17(3):147-167.

Ramos CA, Rouce R, Robertson CS, Reyna A, Narala N, Vyas G, Mehta B, Zhang H, Dakhova O, Carrum G, Kamble RT, Gee AP, Mei Z, Wu MF, Liu H, Grilley B, Rooney CM, Heslop HE, Brenner MK, Savoldo B, Dotti G. In Vivo Fate and Activity of Second- versus Third-Generation CD19-Specific CAR-T Cells in B Cell Non-Hodgkin's Lymphomas. Mol Ther. 2018 Dec 5;26(12):2727-2737.

Raposo T, Gregório H, Pires I, Prada J, Queiroga FL. Prognostic value of tumour-associated macrophages in canine mammary tumours. Vet Comp Oncol. 2014 Mar;12(1):10-9.

Rosenfeld C, Cheever MA, Gaiger A. WT1 in acute leukemia, chronic myelogenous leukemia and myelodysplastic syndrome: therapeutic potential of WT1 targeted therapies. Leukemia. 2003 Jul;17(7):1301-12.

Rowell JL, McCarthy DO, Alvarez CE. Dog models of naturally occurring cancer. Trends Mol Med. 2011 Jul;17(7):380-8.

Rütgen BC, Hammer SE, Gerner W, Christian M, de Arespacochaga AG, Willmann M, Kleiter M, Schwendenwein I, Saalmüller A. Establishment and characterization of a novel canine B-cell line derived from a spontaneously occurring diffuse large cell lymphoma. Leuk Res. 2010 Jul;34(7):932-8.

Sakai O, Igase M, Mizuno T. Optimization of canine CD20 chimeric antigen receptor T

cell manufacturing and in vitro cytotoxic activity against B-cell lymphoma. Vet Comp Oncol. 2020 Dec;18(4):739-752.

Salles G, Barrett M, Foà R, Maurer J, O'Brien S, Valente N, Wenger M, Maloney DG. Rituximab in B-Cell Hematologic Malignancies: A Review of 20 Years of Clinical Experience. Adv Ther. 2017 Oct;34(10):2232-2273.

Sha HH, Wang DD, Yan DL, Hu Y, Yang SJ, Liu SW, Feng JF. Chimaeric antigen receptor T-cell therapy for tumour immunotherapy. Biosci Rep. 2017 Jan 27;37(1):BSR20160332.
Shosu K, Sakurai M, Inoue K, Nakagawa T, Sakai H, Morimoto M, Okuda M, Noguchi S, Mizuno T. Programmed Cell Death Ligand 1 Expression in Canine Cancer. In Vivo. 2016 May-Jun;30(3):195-204.

Sisó S, Marco-Salazar P, Moore PF, Sturges BK, Vernau W, Wisner ER, Bollen AW, Dickinson PJ, Higgins RJ. Canine Nervous System Lymphoma Subtypes Display Characteristic Neuroanatomical Patterns. Vet Pathol. 2017 Jan;54(1):53-60.

Smith C, Økern G, Rehan S, Beagley L, Lee SK, Aarvak T, Schjetne KW, Khanna R. Ex vivo expansion of human T cells for adoptive immunotherapy using the novel Xeno-free CTS Immune Cell Serum Replacement. Clin Transl Immunology. 2015 Jan 16;4(1):e31.

Smith JB, Panjwani MK, Schutsky K, Gnanandarajah J, Calhoun S, Cooper L, Mason N, Powell DJ. Feasibility and safety of cCD20 RNA CAR-bearing T cell therapy for the treatment of canine B cell malignancies. J Immunother Cancer. 2015 Nov 4;3(2):123.

Tagliamonte M, Petrizzo A, Tornesello ML, Buonaguro FM, Buonaguro L. Antigen-specific vaccines for cancer treatment. Hum Vaccin Immunother. 2014;10(11):3332-46.

Trompieri-Silveira AC, Gerardi D, Mouro JV, Costa MT, and Alessi AC: Immunohistochemical expression of B and T-lymphocytes and TGF-b in experimentally transplanted canine venereal tumor. Cieˆ ncia Rural 2009;39:1148–1154.

Tsukahara T, Ohmine K, Yamamoto C, Uchibori R, Ido H, Teruya T, Urabe M, Mizukami H, Kume A, Nakamura M, Mineno J, Takesako K, Riviere I, Sadelain M, Brentjens R, Ozawa K. CD19 target-engineered T-cells accumulate at tumor lesions in human B-cell lymphoma xenograft mouse models. Biochem Biophys Res Commun. 2013 Aug 16;438(1):84-9.

Turtle CJ, Hanafi LA, Berger C, Gooley TA, Cherian S, Hudecek M, Sommermeyer D,

Melville K, Pender B, Budiarto TM, Robinson E, Steevens NN, Chaney C, Soma L, Chen X, Yeung C, Wood B, Li D, Cao J, Heimfeld S, Jensen MC, Riddell SR, Maloney DG. CD19 CAR-T cells of defined CD4+:CD8+ composition in adult B cell ALL patients. J Clin Invest. 2016 Jun 1;126(6):2123-38.

Umeki S, Ema Y, Suzuki R, Kubo M, Hayashi T, Okamura Y, Yamazaki J, Tsujimoto H, Tani K, Hiraoka H, Okuda M, Mizuno T. Establishment of five canine lymphoma cell lines and tumor formation in a xenotransplantation model. J Vet Med Sci. 2013 May 2;75(4):467-74.

Umeki S, Suzuki R, Shimojima M, Ema Y, Yanase T, Iwata H, Okuda M, Mizuno T. Characterization of monoclonal antibodies against canine P-selectin glycoprotein ligand-1 (PSGL-1). Vet Immunol Immunopathol. 2011 Jul 15;142(1-2):119-25.

Urak R, Walter M, Lim L, Wong CW, Budde LE, Thomas S, Forman SJ, Wang X. Ex vivo Akt inhibition promotes the generation of potent CD19CAR T cells for adoptive immunotherapy. J Immunother Cancer. 2017 Mar 21;5:26.

Wagner N, Wagner KD, Xing Y, Scholz H, Schedl A. The major podocyte protein nephrin is transcriptionally activated by the Wilms' tumor suppressor WT1. J Am Soc Nephrol. 2004 Dec;15(12):3044-51.

Wang X, Popplewell LL, Wagner JR, Naranjo A, Blanchard MS, Mott MR, Norris AP, Wong CW, Urak RZ, Chang WC, Khaled SK, Siddiqi T, Budde LE, Xu J, Chang B, Gidwaney N, Thomas SH, Cooper LJ, Riddell SR, Brown CE, Jensen MC, Forman SJ. Phase 1 studies of central memory-derived CD19 CAR T-cell therapy following autologous HSCT in patients with B-cell NHL. Blood. 2016 Jun 16;127(24):2980-90.

Wang Z, Wu Z, Liu Y, Han W. New development in CAR-T cell therapy. J Hematol Oncol. 2017 Feb 21;10(1):53.

Withers SS, Moore PF, Chang H, Choi JW, McSorley SJ, Kent MS, Monjazeb AM, Canter RJ, Murphy WJ, Sparger EE, Rebhun RB. Multi-color flow cytometry for evaluating age-related changes in memory lymphocyte subsets in dogs. Dev Comp Immunol. 2018 Oct;87:64-74.

Withrow SJ, Wilkins RM. Cross talk from pets to people: translational osteosarcoma treatments. ILAR J. 2010;51(3):208-13.

Xu Y, Zhang M, Ramos CA, Durett A, Liu E, Dakhova O, Liu H, Creighton CJ, Gee AP,

Heslop HE, Rooney CM, Savoldo B, Dotti G. Closely related T-memory stem cells correlate with in vivo expansion of CAR.CD19-T cells and are preserved by IL-7 and IL-15. Blood. 2014 Jun 12;123(24):3750-9.

Yang L, Han Y, Suarez Saiz F, Minden MD. A tumor suppressor and oncogene: the WT1 story. Leukemia. 2007 May;21(5):868-76.

Yin Y, Boesteanu AC, Binder ZA, Xu C, Reid RA, Rodriguez JL, Cook DR, Thokala R, Blouch K, McGettigan-Croce B, Zhang L, Konradt C, Cogdill AP, Panjwani MK, Jiang S, Migliorini D, Dahmane N, Posey AD Jr, June CH, Mason NJ, Lin Z, O'Rourke DM, Johnson LA. Checkpoint Blockade Reverses Anergy in IL-13Rα2 Humanized scFv-Based CAR T Cells to Treat Murine and Canine Gliomas. Mol Ther Oncolytics. 2018 Aug 28;11:20-38.

Zandvliet M, Teske E. Mechanisms of Drug Resistance in Veterinary Oncology- A Review with an Emphasis on Canine Lymphoma. Vet Sci. 2015 Aug 12;2(3):150-184.

Zandvliet M. Canine lymphoma: a review. Vet Q. 2016 Jun;36(2):76-104.

Zhang Q, Ding J, Sun S, Liu H, Lu M, Wei X, Gao X, Zhang X, Fu Q, Zheng J. Akt inhibition at the initial stage of CAR-T preparation enhances the CAR-positive expression rate, memory phenotype and in vivo efficacy. Am J Cancer Res. 2019 Nov 1;9(11):2379-2396.

Zolov SN, Rietberg SP, Bonifant CL. Programmed cell death protein 1 activation preferentially inhibits CD28.CAR-T cells. Cytotherapy. 2018 Oct;20(10):1259-1266.